Master's thesis

NTNU
Norwegian University of Science and Technology
Faculty of Natural Sciences
Department of Biology

Åsa Vedøy

Exploring the Link of Inflammation and Adipogenesis Following Exposure to Plastic Chemical

Master's thesis in Biotechnology
Supervisor: Martin Wagner
Co-supervisor: Johannes Völker
November 2022

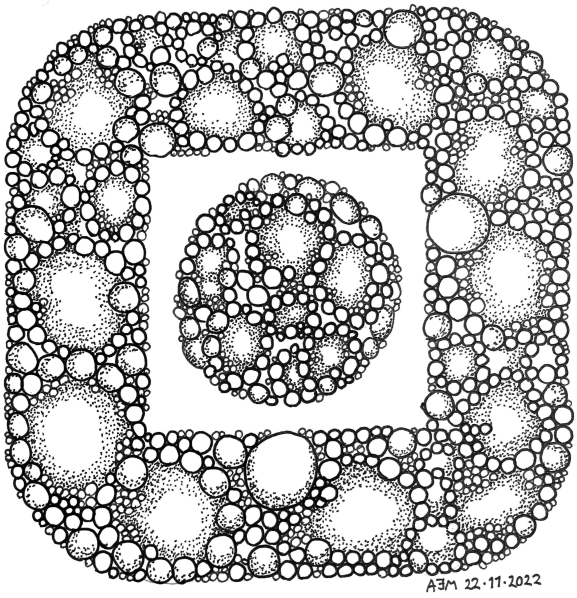

NTNU
Norwegian University of
Science and Technology

Åsa Vedøy

Exploring the Link of Inflammation and Adipogenesis Following Exposure to Plastic Chemical

Master's thesis in Biotechnology
Supervisor: Martin Wagner
Co-supervisor: Johannes Völker
November 2022

Norwegian University of Science and Technology
Faculty of Natural Sciences
Department of Biology

NTNU
Norwegian University of
Science and Technology

Acknowledgements

This master's thesis in molecular biology was conducted at the Department of Biology at the Norwegian University of Science and Technology (NTNU) in the period January 2021 to November 2022.

I would like to thank my two admirable supervisors Martin Wagner and Johannes Völker. I am grateful to Johannes for taking the time to teach me all the laboratory technics, data analysis, and for answering all the questions you had explained the answer to in advance. Thank you for taking the time to supervise me even through you were not connected to NTNU the last year of the work of my thesis. Thanks to Martin for keeping my spirit up, guiding me onto the right path whenever I was lost and always being eager to answer my questions. Further, I would like to thank Felicity Ashcroft for guiding me in the work of transcriptomics and Harini Pechiappan for teaching me how to conduct ELISA. Thank you also, Sarah Stevens for troubleshooting when needed, always staying calm and helping me with the plastic extractions.

Last but not least, thanks to family and friends for patience and support, especially to Dagros, for sympathy and for always believing in me. Additionally, I am highly grateful to Ingrid Gisnås Vardeberg and Anders Jorud Meyer for always having a shoulder to cry on, I do not think I could have finished this thesis without your love and encouragement.

Trondheim, November 2022

Åsa Vedøy

Abstract

The expanding prevalence of obesity is an enormous health issue on a populational level. According to the obesogenic hypothesis adipose tissue is susceptible of exposure to metabolism disrupting chemicals (MDCs), especially during early life. Commercial plastic materials contain an organic polymer matrix and various chemicals, and some of the chemicals are known obesogens or MDCs. It remains however, to identify whether everyday plastic products contain MDCs. We therefore investigated the effects of adipocyte exposure to plastic chemicals extracted from everyday products. To validate our previous findings, we exposed 3T3-L1 to plastic extracts and to investigate whether there is a sensitive exposure window in the adipocyte differentiation, we exposed the cells to the plastic chemicals during the adipogenesis assay in three different windows of exposure. To investigate whether the plastic chemicals were triggering an inflammatory response in the adipocytes, we quantified the interleukin (IL)-6 and tumor necrosis factor α(TNF-α) release after chemical exposure. In the further investigation of the underlying mechanisms for the adipogenic induction, altered gene expression in the adipocytes caused by chemical exposure was studied.

We found that the differentiation phase was a further sensitive window of exposure for all the plastic extracts, along with the positive control, rosiglitazone. The IL-6 release by the adipocytes was higher during the differentiation compared to the end of the experiment, and two of the extracts caused a higher IL-6 release compared to the remaining extracts. In contrast to IL-6, TNF-α was not detected. In the investigation for underlying mechanisms of the induction of adipogenesis, we observed that the extracts caused a similar alteration of several genes, which was different to the effect of rosiglitazone. Our results suggests that plastic chemical exposure early in life could contribute to the obesity pandemic, the link between the inflammatory response and the chemical exposure was however not clear. The underlying mechanisms affected by the plastic extracts imply hypoxia, endoplasmic reticulum (ER) stress and oxidative stress in the cells, all related to the obesity phenotype.

Samandrag

Den aukande førekomsten av fedme er eit enormt helseproblem på befolkningsnivå. Ifølgje den obesogene hypotesa er feittvev utsett for eksponering av metabolismeforstyrrande kjemikalie, spesielt i tidleg alder. Kommersielle plastmateriale er bygd opp av ei organisk polymermatrise og er tilsett ulike kjemikaliar, nokre av desse er identifisert som fedme- og/eller metabolismeforstyrrande. Ein veit ikkje om kvardagsprodukt av plast inneheld metabolismeforstyrrande kjemikaliar. Me undersøk difor effekten av kjemikaliar frå kvardagsprodukt av plast i feittceller. For å stadfeste våre tidlegare funn, eksponerte me 3T3-L1 celler for kjemikaliar ekstrahert frå plastprodukt. For å vidare undersøkje om det var ein sensitiv fase for eksponering av feittceller, eksponerte me cellene for plastkjemikaliar i løpet av ein differensieringsanalyse, anten i differensieringsfasen, i vedlikehaldsfasen eller gjennom analysen. For å undersøkje om plastkjemikaliane utløyste ein betennelsesrespons i feittcellene kvantifiserte me interleukin (IL)-6 og tumornekrosefaktor-α (TNF-α) nivået frigjort av cellene etter eksponering av plastekstrakta. I den vidare undersøkinga av dei underliggjande mekanismane påverka av plastekstrakta, studerte me det endra genuttrykket i feittcellene.

Me fann ut at differensieringsfasen var eit sensitivt tidsvindauge for eksponering av plastkjemikaliane, saman med den positive kontrollen, rosiglitazone. IL-6 frigjeringa var høgare under differensieringa samanlikna med slutten av vedlikehaldsfasen og to av ekstrakta forårsaka ei høgare IL-6 frigjering samanlikna med dei resterande ekstrakta. I motsetjing til IL-6 vart ikkje TNF-α påvist. I den vidare undersøkinga av underliggjande mekanismar påverka av ekstrakteksponeringa observerte me at plastkjemikaliane forårsaka ei liknande endring av fleire gen, i tillegg til å vere ulike frå effekten av rosiglitazone. Resultata våre indikerer at eksponeringa av plastkjemikalar tidleg i livet kan medverka til fedmepandemien, medan linken mellom betennelsesresponsen og den kjemiske eksponeringa var ikkje tydleg. Dei underliggjande mekanismane som vert påverka av plastekstrakta inneber utilstrekkeleg oksygentilføring, endoplasmatisk retikulum (ER) stress og oksidativt stress i cellene, alt relatert til fenotypen til personar med fedme.

Table of Contents

Abbreviations

AC	Adipocyte count
ATX	Autotaxin
BMP	Bone morphogenetic protein
CC	Cell count
C/EBPα	CCAAT/enhancer-binding protein-α
DEHP	Bis(2-ethylhexyl)phthalate
DM	Differentiation media
DMSO	Dimethyl sulfoxide
ELISA	Enzyme-linked immunosorbent assay
ER	Endoplasmic reticulum
FABP4	Fatty acid binding protein
FBS	Fetal bovine serum
FCM	Food contact material
HNC	Highest non-cytotoxic concentration
IBMX	3-isobutyl-1-methylxantine
IL	Interleukin
LC-QTOF-MS/MS	Liquid chromatography coupled to a quadrupole of flight spectrometer
LDC	Lipid droplet count
LDPE	Low-density polyethylene
LPA	Lysophosphatidic acid
LPAR	Lysophosphatidic acid receptor
LPC	Lysophosphatidylcholine
LPP	Lipid phosphate phosphatase
MANF	Mesencephalic astrocyte-derived neurotrophic factor
MDC	Metabolism disrupting chemical
MM	Maintenance media
NC	Negative control
NHANES	National Health and Nutrition Examination Study
PAM	Preadipocyte media
PBS	Phosphate-buffered saline

PLA	Polylactic acid
PP	Polypropylene
PPARγ	Peroxisome proliferator-activated receptor-γ
PS	Polystyrene
PUR	Polyurethane
PVC	Polyvinyl chloride
qPCR	Quantitative polymerase chain reaction
ROS	Reactive oxygen species
SC	Solvent control
TBT	Tributyltin
TNF-α	Tumor necrosis factor-α
WAT	White adipose tissue

1. Introduction

1.1 General background

Obesity is an emerging health problem and a worldwide pandemic (Egusquiza and Blumberg, 2020). In the United States in 2003-2004, obesity among adults was estimated to be 32.9%, this number has increased to 42.4% in 15 years and is still increasing (Ogden et al., 2007, Hales et al., 2020). The expanding prevalence of obesity is an enormous health issue both on an individual level, but also in a global scale. The health burden extends to several organ systems as the excessive adipose tissue is related to a higher prevalence of metabolic syndrome, several types of cancer, cardiovascular diseases, and higher mortality rates (González-Muniesa et al., 2016). Metabolic syndrome is a condition characterized by hyperglycemia, abdominal obesity, dyslipidemia, and hypertension. A combination of these metabolic risk factors collectively increase the risk of heart diseases, type 2 diabetes, and stroke (Ghaben and Scherer, 2019). Additionally, a chronic inflammatory state accompanies the metabolic syndrome and is a low-grade inflammatory response triggered by excess nutrients in metabolic cells. In this case, levels of several circulating inflammatory markers are increased (González-Muniesa et al., 2016). Thus, in addition to excess body weight, obesity cause extensive health burdens and can lead to several medical conditions.

Today, plastics are ubiquitously used. The question remains however, whether plastic products pose a threat to the human health. Plastics are widely distributed and are highly diverse in both chemical composition, properties, and potential functions (Lithner et al., 2011). The global plastic production has increased from 2 million tons in 1950 to over 400 million tons in 2015 and is expected to double over the next 20 years (Heinrich Böll Stiftung, 2019). Plastic polymers are not regarded as toxic *per se*, but several of the chemicals applied in plastic production are hazardous for human health and the environment. These chemicals, and their degradation products may be released during the lifetime of plastic products (Lithner et al., 2011). Several aspects of how plastic chemicals may affect our health are yet not elucidated, thus in this thesis we will further investigate whether plastic chemicals could promote obesity.

1.2 Plastic chemicals

Commercial plastic materials contain an organic polymer matrix and various chemical additives. The organic polymers are the basis of the plastic material and are composed by repeating monomers. The plastic's properties are improved by additives, e.g., antioxidants,

plasticizers, and flame retardants. Additionally, a variety of chemicals are used in the production of the synthetic materials to enable or ease the production or processing of the plastics (Wiesinger et al., 2021). Nonintentionally added substances (NIASs) can also be present in plastics, these including break-down products, impurities of starting materials, unwanted side-products and contaminants from recycling processes (Geueke, 2018). As plastic products are used by the consumer, chemicals may migrate from the plastic into products such as food or in the environment (Groh et al., 2019). Chemical release is an unwanted process, since loss of additive content decreases the polymer lifetime and exposing consumers to the chemicals released (Teuten et al., 2009). Primarily, chemicals may end up in the human body via ingestion, inhalation or dermal absorption of air, dust, water, food, and the application of personal care products (Koch and Calafat, 2009). Plastic chemicals may thus be released from the plastic products and end up in the human body.

Bisphenol A (BPA) is a plastic chemical known to alter the endocrine system. BPA is a monomer and plasticizer used in the production of plastic products like toys, water pipes, eyeglass lenses, drinking containers, along with others (Vandenberg et al., 2007). Even though BPA was shown to stimulate the reproductive system in female rats in 1936, BPA was used as a plastic monomer in polycarbonate plastics and epoxy resins from the 1950s (vom Saal et al., 2007). More recent studies have demonstrated BPA to possess further endocrine disrupting properties, i.e., alterations of the hormone synthesis and metabolism, and hormone concentration in the blood (Koch and Calafat, 2009). In 2011, the European Union prohibited the use of BPA in food contact materials (Regulation10/2011/EU, 2011). However, human can absorb these endocrine disrupting chemical through exposure either by unreacted BPA in the plastic polymer or by remobilized monomers in the final product (Koch and Calafat, 2009). In other words, unbound plastic chemicals can be absorbed by humans and alter the endocrine system.

1.2.1 Metabolism disrupting chemicals

Chemicals termed obesogens or metabolism disrupting chemicals (MDCs) can promote obesity and metabolic changes. The US National Health and Nutrition Examination Study (NHANES) has reported that when comparing adults with equivalent energy consumption and physical activity in 2006 and 1988, the adults in 2006 had a BMI 2.3 kg/m^2 higher than adults in 1988. The study challenged the weight balance model, a model assuming that a greater energy intake

than energy expenditure is expected to increase the fat accumulation in direct proportion (Amato et al., 2021). According to the obesogen hypothesis, environmental chemicals promote obesity by increasing adipocyte commitment, differentiation, and size. These chemicals are abundant in our environment and used in several everyday products, e.g., furniture, electronic devices, and plastic products (Heindel and Blumberg, 2019). In 2015, the obesogen hypothesis was proposed to be expanded to include other metabolic endpoints, e.g., type 2 diabetes and liver lipid abnormalities. As a result, the MDC hypothesis was introduced, a hypothesis proposing that environmental chemicals have the ability to promote metabolic alterations in humans and animals, which may play a considerable role in the pandemic of obesity, type 2 diabetes and metabolic syndrome (Heindel et al., 2017). Obesogens and MDCs are thus environmental chemicals promoting obesity and metabolic alterations.

Tributyltin (TBT) is a well-characterized obesogen widely used in industry and found to be present in aquatic environment. In the 1970s, TBT was used as antifouling agent to prevent adhesions of organisms but had severe effects on the marine life. Even though TBT was banned in the United States in the 1980s, the compound has been found in sea sediments and fish for human consumption in the recent years (Katz and Walker, 2019). TBT is also the main organotin used as polyvinyl chloride (PVC) heat stabilizer, wood preservatives, and has been detected in house dust in several countries in Europe (Heindel and Blumberg, 2019, Fromme et al., 2005). The organotin was among the first obesogens identified and is known to bind and activate the master regulator of adipocyte differentiation, peroxisome proliferator-activated receptor γ (PPARγ) and its heterodimeric partner. *In vitro* studies demonstrate that TBT activation promotes adipocyte commitment and differentiation, while *in vivo* studies found that TBT exposure increase fat accumulation in rodents, fish, snails and daphnia (Amato et al., 2021). Hence, the organotin TBT is found in our surroundings and is shown to promote adipocyte development and lipid storage.

The adipose tissue is an endocrine organ susceptible of metabolic disruption, especially in critical windows of exposure (Nappi et al., 2016). Studies have shown that the total number of adipocytes increases throughout childhood and adolescence and remains constant in adulthood. With this in mind, the difference in adipocyte number between lean and obese individuals is thus established during childhood (Spalding et al., 2008). According to the obesogenic hypothesis the adipose depots are susceptible of exposure to MDCs, especially during

development, i.e., pre- and early postnatal life, and throughout the puberty. Weight gain in adults is primarily due to changes in size in pre-existing adipocytes, an increased adipogenesis caused by MDCs during early development would therefore permanently establish an elevated adipocyte number (Nappi et al., 2016). Considering obese individuals have a higher adipocyte number than lean individuals, the exposure to MDCs could contribute to obesity through the elevation of adipocyte number during the early life.

1.3 Adipocytes and adipogenesis

Adipose tissue is a connective tissue regulating the energy balance and nutritional homeostasis and consist of brown, beige, and white adipocytes. Brown adipose tissue generates body heat through the energy demanding process of non-shivering thermogenesis. Beige adipocytes appear to be bifunctional, changing to brown or white adipocytes depending on stimuli (Heindel et al., 2017). The white adipose tissue (WAT) is our largest energy reserve and controls the energy balance by storing and mobilizing triacylglycerol (Duncan et al., 2007). This active endocrine organ regulates several activities, such as insulin sensitivity, lipid metabolism and satiety by releasing a variety of adipokines, including adipsin, leptin, adiponectin, and resistin. In humans, development of WAT compartments is initiated late in the gestation and the differentiation of adipocytes rapidly escalates in response to increased nutrient availability (Cristancho and Lazar, 2011). In short, adipogenesis, the adipocyte differentiation, is an ordered multistep transformation whereby fibroblast-like progenitor cells become mature adipocytes (Ghaben and Scherer, 2019). In other words, adipocytes exist in various forms and differentiate through the process of adipogenesis.

During the adipogenesis, progenitor cells restrict themselves to the lineage forming a preadipocyte, followed by the differentiation, whereby the cells start to accumulate lipids and further form a functional mature adipocyte. In the early phase of the adipogenesis, a multipotent precursor cell is activated through bone morphogenetic protein (BMP) binding which is required for the adipocyte commitment. Once the precursor cell has committed to the adipocyte lineage, a transcriptional cascade is triggered and the induction of metabolic genes associated with the adipocyte is expressed (Ghaben and Scherer, 2019). The BMP signaling promote the terminal differentiation in the preadipocytes by the activation of the transcription factor SMAD4, which in turn stimulates the transcription of the master regulator of adipogenesis, PPARγ (Huang et al., 2009). PPARγ is a nuclear receptor and transcription factor indispensable

for the differentiation of adipocytes (Farmer, 2006). One of its most important roles is to activate another master regulator of adipogenic transcription, CCAAT/enhancer-binding protein α (C/EBPα) which then induce each other's expression through a positive feedback loop. This results in the induction of other pro-adipogenic factors and thereby maintains the differentiated cell state (Rosen, 2005). In the early stages of differentiation, the lipid accumulation causes the expression of the adipocyte fatty acid binding protein (FABP4) and the glucose transporter GLUT4. At the completion of the differentiation, mature adipocytes also express the peptide hormones leptin and adiponectin, as well as adipose triglyceride lipase, lipoprotein lipase, and perilipin (Ghaben and Scherer, 2019). The functional mature adipocytes are then alternating between the storing and release of lipids dependent on extracellular signals.

Fully differentiated adipocytes are incapable of mitotic division and differentiation of precursor cells occurs to increase the number of adipocytes. Adipose tissue can increase in size either by increasing the size of the preexisting adipocytes (hypertrophy), or by formation of new adipocytes through differentiation of precursor cells (hyperplasia). The hypertrophic potential in mature adipocytes is outstanding as they are able to obtain a diameter of several hundred micrometers (Ghaben and Scherer, 2019). It is however controversial whether adipogenesis occurs in adult adipose tissue. As mentioned, studies have shown that the number of adipocytes stabilizes in adulthood, at the same time, there have been findings obtained in human adipose tissue showing that adipocytes undergo approximately 10% annual turnover (Spalding et al., 2008). Hence, adipogenesis occurs to some degree in adult adipose tissue, and might have a role in the pathology of obesity.

WAT holds the major energy reserve in human and its function is crucial in the regulation of the lipid metabolism. The lipid storage in WAT is in a constant state of flux between the breakdown of triglycerides, lipolysis, and the generation of new triglycerides, lipogenesis (Duncan et al., 2007). As the adipocytes become sensitive to insulin, excess nutrients are converted into triglycerides through lipogenesis (Han, 2016). A shift towards a greater rate of lipolysis occurs however during times of low energy supply, causing a release of fatty acids and glycerol into the bloodstream for use in other organs as energy source (Duncan et al., 2007). Proper adipocyte function is crucial in the regulation of the lipid metabolism and several extracellular stimuli participate in this regulation such as insulin, catecholamines, growth hormone and cytokines (Cawthorn and Sethi, 2008). Lipolysis and lipogenesis are crucial

adipocyte functions in the metabolic regulation which are regulated by several extracellular ligands.

Adipocytes and adipogenesis can be studied *in vivo*, *in vitro* and *ex vivo*. Most of what we know about adipocyte biology and adipogenesis is derived from studies performed *in vitro* (Bahmad et al., 2020). The most frequently used cell line is 3T3-L1 and is especially used in the investigation on the effects of compounds in adipogenesis, inflammation and metabolism. This immortalized cell line is cultured two-dimensional (2D) and can differentiate from fibroblasts to adipocytes (Dufau et al., 2021). Besides 3T3-L1, there are several *in vitro* models for adipogenesis, like the immortalized cell lines C3H/10T1/2, Ob17, 3T3-F442A and BFC-1. These cell lines along with 3T3-L1, are derived from mouse and are commercially available, in contrast to human cell lines which are much more limited (Dufau et al., 2021). Otherwise, *ex vivo* primary cell cultures can be used as adipocyte models to study depot- or age-dependent adipogenic mechanisms more representative of *in vivo* mechanisms. However, these are not as commonly used as the established preadipocyte lines because of the time-consuming isolation procedures, short life span in culture, and major variability (Bahmad et al., 2020). Even though 2D approaches have been highly successful in the interpretation of adipocyte biology, monolayer cell cultures often do not reflect the complexity of the adipose tissue. Therefore, 3D models could be useful and serve as an alternative for studying the complex biology in adipose tissue (Bahmad et al., 2020). Animal models are however problematic as they are both expensive, time consuming and may not completely replicate the human biology because of the species variation (Klingelhutz et al., 2018). Thus, preadipocyte cell lines from animals are ideal models for the study of adipogenesis considering they are less costly and commercially available.

During the adipogenesis assay preadipocytes, like 3T3-L1 cells are induced to differentiate into mature adipocytes. The most common protocol for adipogenesis assay throughout the literature can be divided into three segments: the preadipocyte window, the differentiation window and the maintenance (Figure 1). First, the cells grow confluent and undergo a cell cycle arrest in the preadipocyte window. During the differentiation window, the cells are exposed to an adipogenic cocktail for 2 d leading to differentiation of the cells into adipocytes. Finally, the maintenance starts when the cell culture media with the adipogenic cocktail is replaced by a media added insulin (Student et al., 1980). The adipogenic cocktail contains dexamethasone, 3-isobutyl-1-methylxantine (IBMX/MIX), insulin, and fetal bovine serum (FBS), which

stimulates the cells to develop adipocyte characteristics (Rubin et al., 1978). Dexamethasone stimulates the glucocorticoid receptor pathway and IBMX stimulates the cAMP-dependent protein kinase pathway (Rosen and Spiegelman, 2000). As the cells become sensitive to insulin during the terminal phase of differentiation, insulin activates several signaling transduction pathways and is essential for the adipocyte differentiation (Gregoire et al., 1998, Rosen and Spiegelman, 2000). Rosiglitazone is a strong PPARγ activator and promoter of adipogenesis, and is commonly utilized as a positive control (Gimble et al., 1996). Hence, during an adipogenesis assay preadipocytes are exposed to an adipogenic cocktail to stimulate the cells to develop into adipocytes and further expand by storing lipid droplets.

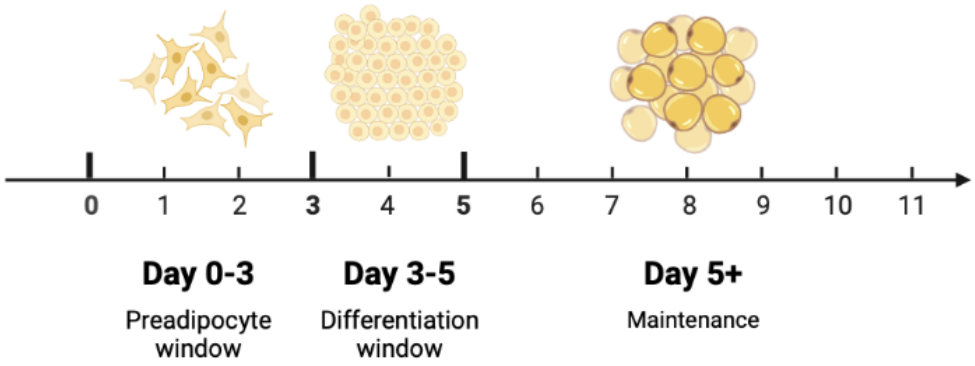

Figure 1: The three phases of adipogenesis assay: preadipocyte window, differentiation window and maintenance.

1.4 Inflammation in obese subjects

Excess nutrients in WAT may result in the release of inflammatory markers leading to infiltration of immunological cells into the tissue. An obesity induced inflammation is described as a metaflammation – a chronic mild inflammatory response initiated by excess nutrients in metabolic cells with an increased level of inflammatory markers (Gregor and Hotamisligil, 2011). An inflammation is a complex biological response which arises to maintain cell homeostasis. This includes host defense, tissue remodeling and metabolic changes. Activation of the immune system can lead to multiple mechanisms such as the recruitment and activation of immune cells, secretion of mediators and regulation of signaling pathways, and epigenetic expression (Martínez et al., 2012). As mentioned earlier, WAT is a dynamic endocrine organ producing and secreting several bioactive peptides, adipokines, including pro-inflammatory markers (Guerre-Millo, 2004). During obesity associated chronic inflammation, there is a higher level of several of these markers, which results in two major

cellular features; adipocyte expansion and infiltration of immunological cells into the adipocyte tissue (Wellen and Hotamisligil, 2003). A metaflammation therefore arises to maintain cell homeostasis and leads to several alteration in the adipocyte epigenetic expression and recruitment of immune cells.

An individual's metabolic health is thoroughly impacted by the balance of hypertrophic and hyperplasic expansion of adipose tissue. Increased size in adipocytes has been associated with insulin insensitivity and increased adipose tissue in individuals since the 1950's century (Salans et al., 1968, Krotkiewski et al., 1983). Later, studies have shown that the increasing adipocyte diameter is positively correlated with the secretion of pro-inflammatory adipokines like interleukin (IL)-6, IL-8, tumor necrosis factor alpha (TNF-α) and monocyte chemoattractant protein-1 (Skurk et al., 2007). When adipocytes increase in size, they increase the contact with neighboring cells and matrix, triggering a mechanical stress in the adipocytes. In addition, they experience hypoxia considering their size because they are reaching the limits of oxygen diffusion. These two factors of hypertrophy contribute to an inflammation which arises in the adipocyte tissue (Halberg et al., 2009). Additionally, there is evidence of impairment in adipocyte differentiation caused by the addition of pro-inflammatory markers to cultured preadipocytes (Gustafson and Smith, 2006). This forms a vicious cycle where the hypoxic state, and the mechanical stress in expanded adipocytes leads to the secretion of adipokines, leading to impairment of differentiation of adipogenic precursors.

Reactive oxygen species (ROS) are molecules containing oxygen that are highly reactive in tissues (Mehrzad, 2022). ROS are produced in cellular organs where the oxygen consumption is high, such as in the mitochondria, peroxisomes and endoplasmic reticulum (ER) (Phaniendra et al., 2015). It is not entirely clear whether there is a direct connection between ROS and obesity. Nonetheless, ROS levels in WAT increase in genetically obese mice and obesity in mice induced by high-fat diet (Furukawa et al., 2004). ROS can be generated in adipocytes during nutrient excess or by macrophages, which are accumulated in WAT in obesity (Hauck et al., 2019). When there is an imbalance between oxidants and antioxidants, oxidative stress occurs. This condition compromises the cells functions by causing damage in DNA, proteins, carbohydrates, and lipids and leading to unspecific inflammatory effects. During normal metabolism however, the mitochondria generate a low amount of ROS that are usually eliminated by intracellular antioxidant enzymes (Mehrzad, 2022). Thus, increased levels of

ROS are found in obese mice, this overload of ROS leads to oxidative stress which is damaging cell structures and can lead to unspecific inflammatory effects.

Chemicals extracted from plastic products have been demonstrated to exert a baseline toxicity and induce oxidative stress. Zimmermann et al. (2019) demonstrated several plastic extracts to exert a baseline toxicity in *A. fischeri* (Zimmermann et al., 2019). Plastic chemicals extracted from all the analyzed PVC, polyurethane (PUR) and polylactic acid (PLA), and the majority of the low-density polyethylene (LDPE) products were observed to have a high efficiency in the generation of baseline toxicity. Chemicals extracted from some of their polypropylene (PP) and polystyrene (PS) product induced baseline toxicity as well. In the same study, they demonstrated that several of their plastic extracts induced oxidative stress in a human cell line. Among these extracts, plastic chemicals from PP, PS, PUR, and PVC induced the Nrf2-ARE regulated oxidative stress response. Several of the plastic extracts used by Zimmermann et al. (2019) were further analyzed in a nontarget liquid chromatography coupled to a quadrupole of flight spectrometer (LC-QTOF-MS/MS) analysis (Völker et al., 2022a). We detected 55 300 features (e.g., unidentified chemicals) across the analyzed samples and between 6% and 33% of the features in each sample were tentatively identified. The tentatively identified chemicals were further cross-referenced against a list of known MDCs and more than half of the analyzed extracts contained between 1 to 10 MDCs. In this master thesis, we further focused on extracts from plastic consumer products of the previously conducted investigations by Völker et al. (2022a) and Zimmermann et al. (2019).

1.5 The rationale of the study

On a daily basis, we utilize plastic products containing a large amount of chemicals. In our previous study, we exposed 3T3-L1 cells to chemicals extracted from several plastic products and found several PP, PS, PVC and PUR plastic extracts promoting adipogenesis in the adipocytes (Völker et al., 2022a). The adipogenesis induction was not PPARγ mediated by most of the plastic extracts. Accordingly, we aimed to better understand the underlying mechanisms of the most potent plastic extracts and their potential harm on human health.

In the investigation of how the plastic extracts affect the adipogenesis of 3T3-L1 cells, we want to look further into when the extract exposure is the most potent. An earlier study demonstrated that MDCs could enhance the development of adipocytes and lipid storage dependent on exposure windows. The differentiation window was showed to be more sensitive for exposure

of bis(2-ethylhexyl)phthalate (DEHP) and TBT compared to the predifferentiation and maintenance window in the adipogenesis assay (Biemann et al., 2012). Finding a potential sensitive window of exposure for each extract could implicate when the plastic chemicals affect the development of adipocytes.

Further on, we want to investigate whether the 3T3-L1 cells release inflammatory markers in response to chemical exposure and potential gene alterations. The study performed by Völker et al. (2022a) revealed two characteristics associated with unhealthy adipocytes as a result of plastic extract exposure: increased adipocyte size and large lipid storage. An elevated inflammation is also a characteristic of unhealthy adipocytes, however, the inflammatory effects of the plastic extracts were not investigated. We, therefore, want to further explore whether the selected plastic extracts are promoting a shift in the development towards unhealthy adipocytes, by studying a potential cytokine release after plastic chemical exposure to 3T3-L1 cells. Finally, we want to perform an analysis of the gene expression. Based on the results obtained in Völker et al. (2022a), we know that two of the plastic extracts analyzed in this thesis activate PPARγ. To further explore which mechanisms the plastic extracts are altering, we aim to conduct a transcriptomic analysis.

Hence, in this thesis, we aimed to further study the effect of the exposure of plastic extracts on 3T3-L1 preadipocytes during the adipogenesis with the following objectives:

1. We aim to verify the results obtained in Völker et al. (2022a), confirming the adipogenic effect of the plastic extracts in the 3T3-L1 cells.

2. We want to identify whether there is a specific sensitive window of exposure in the adipogenesis, by using the most potent plastic extracts from Völker et al. (2022a).

3. We want to investigate if plastic chemicals trigger a cytokine release in 3T3-L1 cells during the adipogenesis assay.

4. We aim to better understand the underlying mechanism for the induction of adipogenesis by the plastic chemicals.

2. Methods and materials

2.1 Plastic samples and extraction

We selected six plastic extracts from our previous study (see Table 1), which induced potent adipogenic responses (Völker et al., 2022a). The petroleum-based plastic samples are made of several major polymer types on the market: PP, PS, PUR, and PVC. Plastic sample PS2 is a food contact material (FCM) in contrast to the remaining five which are products not in contact with food. To extract the polar chemicals in the plastic samples, methanol was used as a solvent, thus not dissolving the analyzed polymers.

Plastic extractions was conducted by Völker et al. (2022a) and the remaining extracts were further analyzed in this study. Given that only limited amount of extract of some of the samples (PP4, PUR3, PUR4) was available for further analysis, an additional extraction of these plastic samples was conducted. The plastic products utilized for the extraction were available from the previous study. The plastic extraction was conducted by first cutting the plastic products into 0.5–0.8 x 2 cm pieces. Foamy samples were cut to a depth of 0.5 cm. The plastic samples were placed in separate glass vials and for each 3 g of plastic 20 mL methanol was added. During the extraction, the vials were placed in an ultrasonic bath for 1 h at room temperature. The methanol was transferred into clean glass vials and dimethyl sulfoxide (DMSO) was added with a volume of 1% of the methanol. Evaporation of the methanol was carried out by placing the extracts under a gentle stream of nitrogen until the remaining volume of DMSO was reached. The plastic extracts were stored at -20°C prior to analysis. To simplify, “1 mg plastic” corresponds to the chemicals extracted from 1 mg of plastic.

Table 1: Plastic products analyzed in this study.

Sample	Polymer type	Plastic product
PS2	Polystyrene	Fruit tray
PP4	Polypropylene	Handkerchief packaging
PVC2	Polyvinyl chloride	Place mat
PVC4	Polyvinyl chloride	Floor covering
PUR3	Polyurethane	Acoustic foam
PUR4	Polyurethane	Shower slippers

2.2 Culturing of 3T3-L1

2.2.1 3T3-L1 cell line

The preadipocyte cell line 3T3-L1 is a useful *in vitro* model and can differentiate into adipocytes after induction. The 3T3-L1 cell line was isolated from mouse embryos and expanded based on their ability to accumulate lipids (Green and Meuth, 1974). The preadipocyte cell line has served as a useful *in vitro* model in the study of adipogenesis and function. Exposing the cells to the adipogenic cocktail cause an upregulation of the adipogenic gene expression program which among others increases glucose uptake and triglyceride synthesis (MacDougald and Lane, 1995).

2.2.2 Maintenance of 3T3-L1 cells

Preadipocytes were cultured in preadipocyte media (PAM) and passaged at 60-80% confluency. 3T3-L1 preadipocytes (ZenBio Inc.) were thawed at passage 9 and cultured at 37°C and 5% CO_2 in 19 mL PAM (DMEM-high glucose, 10% bovine calf serum (BCS) and 1% penicillin/streptomycin) in T75 flasks (Nunc EasYFlasks, Thermo Scientific; Tissue Culture Flask, VWR; reagents are listed in Table A1). After 24 h, the media was exchanged to remove DMSO and dead cells. When reaching 60–80% confluency, the cells were passaged. When passaging the cells, the media was removed, and the cells were rinsed with 10 mL phosphate-buffered saline (PBS, Table A2). To bring the cells into solution, 1 mL 0.05% trypsin was dispersed over the cells and the flask was incubated for 2–3 min at 37°C. The flask

was tapped to detach the cells from the surface and 9 mL PAM was added. To obtain a 1:5 dilution, 2 mL of the cell suspension was transferred to a new flask with 18 mL PAM. The following day, the media was changed to remove residual trypsin. Culturing 3T3-L1 over multiple passages can lead to a decline in differentiation efficiency (Zebisch et al., 2012), thus, cells of passage 10 were used for experiments to ensure differentiation capability.

2.3 Media comparison

A media comparison of Gibco DMEM and Sigma DMEM was conducted to investigate whether the media by different suppliers influenced the adipogenesis assay. The first and second adipogenesis experiments was conducted with Gibco DMEM cell culture media (Table 2). Because of delayed delivery, Sigma DMEM was further used. Since the Sigma DMEM has a lower L-glutamine content than Gibco DMEM, we decided to compare them. When conducting the adipogenesis assay with a media comparison, Gibco DMEM was no longer available, and BioWest DMEM was used instead as the ingredient list of Gibco and BioWest DMEM are identical.

Table 2: The supplier of the DMEM used in the preadipocyte media (PAM), differentiation media (DM) and maintenance media (MM) in the adipogenesis assay experiments with a description of the investigation.

Experiment	PAM	DM	MM	Investigating
1	Gibco	Gibco	Gibco	Critical window of exposure
2	Sigma	Gibco	Gibco	Critical window of exposure
3-5 and 8-9	Sigma	Sigma	Sigma	Critical window of exposure
6	BioWest, Sigma	BioWest, Sigma	BioWest, Sigma	Media comparison
7	Sigma	Sigma	Sigma	Immunological effects

The adipogenesis assay was performed according to the procedure described in section 2.4, with media based on BioWest DMEM and Sigma DMEM. Through the adipogenesis assay the cells were cultured in either of the two different cell culture media or Sigma DMEM added 1% L-glutamine. The cells were exposed to a dilution series of the positive control, rosiglitazone, throughout the experiment. This was done to compare the dose-response relationship of rosiglitazone in the different media types to the results from the obtained data.

2.4 Adipogenesis assay and critical window of exposure

The adipogenesis assay was conducted with 3T3-L1 preadipocytes to obtain differentiated adipocytes. The 11-day experiment include the pre-differentiation (day 1-3), differentiation (day 3-5) and maintenance (day 5-11). The assay was repeated nine times, one of the experiments were carried out to compare the cell culture media and one was conducted to obtain media samples for the immunological analysis described in section 2.5. The remaining seven experiments was conducted to study the critical window of exposure, resulting in four biological replicates for each plastic extract exposure (Table 2). The cells were exposed to a dilution series of the extracts in three windows: during the differentiation (day 3-5), maintenance (day 5-11) or throughout the assay (day 3-11). To study the critical window of exposure, each experiment included three plates seeded with preadipocytes, one plate for each of the exposure windows. This, in order to compare the adipogenic effects in the cells after exposure during the three different windows.

During the first part of the adipogenesis assay, the cells are seeded, they go through growth arrest and thereafter the adipogenic cocktail is added to the cells. In the pre-differentiation window, the preadipocytes were seeded in 96-well plates (CLS3340, Corning; Greiner Cellstar, Sigma). The number of cells in suspension was counted with flow cytometry (NovoCyte Quanteon Flow Cytometer Systems 4 Lasers, Agilent) and diluted according to their density before seeding them in three 96-well plates with a start density of 15 000 cells per well. The first day of the assay, 24 h after the seeding, we conducted a media exchange to start the 48-h growth arrest period, whereby the cell growth was inhibited by cell-cell contact.

In the following 48 h (day 3-5), the differentiation window started when PAM was replaced by 200 mL differentiation media $well^{-1}$ (DM: DMEM-high glucose, 10% fetal bovine serum (FBS), 2% HEPES, 1% penicillin/streptomycin, 1 μg mL^{-1} human insulin, 0.8 M IBMX and 6.25 nM dexamethasone). In addition to the differentiation media, the plastic extracts were added to the two 96-well plates exposed throughout and during the differentiation window. The extracts and positive control were diluted in the differentiation media, in a dilution series prior to cell exposure. The highest concentration of rosiglitazone was prepared by adding 1.2 μL of 300 μM rosiglitazone to 1198.8 μL media, obtaining a 1:1000 dilution. In the further successive steps of the dilution series rosiglitazone was diluted 1:4 resulting in concentrations of 1.17,

4.68, 18.75, 75 and 300 nM. The plastic extracts were first diluted 1:1000 by adding 1.8 µL of 15 mg μl^{-1} plastic extract to 1798.2 µL media and further diluted 1:2 in the dilution series resulting in concentrations 0.1875, 0.375, 0.75, 1.5 and 3 mg $well^{-1}$ (200 µL media per well). The plastic extracts and rosiglitazone are solved and diluted respectively, in DMSO, and it was therefore utilized as solvent control (SC). The SC was diluted 1:1000 in the respective media before added to the cells. A negative control (NC) was also included in each plate, where four wells were added PAM throughout the assay.

Maintenance of the cells started at day 5, whereby the media was exchanged every other day until fixation at day 11. After the differentiation window, the media was replaced by 200 µL maintenance media $well^{-1}$ (MM: DMEM-high glucose, 10% FBS, 2% HEPES, 1% penicillin/streptomycin and 1 μg mL^{-1} human insulin). The maintenance media contained the plastic extracts, rosiglitazone or DMSO according to the mentioned dilutions in the plates designated for the exposure during the maintenance phase or throughout the experiment. During the following six days of maintenance the media was exchanged every other day. On day 11, the media was removed, the cells were rinsed twice with PBS and fixed with 50 mL 2% paraformaldehyde $well^{-1}$ for 15 min on ice. The cells were further rinsed twice with PBS and stored over night at 4°C prior to staining. The following day, the PBS was removed and 100 mL $well^{-1}$ of a NucBlue and NileRed staining solution (19.5 mL PBS, 500 µL AdipoRed and 1 drop NucBlue mL^{-1}) was added to the cells for 40 min in the dark at room temperature. The staining solution was removed, and the cells were rinsed with PBS. The fixed and stained adipocytes were stored in 200 mL PBS $well^{-1}$ at 4°C prior imaging. Short time after the staining was carried out, the imaging was executed using a Cytation 5 Cell Imaging Multimode reader (BioTek). Autofocus was used to select the image plane, and three images was captured per field (Brightfield, NucBlue and NileRed) with nine fields per well. NucBlue staining was detected by a 365 LED with DAPI filter cube (Ex 377/50, Em 477/60), and a 523 LED with RFP filter cube (Ex 531/40, Em 593/40) for NileRed.

2.5 Immunoassay

We investigated whether the plastic extracts promote an inflammatory effect in the adipocytes after exposure throughout the adipogenesis assay, by conducting an immunoassay. We hypothesized whether there was a cytokine release during the differentiation or if it increased during the assay. From an adipogenesis assay where the cells were exposed to the plastic extract

throughout the experiment (experiment 7), we aspirated the media on the first day after the differentiation window (day 5) and the last day of the experiment (day 11). The sampled media was analyzed in an enzyme-linked immunosorbent assay (ELISA). The media samples were stored separately at -80°C prior to the quantification of released IL-6 and TNF-α. The immunoassay was repeated for sample PS2, PVC4, PUR4, the SC and rosiglitazone with aspirated media from experiment 8.

The ELISA was conducted shortly after the adipogenesis assay ended using ELISA Mouse IL-6 DuoSet kit and ELISA Mouse TNF-α DuoSet kit both from R&D systems according to the manufacturer's instructions (Appendix). In short, a 96-well plate was initially coated with the respectively IL-6 or TNF-α Goat Anti-Mouse Capture Antibody overnight. The plate was then blocked to cover the remaining binding surfaces before addition of the media samples and the dilution series of IL-6 or TNF-α Recombinant Mouse Standard. Instead of a 2-h incubation at room temperature, the plate was incubated at 4°C overnight to increase the probability of substrate binding. The next day, IL-6 or TNF-α Biotinylated Goat Anti-Mouse Detection Antibody was added, followed by streptavidin conjugated to horseradish-peroxidase. The substrate solution and stop solution was added respectively before determining the optical density using a Cytation 5 Cell Imaging Multimode reader (BioTek) at 450 nm and at 540 nm for wavelength correction.

2.6 Transcriptomics

To achieve a greater understanding of the mechanisms by which the plastic extracts induce adipogenesis, we chose to conduct quantitative polymerase chain reaction (qPCR). To include further plastic samples and to verify the altered gene expression observed in an unpublished RNA sequencing conducted prior to the thesis, a qPCR was carried out. Six genes of interest were selected based on the results of the RNA sequencing. Prior to the RNA sequencing, the adipogenesis assay was conducted and the cells were exposed to PP4, PS2, PVC2, PVC4 and PUR4 throughout the experiment. At day 11, the cells were lysed by applying Invitrogen's Trizol reagent according to their procedure. RNA from the adipocytes exposed to PP4, PUR4 and PVC2, as well as the positive control and SC, was further extracted, quality-tested using a Nanodrop (NanoDrop One/One^{c} Microvolume UV-Vis Spectrophotometer, ND-ONE-W, Thermo Scientific) and Bioanalyzer (2100 Bioanalyzer instrument, Agilent), and further

sequenced. Adipocytes exposed to the two remaining plastic extracts, PS2 and PVC4, were stored in Trizol for 10 months.

2.6.1 RNA extraction

RNA from adipocytes exposed to PS2 and PVC4 was extracted using Qiagen's RNeasy mini kit, likewise as in the sequenced samples. The applied protocol is a combination of the TRIzol and the mini kit procedures (Appendix). The TRIzol samples were first added to chloroform, which causes a phase separation that separates the proteins (organic phase) and the DNA (interphase) from the RNA remaining in the aqueous phase (Rio et al., 2010). The aqueous phase was removed, and ethanol added, further the RNA was extracted according to the mini kit procedure. Finally, the RNA was resuspended in 30 µL RNAse free water, and the concentration and purity of the RNA was measured by NanoDrop One/One^c Microvolume UV-Vis Spectrophotometer (ND-ONE-W) from Thermo Scientific. The four samples containing the highest RNA concentration and with an A260/280 absorption ratio >1.7 were further used for cDNA synthesis. In prior to further analysis, the RNA samples were stored at -80°C.

2.6.2 cDNA synthesis

Reverse transcription was performed on all five RNA samples, the positive control, and the SC. Before the reverse transcription, the RNA samples were diluted based on the NanoDrop results to obtain the same RNA concentration. QuantiTect Reverse Transcription Kit from Qiagen was used for the reverse transcription and conducted according to their protocol. Genomic DNA was first eliminated before the reverse transcription mix was added to the RNA and incubated in a T1000 Thermal Cycler from Bio Rad at 42°C in 42 min and 3 min at 95°C. The cDNA samples were stored at -20°C in prior to qPCR.

2.6.3 qPCR

The qPCR analysis was performed on the cDNA samples with the selected primer sequences (Table 3). The analysis was conducted using LightCycler 480 SYBR Green I Master and LightCycler 96 Instrument from Roche. The qPCR was carried out according to Roche's protocol by first diluting the cDNA samples 1:10 and further adding each sample in a qPCR 96-well plate along with the selected primers mixed with the SYBR Green mix. The qPCR program is listed in Table 4. The cDNA samples were analyzed twice with the primers for *Ywhaz, Gapdh, Fabp4* and *Enpp2.*

Table 3: Primers with their respective sequences used for qPCR.

Gene	Sequence	Function
Mouse Enpp2	Forward 5' CTGTCTTTGATGCTACTTTCC	Target gene
	Reverse 5' TCACAGACCAAAAGAATGTC	
Mouse Serpinb6a	Forward 5' ACTGAGTACAGTGGAAAAGG	Target gene
	Reverse 5' CATGTTGTAATTCTCCTCCAG	
Mouse Amotl2	Forward 5' AGAAGACCATGAGGAACAAG	Target gene
	Reverse 5' TTCCAATCTCTCTCTAAGGTC	
Mouse Manf	Forward 5' CAAGATCATCAATGAGGTGTC	Target gene
	Reverse 5' GGATCTTCTTCAGCTCTTTC	
Mouse Ppap2b	Forward 5' AGGGCTACATTCAGAACTAC	Target gene
	Reverse 5' GAAGGTAGAGCACCAGATAC	
Mouse Tcf21	Forward 5' ATTCACCCAGTCAACCTG	Target gene
	Reverse 5' AGGATGCTGTAGTTCCAC	
Mouse Slc2a1	Forward 5' AAGTCCAGGAGGATATTCAG	Reference gene
	Reverse 5' CTACAGTGTGGAGATAGGAG	
Mouse Cfd	Forward 5' TTTAAGCTATCCCAGAATGC	Reference gene
	Reverse 5' GATTGACACTCTGAGTTGATG	
Mouse Pparg	Forward 5' AAAGACAACGGACAAATCAC	Reference gene
	Reverse 5' GGGATATTTTGGCATACTCTG	
Mouse Fabp4	Forward 5' GTAAATGGGGATTTGGTCAC	Reference gene
	Reverse 5' TATGATGCTCTTCACCTTCC	
Mouse Gapdh	Forward 5' TGCACCACCAACTGCTTAGC	Housekeeping gene
	Reverse 5' GGATGCAGGGATGATGTTCT	
Mouse Ywhaz	Forward 5' ACTTAACATTGTGGACATCG	Housekeeping gene
	Reverse 5' GGATGACAAATGGTCTACTG	
Mouse Nono	Forward 5' CTTCTTGCTGACTACATTTCC	Housekeeping gene
	Reverse 5' CATACTCATACTCAAAGGAGC	
Mouse Rn18s	Forward 5' CAGTTATGGTTCCTTTGGTC	Housekeeping gene
	Reverse 5' TTATCTAGAGTCACCAAGCC	

Table 4: qPCR program run by the LightCycler 96 Instrument

Stage	Degrees	Time	Degrees/s ramp rate
Preincubation	95	5 min	4.4
Amplification (45 cycles)	95	10 s	4.4
	55	10 s	2.2
	72	10 s	4.4
Melting	95	5 s	4.4
	65	1 min	2.2
	97	Cont.	0.11
Cooling	40	10 s	1.5

2.7 Data analysis

2.7.1 Adipogenesis assay and critical window

The images captured by the Cytation 5 Cell Imaging Multimode reader were analyzed by a Cell profiler pipeline available at Zendo (Völker et al., 2022b). The pipeline distinguishes cells in the images based on the identified nuclei stained with NucBlue. Lipid droplets were identified in the NileRed images, and both the cells and the lipid droplets were counted. The lipid content in each cell was measured, and adipocytes and mature adipocytes were identified. The adipocytes were defined as a cell containing at least one lipid droplet and the mature adipocyte had a lipid droplet area ≥ 1000 pixels, which is equivalent to ≥8 average lipid droplet. In addition, the total area occupied by the lipid droplet was measured as well as the average intensity of the NileRed staining. The pipeline was not able to distinguish the nuclei in the cells from the first experiment because of weak NucBlue staining. The cell counting data (cell count, adipocyte count, mature adipocyte count) was therefore not further analyzed. In addition, the lipid staining in experiment 3 and 4 was too bright in the images for the pipeline to distinguish the lipid droplets, which resulted in an unrepresentative output. The lipid quantification data (lipid droplet count, total area of lipid droplets, and total intensity) was therefore excluded from the further analysis. Otherwise, the nuclei count was used to evaluate the cytotoxicity of the plastic extracts. The threshold of cytotoxicity was a nuclei count <20% compared to the SC. If cytotoxicity occurred, this part of the data set was not further analyzed.

The adipogenic effects were analyzed in GraphPad Prism, version 9.1.2 (226). The concentration was first transformed using the decadic logarithm and then fitted using a four-parameter logistic regression (Equation 1):

$$Y = P_F + \frac{\Delta P}{1+10^{(Log(EC50)-X)*m}} \quad (1)$$

P_F represents the floor plateau on the Y axis, ΔP is the difference between the ceiling plateau and the floor plateau, EC50 presents the half-maximal effective concentration and m is the hill slope.

The dose response relationships were normalized to be in a range from the lowest mean value (0%) and highest mean value (100%) of rosiglitazone (throughout exposure) in each endpoint (Equation 2):

$$Y = \frac{x - min(x)}{\max(x) - \min(x)} * 100 \quad (2)$$

Y is the normalized value of x, min(x) represents the lowest mean value in the throughout exposure of rosiglitazone and max(x) is the highest mean value from the throughout exposure of rosiglitazone. The two last mentioned variables are dependent on which endpoint x is obtained from.

2.7.2 Immunoassay

Results from the immunoassay were analyzed in GraphPad Prism, version 9.1.2 (226). The cytokine concentrations in the standard samples were analyzed with a four-parameter logistic curve (Equation 1). The measured optical density in the analyzed media samples were interpolated according to the standard curve. Responses outside the range of the standard curve were excluded from the dataset. The samples with a higher response than the range of the standard curve was diluted and tested again. A one-way ANOVA was used to determine whether there was a statistically significance between cytokine release caused by the SC and the plastic extracts.

2.7.3 Transcriptomics

LinRegPCR (version 2017.1) and qbase+ (version 3.2) were used to analyze the amplification curves generated by LightCycler 96 (Ruijter et al., 2009). In LinReg, the qPCR efficiency and Ct values was calculated based on the amplification curves. These values were then statistically analyzed in qbase+, by scaling the values to the SC and normalize them to *Ywhaz* from the second experiment.

3. Results

3.1 Comparison of the impact of different cell culture media

A media comparison was conducted to identify the impact of L-glutamine on the 3T3-L1 adipogenesis assay. At the time the adipogenesis assays were carried out, there was a shortage in supply of Gibco cell culture media, and it was therefore replaced by Sigma cell culture media which contained a lower level of L-glutamine than the Gibco media. To ensure comparability of the obtained data we decided to compare the impact of the different cell culture media on the adipogenesis assay. Since the Gibco media was not available when conducting the media comparison, BioWest cell culture media was used instead of Gibco. The ingredient list in BioWest media was identical to the Gibco media, the BioWest media was however beyond its expiration date. The impact of cell culture media with different L-glutamine content in the cells was therefore investigated to ensure comparability of the obtained data.

In general, the cell count (CC) and lipid droplet count (LDC) in the different media treatments were very similar (Figure 2). Rosiglitazone exposure in BioWest media caused a similar CC and LDC dose-response relationship in the cells as the Sigma media from the media comparison. Overall, these two media caused a slightly lower CC and LDC dose-response relationships than the Sigma media combined of all experiments. However, in the highest concentration of rosiglitazone the three mentioned media treatments caused a CC of approximately 600 cells per field, and it resulted in approximately 2300 LDC per field in the cells. Sigma media with added glutamine displayed both a lower CC and LDC in the adipocytes, reaching 500 cells per field and 1500 lipid droplets per field. Dose response-relationships for the remaining four endpoints can be found in Appendix (Figure A.1). The addition of glutamine did not improve the response of the assay but rather reduced it. Thus, the glutamine addition was not a relevant factor. The treatment with Sigma media resulted in a slightly higher response compared to BioWest. Also considering that the BioWest media was expired, we used Sigma media for the main experiments in this thesis.

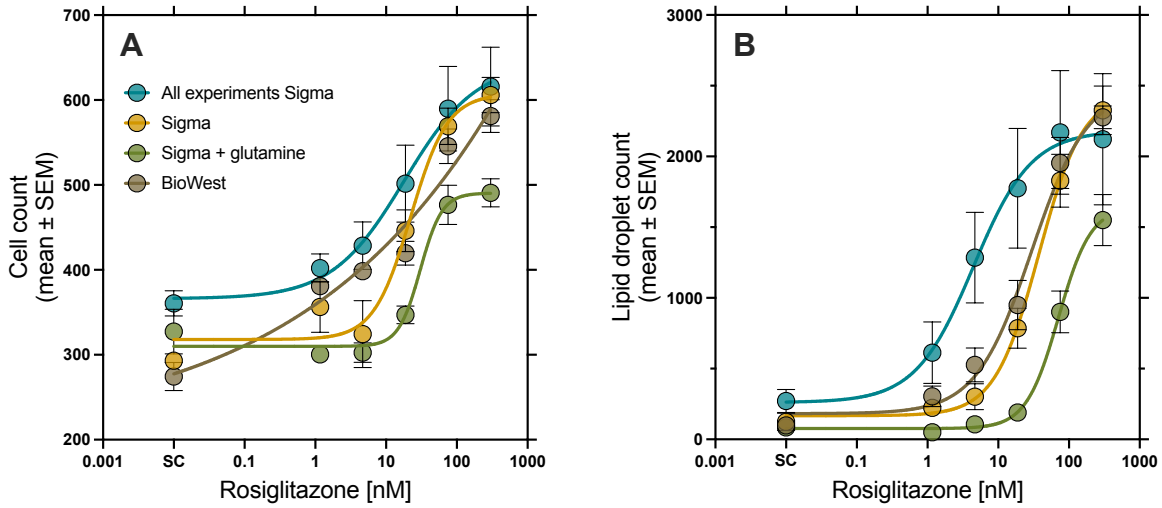

Figure 2: Impact of different cell culture media on 3T3-L1 cells exposed to rosiglitazone throughout the adipogenesis assay. The media comparison was carried out with Sigma media, Sigma media with added glutamine and BioWest media and compared to the average of all the experiments using Sigma media. The effect of the different media was estimated through A) cell count and B) lipid droplet count, with graphs fitted with a four-parameter logistic regression. The results are present as mean of four technical replicates ± SEM, not including the data representing the average of all experiments using Sigma media. The dots in the cell count (N = 7) and lipid droplet count (N = 6) graphs represent the mean ± SEM, where the biological replicates (N) are averages of the four technical replicates from each experiment.

3.2 Effect of plastic chemicals on adipogenesis

In our previous study, we demonstrated that chemicals extracted from several plastic products induced adipogenesis and thereby being similar or even more potent than the positive control rosiglitazone (Völker et al., 2022a). Under standard experimental conditions, the 3T3-L1 cells differentiate into adipocytes and increased their storage of lipid droplets. When the cells are exposed to rosiglitazone or a plastic extract throughout the assay there is an increased adipogenic effect resulting in more and larger adipocytes. The objective was to identify a critical window of exposure in the adipogenesis assay and in that occasion the reproducibility of our earlier results was also reviewed.

Throughout exposure of rosiglitazone and plastic extract exposure are promoting the adipogenesis in 3T3-L1 cells during the adipogenesis assay. Dependent on the dose of rosiglitazone the number of adipocytes increased (Figure 3). The highest concentration of rosiglitazone caused a mean adipocyte count (AC) of 327 adipocytes per field while the SC caused an AC of 47 per field. Among the plastic extracts, the chemicals extracted from PP4, PVC2 and PVC4 induced the greatest adipogenic effect in the cells, with an AC between 400 and 500 per field (Figure 4). PUR3 exposure was cytotoxic in the three highest concentrations.

Despite this, the highest AC caused by the highest non-cytotoxic concentration (HNC) of PUR3 was equivalent to the effect of the third highest concentration of rosiglitazone to the cells (more details regarding the highest non cytotoxic concentration in Table A.3). Finally, the highest PS2 and PUR4 concentration caused the lowest adipogenic effect in the cells, resulting in an AC of approximately 110 adipocytes per field. In general, the greatest adipogenic effect was observed in the cells exposed to PP4, PVC2 and PVC4, and the lowest AC was observed in the cells exposed to PS2 and PUR4.

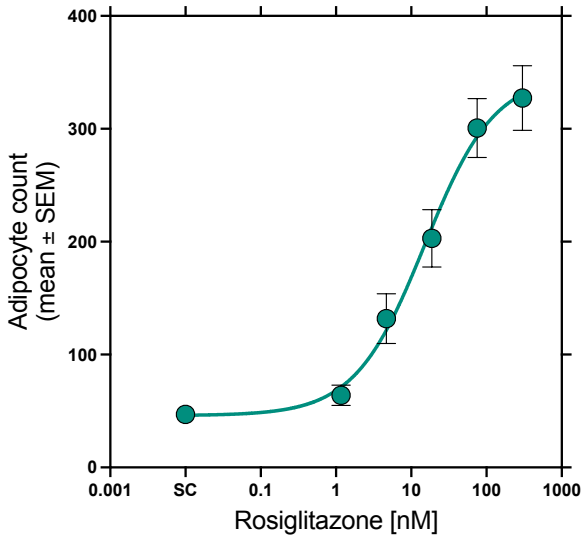

Figure 3: The effect of rosiglitazone on the adipocyte count in 3T3-L1 cells exposed throughout the adipogenesis assay. The adipocyte counts (N = 5) are fitted with a four-parameter curve where the dots represent the mean ± SEM. The biological replicates (N) are averages of the four technical replicates from each experiment.

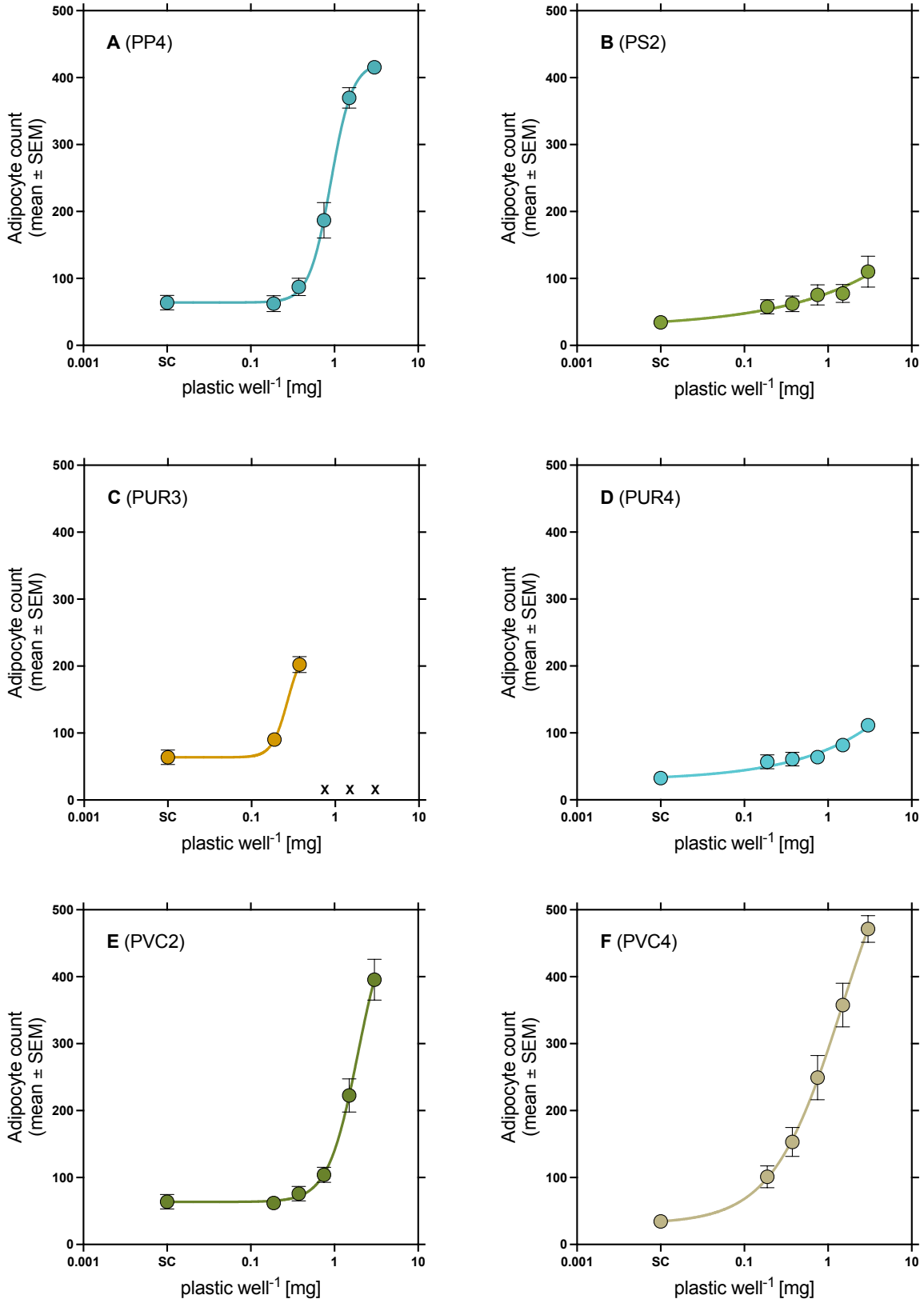

Figure 4: The effect of plastic extracts on the adipocyte count in 3T3-L1 cells exposed throughout the adipogenesis assay. The adipocyte counts are fitted with a four-parameter logistic regression. The average adipocyte count ± SEM is illustrated with the dots with A) PP4 (N = 2), B) PS2 (N = 3), C) PUR3 (N = 2), D) PUR4 (N = 3), E) PVC2 (N = 2) and F) PVC4 (N = 3). The biological replicates (N) are averages of the four technical replicates from each experiment. The x in the PUR3 graph marks cytotoxic concentrations.

3.3 Effect of exposure during different windows of adipogenesis

When conducting the adipogenesis assay, the cells were either exposed in different windows of exposure to compare the impact of plastic chemical exposure on the distinct stages of adipogenesis. During the assay the 3T3-L1 cells were exposed to one of the six plastic extracts either during the differentiation (day 3-5), the maintenance (day 5-11) or throughout (day 3-11) (Figure 1) to identify the most sensitive stages to plastic chemical exposure during adipogenesis. Their effect on the cells was determined via six endpoints: cell count, adipocyte count, mature adipocyte count, lipid droplet count, total intensity, and total area of lipid droplets.

3.3.1 Effect on proliferation and differentiation of adipocytes

Comparing the proliferative and differentiation effects after the exposure in different windows of adipogenesis, the throughout exposure of 3T3-L1 cells to the plastic extracts resulted in the highest CC per field (Figure 5). In general, the strongest effect on the CC was observed after throughout extract exposure, while the exposure during the differentiation and maintenance phase caused a lower proliferation and differentiation. The preadipocyte number remained stable independently of the exposure. These tendencies were also observed in the positive control, rosiglitazone. Here, the proliferation and differentiation were highest in the cells after the throughout exposure, reaching approximately 650 cells per field. Further on, the exposure during the differentiation caused a CC at 550 cells per field and the exposure during the maintenance resulted in 500 cells per field. The CC dose-response relationships from the rosiglitazone exposure to the cells support this trend and the same was observed for the AC (Figure 6). Compared to the plastic extracts, rosiglitazone had a lower proliferative and differentiation effect than PP4, PVC2 and PVC4. However, the effect of throughout rosiglitazone exposure to the cells was similar to the PUR3 throughout exposure and even greater than the effect of the throughout exposure of PS2 and PUR4 to the cells. The results from the exposure of rosiglitazone to the cells suggest that the cells proliferate and differentiate to a greater extent when exposed throughout the assay compared to exposure during the differentiation and maintenance window. Further on, the proliferation and differentiation in the cells exposed to the plastic extracts were affected to different extents dependent on the exposure.

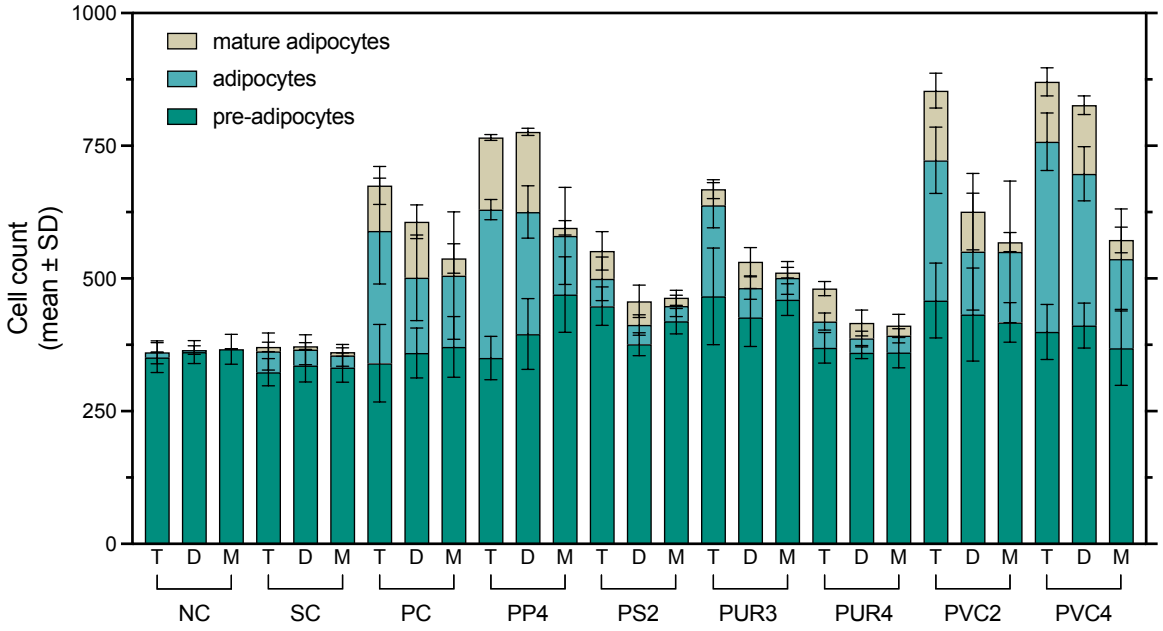

Figure 5: Effect of rosiglitazone (PC) and plastic extracts on the number of preadipocytes, adipocytes, and mature adipocytes in 3T3-L1 cells exposed either throughout the experiment (T), during differentiation (D) or during maintenance (M). The cell numbers (mean ± SD) are obtained from the highest non-cytotoxic concentration of the extracts (details in Table A.3). The biological replicates are as follows: NC, SC and PC (N = 5), PP4, PVC2 and PUR3 (N = 2), PS2, PVC4, PUR4 (N = 3).

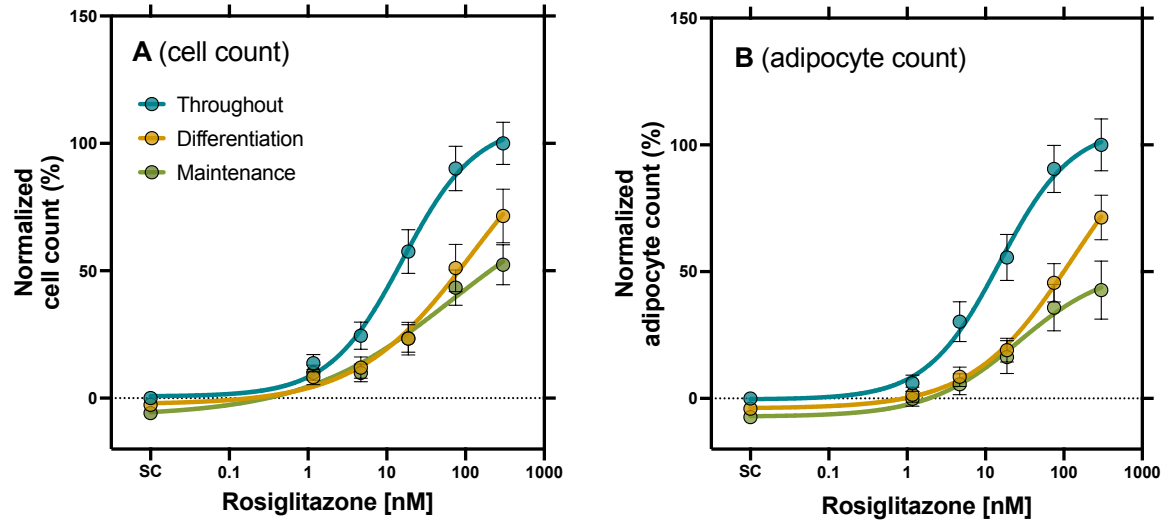

Figure 6: Effect of rosiglitazone exposure on the A) cell count (N = 7) and B) adipocyte count (N = 5) in 3T3-L1 cells exposed either throughout the experiment, during the differentiation or during the maintenance. The mean cell count and adipocyte count ± SEM are fitted with a four-parameter logistic regression and normalized to the rosiglitazone throughout exposure data. Biological replicates (N) are a mean of the four technical replicates from each experiment.

Several similar effects were observed between the different plastic extracts dependent on the window of exposure. PP4 exposure resulted in a comparable CC after exposure throughout the assay and during the differentiation (Figure 7). The maintenance exposure was causing a lower CC, than the two other exposure windows, the CC was however increasing with the dose. The exposure of PS2 resulted in a similar CC after exposure during the differentiation and maintenance window of the assay. The throughout exposure of this extract caused a higher CC, approximately 65% of the effect of the throughout exposure of rosiglitazone to the cells. Similar to PS2, exposure of the PUR3 and PUR4 extract to the cells resulted in a comparable effect of exposure during the differentiation and maintenance window of the assay (Figure 8). Additionally, the throughout exposure of PUR3 and PUR4 caused a higher CC than the two other exposure windows. Throughout exposure of PVC2 caused a higher CC than the two other windows of exposures, like the effects of the exposure of PS2, PUR3 and PUR4 to the cells during the adipogenesis assay (Figure 9). PVC4 exposure caused a similar effect as the PP4 exposure to the cells; the exposure throughout the assay and during the differentiation caused a comparable CC higher than the maintenance exposure. To summarize, the throughout and differentiation PP4 and PVC4 exposure to the cells caused a similarly high proliferation and differentiation, the PS2 and PUR4 exposure caused a generally low proliferation and differentiation and along with PUR3 and PVC2 they caused the highest CC after throughout exposure of the cells.

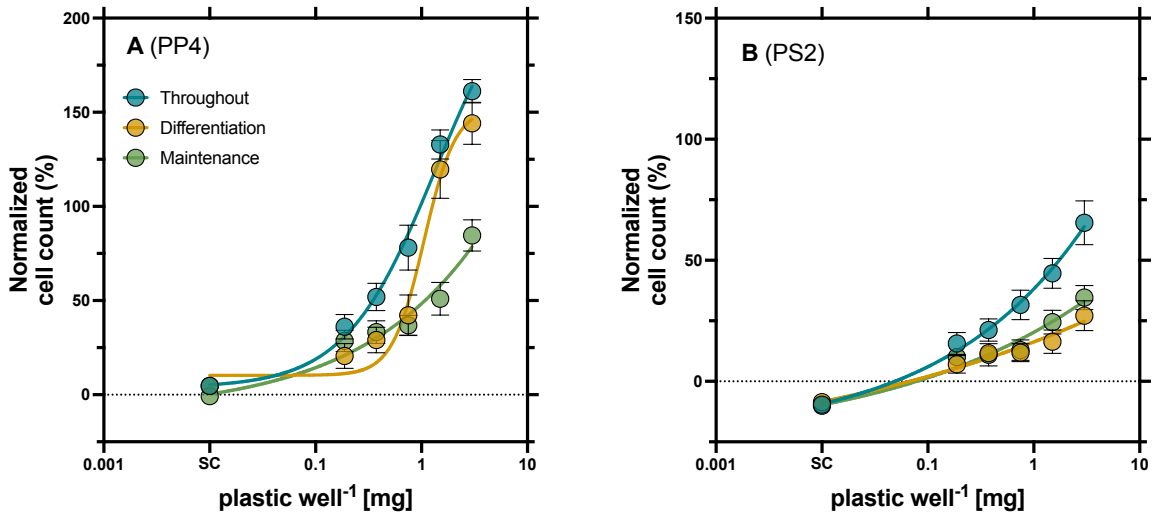

Figure 7: The effect of exposure of 3T3-L1 cells to A) PP4 (N = 3) and B) PS2 (N = 4) on the average cell count ± SEM during three windows of exposure. The data is fitted with a four-parameter logistic regression and normalized to the throughout exposure of rosiglitazone. The biological replicates (N) are a mean of the four technical replicates from each experiment.

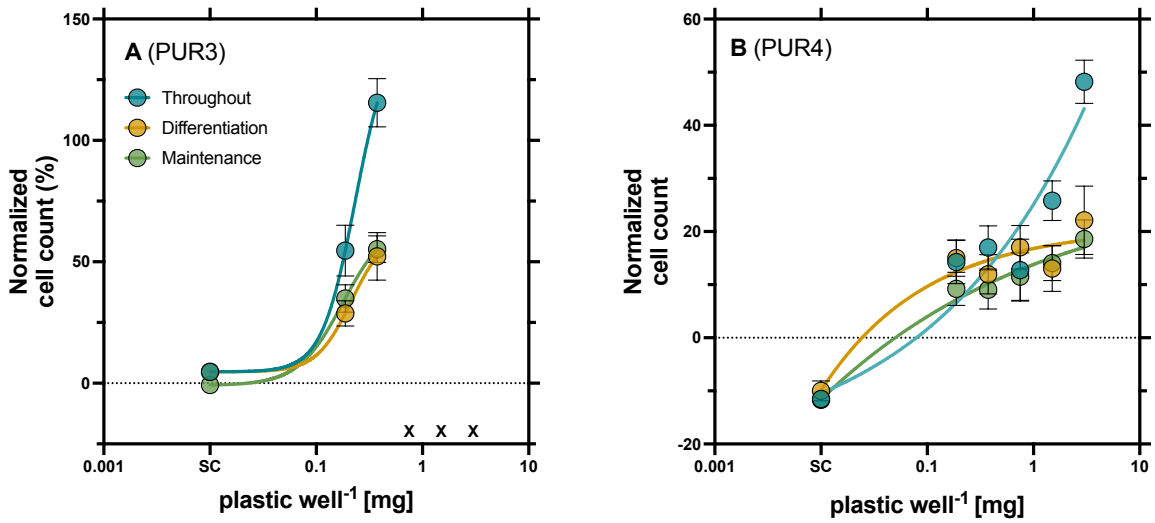

Figure 8: The effect of exposure of 3T3-L1 cells to A) PUR3 (N = 3) and B) PUR4 (N = 4) on the average cell count ± SEM during three windows of exposure. The data is fitted with a four-parameter logistic regression and normalized to the throughout exposure of rosiglitazone. The "x" in the PUR3 graph represent the analyzed cytotoxic concentrations (further details in Table A.3). The biological replicates are a mean of four technical replicates from each experiment.

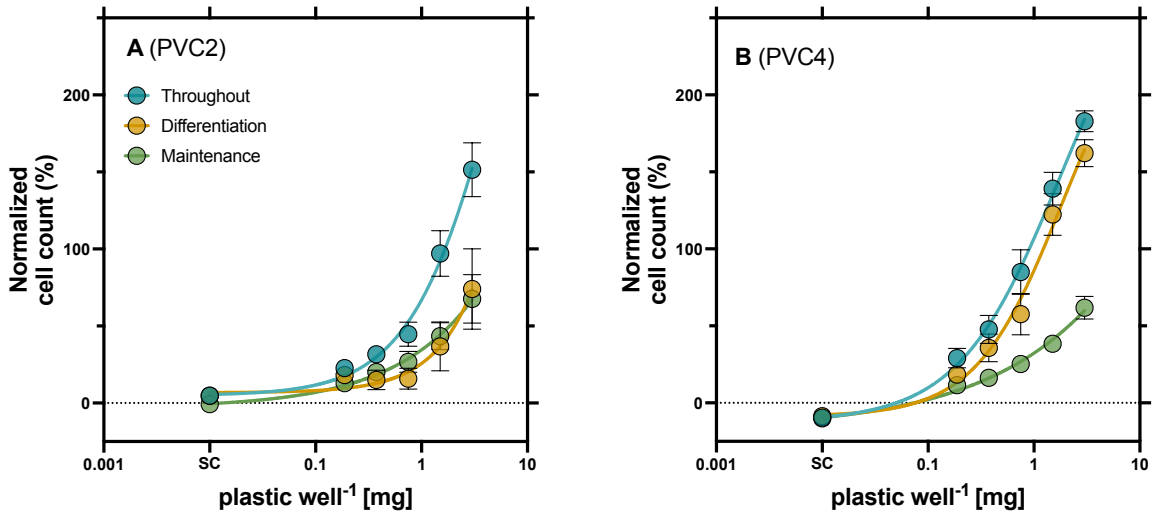

Figure 9: The effect of exposure of 3T3-L1 cells to A) PVC2 (N = 3) and B) PVC4 (N = 4) on the average cell count ± SEM during three windows of exposure. The data is fitted with a four-parameter logistic regression and normalized to the throughout exposure of rosiglitazone. The biological replicates (N) are a mean of four technical replicates from each experiment.

3.3.2 Effect on lipid accumulation

As the adipocytes develop into mature adipocytes, they store lipids and increase in size. Exposure of the adipocytes to rosiglitazone during the differentiation window resulted in the highest lipid accumulation, while the exposure during the maintenance caused a significantly lower lipid content (Figure 10). The lipid accumulation in the cells exposed to rosiglitazone during the maintenance window was lower than 50% of the effect of the throughout exposure

of rosiglitazone. At the same time, the lipid accumulation in the cells exposed through the differentiation window was approaching 150% of the lipid accumulation caused by the exposure throughout the assay. The dose response relationships indicates that the differentiation window is a further sensitive window of exposure by the highest concentrations of rosiglitazone, compared to the exposure during the maintenance and throughout.

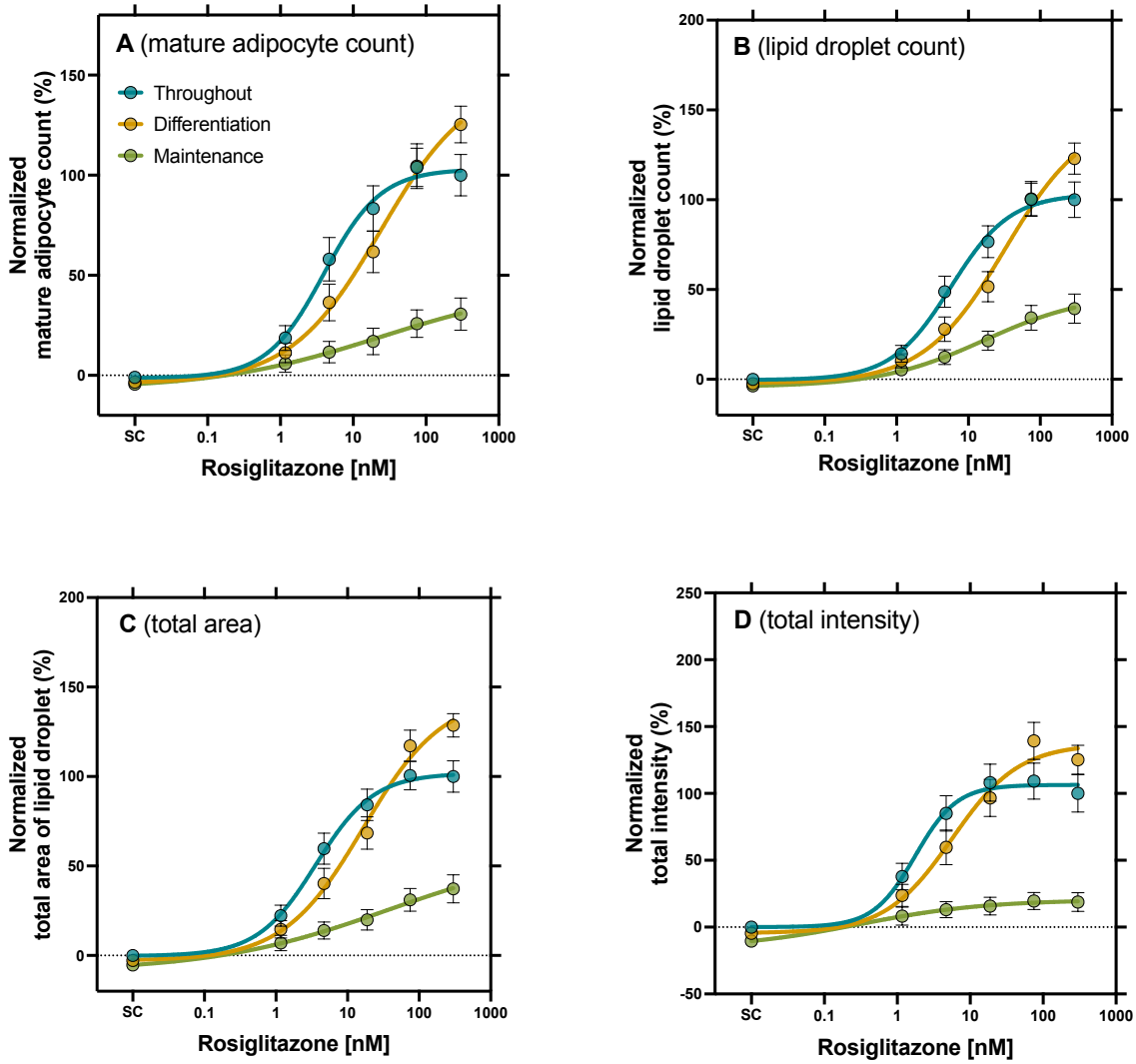

Figure 10: Effect of the exposure of rosiglitazone to 3T3-L1 cells in three windows of exposure on the A) mature adipocyte count (N = 5), B) lipid droplet count (N = 6), C) total area of lipid droplets (N = 6) and D) total intensity of the NileRed staining (N = 6), which are analyzed per field. The mean ± SEM are fitted with a four-parameter logistic regression and normalized to the throughout exposure of rosiglitazone. The biological replicates (N) are an average of four technical replicates from each experiment.

The exposure of PP4 and PS2 throughout and during differentiation window resulted in a comparable LDC for each of the extract (Figure 11). PP4 exposure throughout the assay and during the differentiation window resulted in a higher LDC than exposure of rosiglitazone. Both exposure windows caused a similar dose-response relationship curve reaching

approximately 125% of the throughout exposure of rosiglitazone. Exposure during the maintenance caused a lower effect than the two other exposure windows, however the LDC increased with the concentration of PP4. As for PP4, the throughout and differentiation exposure of PS2 was following a similar dose response relationship. Exposure of the highest concentration of PS2 did however only reach ca. 50% of the LDC obtained after throughout exposure of rosiglitazone. The maintenance exposure to the cells did not alter the LDC in response to the increasing concentration of PS2 and the obtained LDC was approximately 15% of the effect of throughout exposure of rosiglitazone.

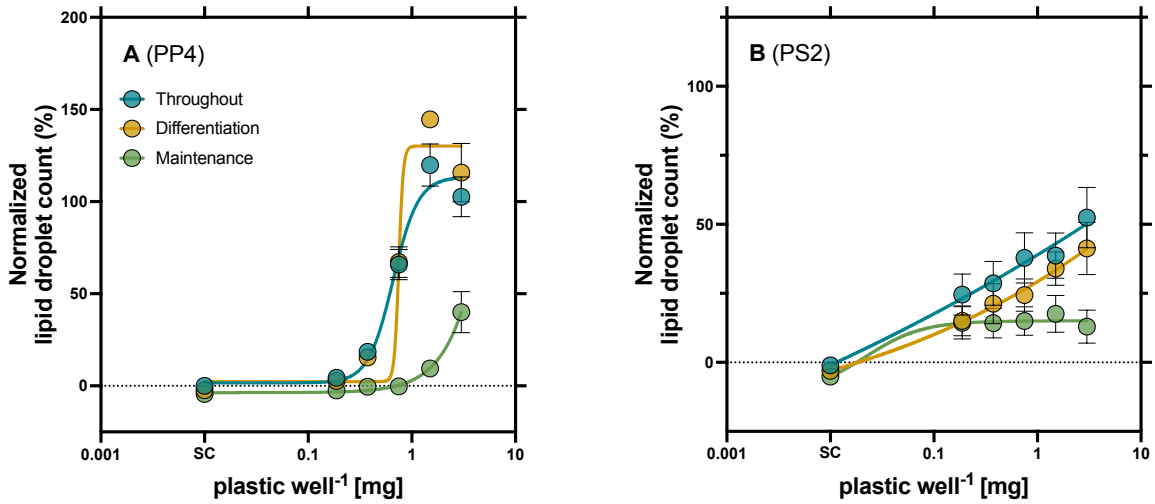

Figure 11: The effect of exposure of 3T3-L1 cells to A) PP4 (N = 3) and B) PS2 (N = 3) in three different windows on the lipid accumulation. The average lipid droplet counts ± SEM are fitted with a four-parameter logistic regression and normalized to the throughout exposure to rosiglitazone. The biological replicates (N) are a mean of the four technical replicates from each experiment.

Exposure of 3T3-L1 cells to the HNC of PUR3 and PUR4 throughout the assay and during the differentiation window caused a higher LDC compared to exposure during the maintenance (Figure 12). In general, PUR3 and PUR4 extracts at the HNC caused a lower LDC in the cells than rosiglitazone and resulted in 32% and 68%, respectively, of the LDC after throughout exposure of rosiglitazone. The maintenance exposure caused the lowest effect on the lipid accumulation and resulted in 0.25% and 15.4% of the LDC caused by the throughout rosiglitazone exposure. The three highest analyzed concentrations of PUR3 were cytotoxic to the cells in all three windows of exposure (further details on HNC in Table A.3). The effect of PUR3 and PUR4 on lipid accumulation in the cells was in total lower than rosiglitazone, while the effect of the maintenance exposure window was lower compared to the throughout and differentiation window.

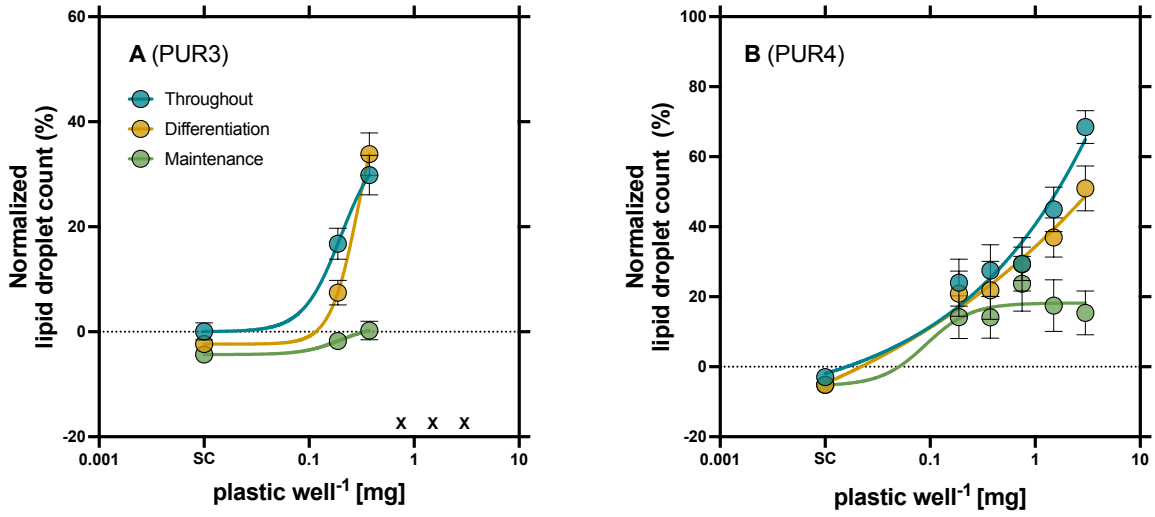

Figure 12: The effect of A) PUR3 (N = 3) and B) PUR4 (N = 3) exposure in three different windows on the lipid accumulation in 3T3-L1 cells. The average lipid droplet counts ± SEM are fitted with a four-parameter logistic regression and normalized to the throughout exposure to rosiglitazone. The "x" in the PUR3 graph represent the analyzed cytotoxic concentrations of PUR3. The biological replicates (N) are a mean of four technical replicates obtained in each experiment.

The two PVC extracts induced a high lipid accumulation in 3T3-L1 cells during the throughout and differentiation window (Figure 13). The LDC after exposure to PVC2 and PVC4 was close to 150% of the effect of throughout rosiglitazone exposure. PVC2 caused the greatest effect on the lipid accumulation after exposure throughout the assay, while PVC4 exposure caused a higher LDC after exposure to the cells during the differentiation window. The effect of PVC exposure through the maintenance window was significantly lower than exposure throughout the assay and during the differentiation, comparable with the effect of rosiglitazone and the other plastic extracts.

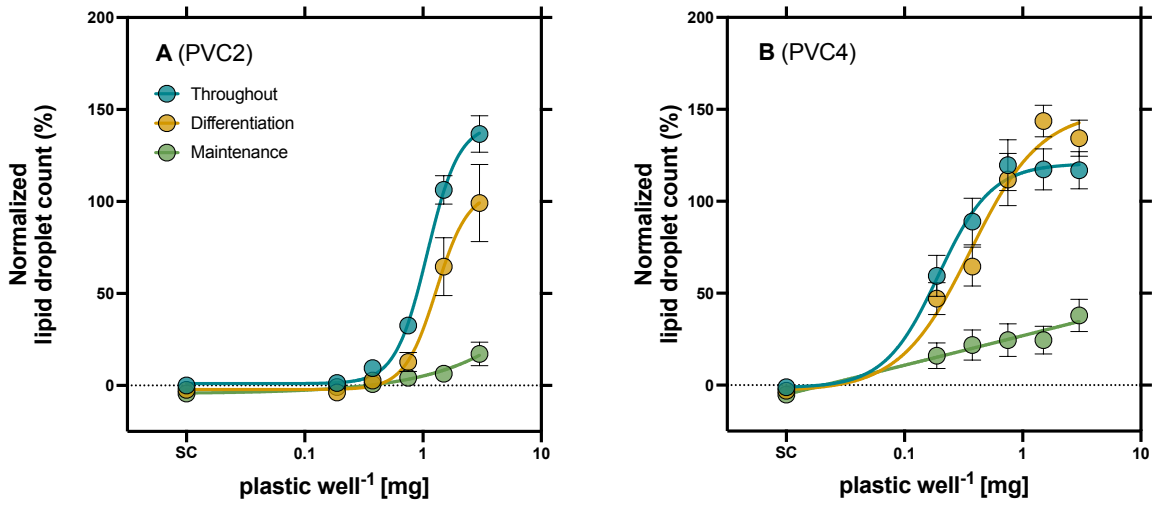

Figure 13: The effect of A) PVC2 (N = 3) and B) PVC4 (N = 3) exposure in three different windows on the lipid accumulation in 3T3-L1 cells. The average lipid droplet counts ± SEM are fitted with a four-parameter logistic regression and normalized to the throughout exposure to rosiglitazone. The biological replicates (N) are a mean of the four technical replicates from each experiment.

Summarizing the proliferative, differentiation and lipid accumulative effects of the plastic extracts, several of the extracts can be compared. The cells exposed during the differentiation and throughout the assay obtained both a comparable high CC and LDC, in the case of PP4 and PVC4 exposure. In the lipid accumulation results, the exposure during the differentiation even caused a higher effect in the two highest concentrations than the throughout exposure. Compared to rosiglitazone, the average CC and LDC was determined to be approximately 50% higher after exposing the cells to PP4 and PVC4 throughout the assay and during the differentiation window. Hence, the data suggest exposure to PP4 and PVC4 during the differentiation is equivalent to exposure throughout the adipogenesis assay. Further, the proliferative effect of PS2, PUR3, PUR4 and PVC2 on the cells exposed throughout the assay was higher compared to the two other exposure windows. The lipid accumulation was however similar in the cells exposed throughout the assay and during the differentiation window of these extracts. PS2 and PUR4 exposure did however cause a generally lower adipogenic effect compared to rosiglitazone and the other plastic extracts. The remaining four endpoints of the plastic exposure display similar effects as presented here (Figure A.2-A.7). Overall, the total effect of the plastic extracts on the lipid accumulation was varying compared to the positive control, the results do however suggest that exposure of the plastic extracts during the differentiation window caused larger adipocytes compared to the throughout exposure.

3.4 Effect of plastic chemicals on cytokine release

During the adipogenesis assay the differentiation occurs between day 3 and 5, the media sampled at day 5 represents the media exposed to the cells during the differentiation phase while day 11 was the last day of the assay and thus at the end of the maintenance stage. These samples were utilized to quantify released IL-6 and TNF-α from the cells by ELISA.

While TNF-α was not detected in the media samples from both time points, exposure of 3T3-L1 cells to plastic extracts induced release of IL-6. The IL-6 concentrations were in general higher in all media samples from day 5 than day 11 (Figure 14). In addition, the mean IL-6 concentration in the media from the cells exposed to several of the plastic extracts was statistically different to the media from the cells exposed to the SC (Table A.4). In the first experiment, the IL-6 level in the media of the cells exposed to PS2 from day 5 was higher than the range of the standard curve. ELISA was therefore repeated for media of the cells exposed to PS2, PUR4, PVC4, rosiglitazone and the SC. The media of the cells exposed to the plastic extracts from day 5 analyzed in the first experiment contained a significantly lower IL-6 level compared to the media of cells exposed to the SC (Figure 14, A). The IL-6 concentration in the media of cells exposed to the SC was 24.7 pg/mL and the IL-6 concentrations in the media of the cells exposed to the following exposures were significantly lower, including the HNC of rosiglitazone ($P<0.0001$), both concentrations of PP4 ($P<0.0001$), PUR4 ($P<0.0001$) and PVC4 ($P<0.0001$), and the second highest concentration (1:2) of PUR3 ($P = 0.0007$). The media of cells exposed to the HNC of PUR3 from day 5 of the adipogenesis assay, did however contain an IL-6 concentration higher than the SC ($P<0.0001$) with a mean concentration of 32.8 pg/mL. Media obtained from the cells exposed to PS2 and PUR3 from day 11 had a significantly higher IL-6 level than the media from cells exposed to the SC. The IL-6 concentration in media obtained from the cells exposed to PS2 1:2 ($P<0.0001$) and HNC ($P = 0.004$) were 13.2 pg/mL and 27.8 pg/mL, respectively. In the media of the cells exposed to PUR3 1:2 ($P<0.0001$) and HNC ($P = 0.004$) the IL-6 concentration was 12 pg/mL and 10 pg/mL. Hence, the adipocytes released a higher level of IL-6 during the differentiation window compared to the last days of the adipogenesis assay, and the cytokine level was further increased in response to the exposure to PS2 and PUR3.

In the second experiment, the IL-6 concentration in the media of the cells exposed to PS2 from day 5 was 50 times higher than in the media of the cells exposed to the SC (Figure 14, B). The IL-6 release from the cells exposed to PS2 during the differentiation window was highly increased ($P<0.0001$). Exposure of the HNC of PS2 resulted in an IL-6 concentration at 1198 pg/mL, while the exposure of 1:2 PS2 caused an IL-6 concentration at 760 pg/mL. The media obtained from the cells exposed to PS2 from day 11 was also increased compared to the media of the cells exposed to the SC. The IL-6 concentration in the media of the cells exposed to the HNC of PS2 media was 40.7 pg/mL ($P<0.0001$) and 35.3 pg/mL in the media of the cells exposed to PS2 1:2 ($P = 0.0001$). The IL-6 concentration in the remaining media samples from day 5 was not significantly different from the media of the cells exposed to the SC, including rosiglitazone, PUR4 and PVC4. Additionally, most of the media samples from day 11 were lower than the range of the standard curve, and therefore not included. The media containing the highest mean IL-6 concentrations were thus obtained from the cells exposed to PS2, both from day 5 and 11 of the adipogenesis assay.

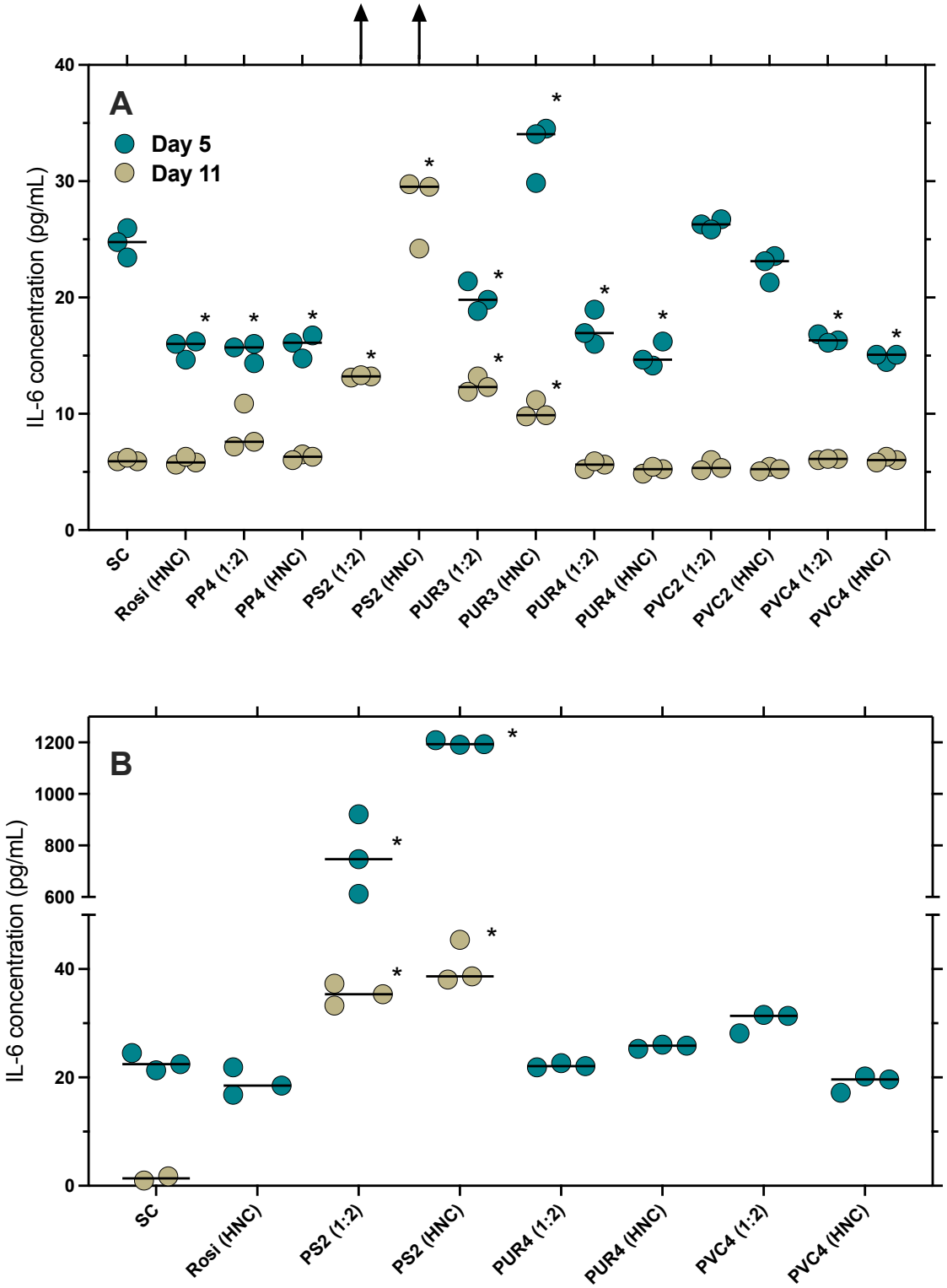

Figure 14: IL-6 concentrations (pg/mL) in the media samples obtained at day 5 and 11 of the adipogenesis assay from 3T3-L1 exposed to the respective plastic extracts. The highest non-cytotoxic concentration (HNC) of the extract and the second highest concentration (1:2) were analyzed. The results in A) and B) were obtained from one biological replicate each, by ELISA. Note that the y-axis in B) is split because of major differences in the concentrations. Rosi = rosiglitazone. * = P<0.001.

3.5 Alteration in adipocyte gene expression after plastic exposure

We carried out qPCR to study whether the gene expression in the adipocytes changed after exposure of different plastic extracts throughout the adipogenesis assay. Based on the RNA sequencing conducted prior to this master thesis several, target genes were selected for analysis of adipocytes exposed to other plastic extracts than those used in the sequencing. After extraction of RNA and reverse transcription, cDNA from adipocytes exposed to PP4, PS2, PUR4, PVC2 and PVC4 throughout the adipogenesis assay was investigated using qPCR. Four of the selected genes were not amplified during the qPCR analysis, these include *Amotl2, Rn18s, Slc2a1* and *Tcf21.* Further on, we observed a large biological variance in several RNA samples and the qPCR analysis was therefore repeated with *Enpp2, Fabp4, Gapdh* and *Ywhaz*. The results from this experiment obtained a lower biological variance than in the first experiment (Figure A.9) and are thus the results presented in this section. The *Ywhaz* gene expression was relatively consistent in all samples and therefore used to normalize the expression of the other genes.

Gapdh and *Nono* were not consistently expressed in the RNA samples and were therefore not used for normalization of the chosen genes. The two housekeeping genes *Gapdh* and *Nono* were selected as reference genes. The gene expression of these genes varied among the samples with a great biological variance (Figure 15). The gene expression of *Gapdh* and *Nono* was thus not used for normalization of the remaining target genes.

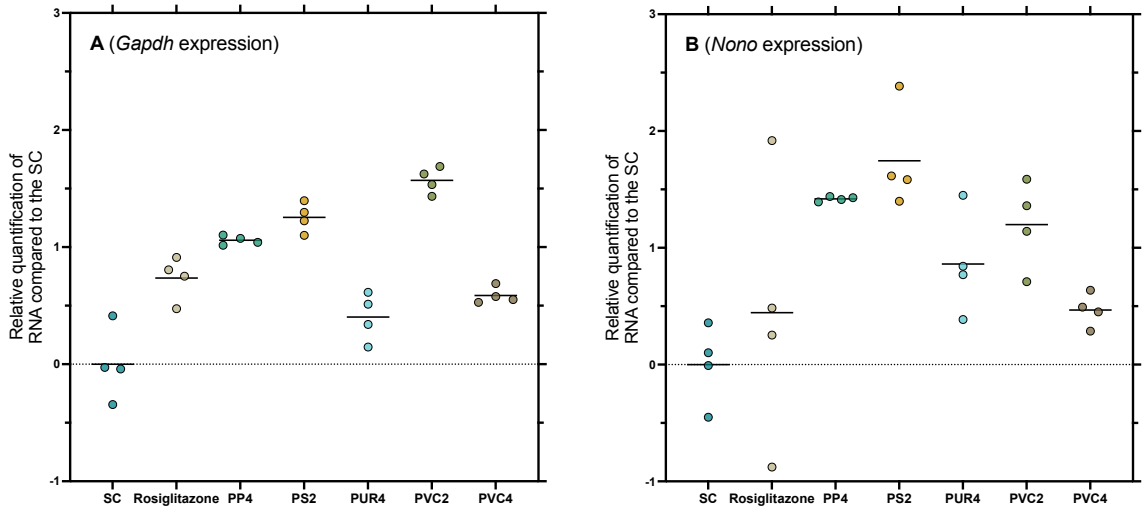

Figure 15: Expression of the housekeeping genes *Gapdh* and *Nono* in 3T3-L1 cells after exposure to plastic extracts throughout the adipogenesis assay. The relative gene expression is scaled to the SC, normalized to *Ywhaz* and transformed logarithmically. The dots in the graphs represent the four biological replicates with the mean of the relative quantification of A) *Gapdh* and B) *Nono* expression.

In general, the reference genes were upregulated in the adipocytes exposed to the plastic extracts and the positive control compared to the SC (Figure 16). *Cfd* expression was slightly upregulated in the adipocytes exposed to rosiglitazone compared to the SC and was further upregulated in the cells exposed to PP4, PS2, PUR4, and PVC2. The exposure to these extracts resulted in an elevated gene expression between 0.75 and 1.75 higher than the SC. The mean *Fabp4* expression in the cells exposed to rosiglitazone was approximately 1.25 higher than the SC. The plastic exposures caused a lower expression of *Fabp4* than rosiglitazone between 0.5 and 1 higher than the SC. Finally, the mean *Pparg* expression was upregulated in the cells exposed to rosiglitazone compared to the SC. The expression of *Pparg* in the adipocytes exposed to the plastic extract was similar with rosiglitazone, between 0.5 and 1 higher expression compared to the SC. The biological variation is however notably large in the gene expression results of *Cfd* and *Pparg.* Despite the large biological variation, the average gene expression indicates an upregulation in the expression of *Cfd, Fabp4,* and *Pparg* in the cells exposed to the plastic extracts and rosiglitazone.

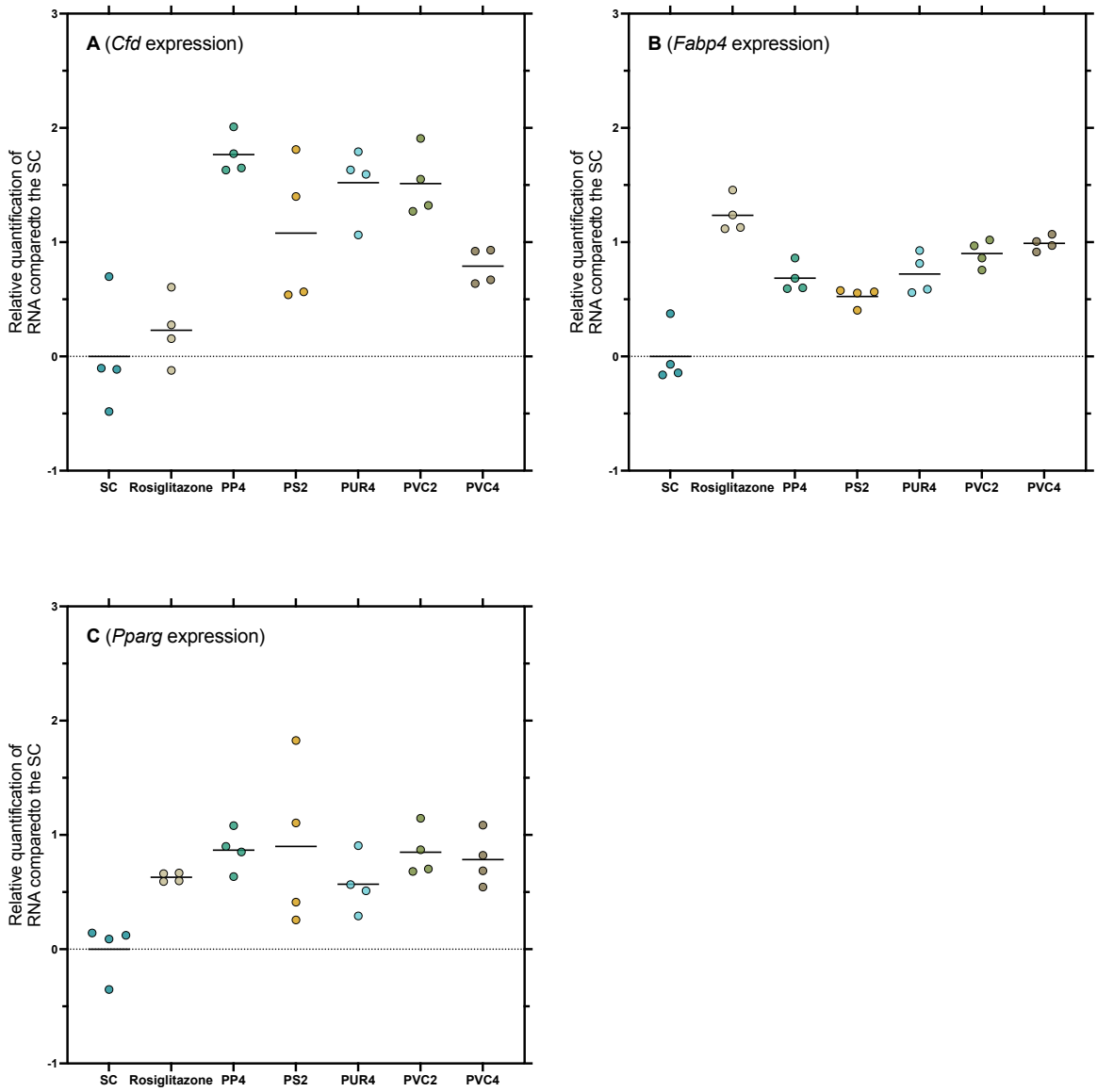

Figure 16: Expression of the reference genes, *Cfd, Fabp4* and *Pparg* in 3T3-L1 cells after exposure to plastic extracts throughout the adipogenesis assay. The relative gene expression is scaled to the SC, normalized to the expression of *Ywhaz* and transformed logarithmically. The graphs represent the mean of the four biological replicates in a relative quantification of A) *Cfd,* B) *Fabp4* and C) *Pparg* expression.

The four target genes *Enpp2, Lpp3, Manf,* and *Serpinb6a* were expressed in the adipocytes dependent on the extract exposure (Figure 17). The mean expression of *Enpp2* in the adipocytes exposed to rosiglitazone was downregulated with an expression 0.5 lower that the SC. The adipocytes exposed to the plastic extracts expressed however a higher level of the same gene. PP4, PVC2, and PVC4 caused an average gene expression in the cells close to 0.5 higher than the SC, while PS2 and PUR4 caused a lower mean expression, close to the mean of the SC. Further, rosiglitazone caused a downregulation of *Lpp3 compared with the SC*. Exposure of PVC4 caused a mean expression at approximately -0.25 compared to the SC, similar to rosiglitazone. The mean *Lpp3* expression in the cells exposed to PVC2 was close to the

expression in the SC, while the mean expression in the cells exposed to PP4, PS2 and PUR4 was approximately 0.5 higher than the SC. The expression of *Manf* increased in the cells exposed to rosiglitazone and was close to 0.25 higher than the SC. PP4, PS2, PUR4 and PVC2 exposure resulted in a higher expression of *Manf* with an expression 0.5-1 higher than the SC. The gene was however downregulated in the cells exposed to PVC4. The *Serpinb6a* expression in the cells exposed to rosiglitazone was slightly lower than the SC, close to -0.5. The adipocytes exposed to PP4, PS2, PUR4 and PVC2 expressed a higher level of the gene, 0.5–1 higher than the SC. The mean expression of *Serpinb6a* in the cells exposed to PVC4 was however approximately the same as in the SC. It is worth noting the large biological variation in the gene expression results of *Lpp3, Manf,* and *Serpinb6a.* An overview of the alterations in all gene expression in the exposed adipocytes are summarized in a heatmap (Figure 18). In general, the cells exposed to rosiglitazone and PVC4 expressed a lower level of the four target genes than the remaining plastic extracts.

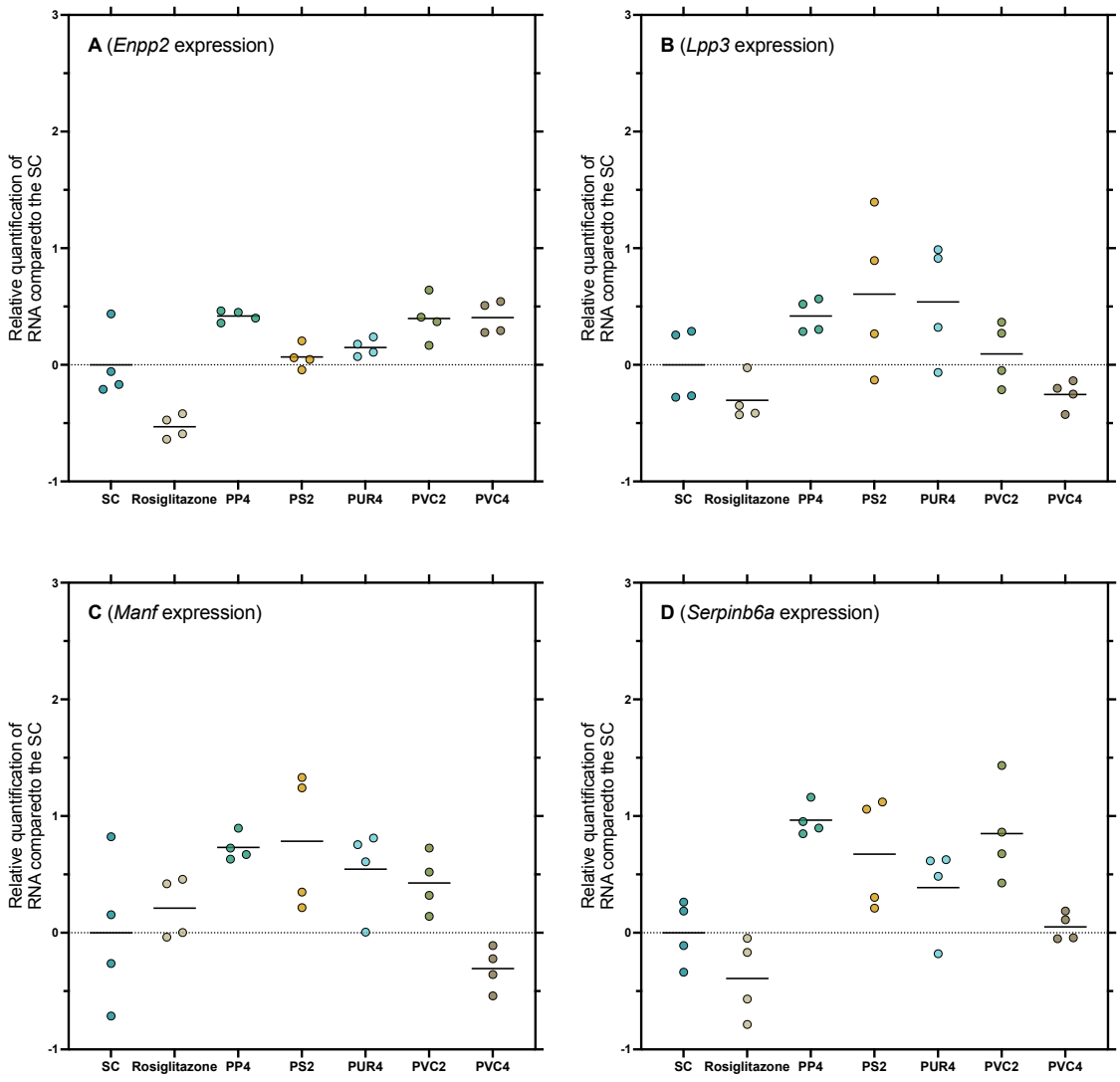

Figure 17: Gene expression of *Enpp2, Lpp3, Manf* and *Serponb6a* in 3T3-L1 exposed to plastic extracts throughout the adipogenesis assay. The relative gene expression is scaled to the SC, normalized to the gene expression of *Ywhaz* and transformed logarithmically. The graphs represent the mean of the four biological replicates in a relative quantification of A) *Enpp2,* B) *Lpp3,* C) *Manf* and D) *Serpinb6a* expression.

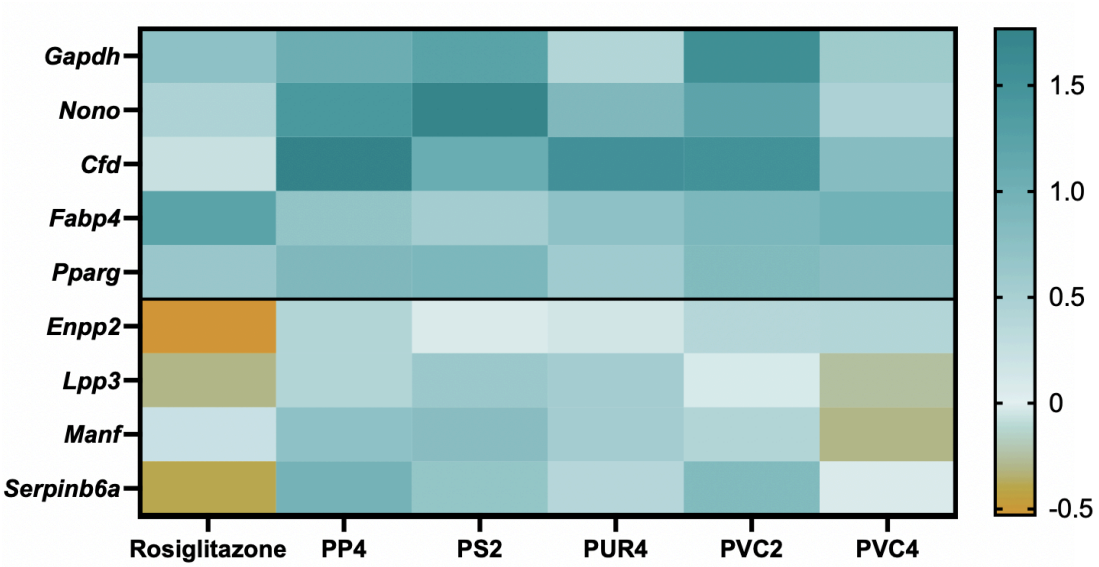

Figure 18: Overview of the mean alteration in gene expression after exposure of plastic extracts to 3T3-L1 cells throughout the adipogenesis assay. The relative quantification of the gene expression is scaled to the SC, logarithmically transformed, and normalized to the gene expression of *Ywhaz* in the adipocytes.

4. Discussion

4.1 Media comparison

To identify the potential impact of different suppliers of DMEM and the addition of L-glutamine to the cell culture media, a media comparison was conducted. The degree of differentiation of 3T3-L1 cells is highly dependent on cell culture conditions, including the hormonal supplements, timing of induction, and even the persons involved with the cell culture (Kraus et al., 2016). Optimization of experimental conditions are therefore critical in ensuring experimental reproducibility. The results showed a similar proliferative and lipid accumulative effect in the adipogenesis of the cells, independent from the media supplier and composition. We observed some minor differences, however, this could be also due to the biological variations of the assay. The similar effects of the media treatments suggest the addition of L-glutamine did not impact the adipogenesis efficacy and thus our results obtained with media from Sigma can be compared to previous experiments conducted with cell media from other suppliers. Because the Sigma media gave a higher response in the cells and the BioWest media was expired, we decided to continue using Sigma media in the further experiments.

4.2 Effect of plastic chemicals on adipogenesis

During the adipogenesis assay, the 3T3-L1 preadipocytes develop into mature adipocytes. In the pre-differentiation window the cells enter the growth-arrest by contact inhibition (Zebisch et al., 2012). Hormonal induction does however cause proliferation and re-entry into the cell cycle of the preadipocyte, which marks the beginning of the differentiation. As the cells further differentiate their ability of mitotic division is depleted (Fajas, 2003). The proliferation thus indicates the number of cells where the adipogenesis is initiated. The lipid accumulation is however increased during the terminal phase of the adipogenesis and continues throughout the maintenance (Niemelä et al., 2008). The LDC does therefore represent maturation and maintenance of the adipocytes. Hence, CC and LDC were selected as endpoints to represent two different parts of the adipogenesis.

Chemicals extracted from plastic consumer products induced adipogenesis in 3T3-L1 cells. Plastic extracts PP4, PVC2, and PVC4 caused a similarly high adipogenesis, while PS2, PUR3, and PUR4 caused a limited adipocyte count (Figure 4). The induction of adipogenesis implies a content of MDCs in the plastic products. The selected plastic extracts caused similar adipogenic responses in comparison to our previous findings (Völker et al., 2022a). However,

we observed some differences in the magnitude of the responses. The throughout exposure of the positive control to the adipocytes in the experiments conducted by Völker et al. (2022a) resulted in approximately 100 cells more per field and 400 lipid droplets more per field compared to the results in this thesis. Lower adipogenic effect can be caused by inadequate training in handling cells in culture, as technical details might contribute to result variability. Simple handling steps such as PBS washing are identified to significantly change assay outcomes (Hirsch and Schildknecht, 2019). The exposure of the extracts does however reflect the same relationship to the positive control in the two studies. Despite the lower response to the exposures in this thesis, our results are confirming the reproducibility of the results from Völker et al. (2022a). The analyzed extracts promoted differentiation in the 3T3-L1 cells during the adipogenesis, even though it was in a slightly lower manner compared to the study conducted by Völker et al. (2022a),

4.2.1 Critical window of exposure

To identify critical windows of exposure during adipogenesis, we exposed 3T3-L1 cells to the selected plastic extracts and the positive control rosiglitazone either during the differentiation window, the maintenance stage, or throughout the assay (Figure 1). Rosiglitazone exposure to the cells throughout the assay caused a higher proliferation and differentiation compared to exposure during the two remaining windows (Figure 6). The lipid accumulation was highest in the cells after exposure of rosiglitazone during the differentiation compared to the two other exposure windows (Figure 10). Exposure to PP4 and PVC4 throughout the assay and during the differentiation window caused a similarly high proliferation and differentiation, while PS2, PUR3, PUR4, and PVC2 caused the highest proliferation and differentiation by exposure throughout the assay (Figure 7–9). The lipid accumulation in the cells exposed to the plastic extracts exclusively during the differentiation stage were similarly high or higher than the throughout exposure (Figure 11–13). In general, exposing the cells only during maintenance caused a lower adipogenic effect compared to the two other exposure windows.

Rosiglitazone exposure of the 3T3-L1 cells caused an increasingly proliferative and differentiative effect according to the dose (Figure 6). The positive control is a thiazolidinedione (TZD), an insulin-sensitizing compound previously used as an anti-diabetic drug. In adipose tissue, the binding of rosiglitazone to PPARγ stimulates adipogenesis in pre-adipocytes (Fryklund et al., 2022), in line with the results observed here, as the proliferation

increased according to the dose in all three windows of exposure. Rosiglitazone caused an increasing proliferative and differentiative effect in the cells in the following order, maintenance exposure, differentiation exposure, and exposure throughout the assay. If there was no window of exposure, it would be expected that the proliferation and differentiation would increase accordingly to the length of the exposure. The throughout exposure lasted 8 days and caused the highest proliferation and differentiation. However, exposure during the differentiation lasted 2 days and resulted in a higher proliferation than maintenance exposure lasting 6 days. Hence, the stronger proliferative effect of rosiglitazone during the differentiation phase supports the hypothesis of a sensitive exposure window.

Regarding the lipid accumulation, the exposure to rosiglitazone during the differentiation window caused the highest effect, second highest effect was obtained by the exposure throughout the assay, while the maintenance exposure caused the lowest lipid accumulation (Figure 10). Since the throughout exposure window caused a higher CC compared to the differentiation window, the throughout exposure caused more and smaller adipocytes than the differentiation exposure of rosiglitazone. This is in line with the literature reporting that the development of small insulin sensitive adipocytes is one of the most well-described effects of treatment of TZDs (Fryklund et al., 2022). Given that lipid accumulation occurs over time, an earlier exposure and activation would kickstart the adipogenesis and lipid accumulation in the cells. It takes time for the cells to mature, and lipid parameters are dominated by the mature adipocytes. In other words, the maintenance exposure might cause a lower lipid accumulation because of a later start and will not have time to build up the same lipid pool as the cells exposed earlier. When drawing a line to human exposure, the high lipid accumulative effect caused by exposure during the differentiation and the low effect resulting from the exposure during the maintenance, suggest that the early life, when the majority of adipogenesis occurs (Spalding et al., 2008), is a critical stage of exposure and exposure later in life does not affect humans to the same extents. Our results do therefore support the obesogen hypothesis which postulates that the adipose depots are susceptible of exposure to obesogens, especially during development (Nappi et al., 2016). Considering both the proliferation and the lipid accumulation resulting from an exposure to rosiglitazone suggests that the differentiation window is a sensitive window of exposure compared to the maintenance phase.

There was not a significant difference between the proliferative effect after the exposure during the differentiation and the maintenance of PS2, PUR3, PUR4, and PVC2 (Figure 7–9). The

throughout exposure to the extracts caused a higher proliferation and differentiation compared to the two other exposure windows. Thus, the proliferative effect did not differ between the cells exposed during the differentiation window and during the maintenance window, indicating that the extracts are inducing adipogenesis throughout the assay and there is no specific sensitive window of exposure. It is however important to consider that the plastic extracts can contain other chemicals in addition to MDCs that may interfere with adipogenesis. In the nontarget analysis performed by Völker et al. (2022a), most of the features in the plastic extracts were not identified. Yet, PS2, PUR3, PUR4, and PVC2 exerted both baseline toxicity and oxidative stress (Zimmermann et al., 2019) which can compromise the ability of 3T3-L1 cells to differentiate and mature (Mehrzad, 2022). The cells exposed throughout the assay and during the maintenance windows are exposed to these chemicals up to 6 days longer than the cells exposed during the differentiation window and may therefore further affect the adipogenesis in these cells. The cells exposed throughout the assay or during the maintenance window obtained, however, a proliferation higher or as high as the cells exposed exclusively during the differentiation. These results are implying the adipocytes are not sensitive to exposure of the plastic extracts in a specific exposure window of the adipogenesis.

The lipid accumulation was affected in the same degree after exposure to PS2, PUR3, PUR4, and PVC2 during the differentiation window as throughout the assay (Figure 11–13). Even though the lipid accumulation was significantly lower in the cells exposed during the maintenance, there is an increasing accumulation according to the extract concentrations. The adipocytes exposed during the maintenance did however have a shorter time of accumulating lipids and maturation after the initial plastic chemical addition. The cells exposed to the extracts exclusively during the maintenance did accumulate a higher amount of lipids compared to the adipocytes exposed to the SC, demonstrating that the chemical activation also occurs during the maintenance. Even though the proliferation results did not imply a sensitive window of exposure, PS2, PUR3, PUR4, and PVC2 exposure increased the lipid accumulation in the exposed cells. This increase in lipid accumulation was observed after exposure during the differentiation window compared to exposure during the maintenance phase, demonstrating that the chemicals induce lipid accumulation early in the adipogenesis.

PP4 and PVC4 exposure during the adipogenesis assay resulted in similar adipogenic effects in the cells. The proliferative effect in the cells was similarly high after exposure of PP4 and PVC4 during the differentiation window and throughout the assay (Figure 7 and 9). Based on

the proliferative and differentiative effects, it seems like the exposure during the differentiation was equivalent to the throughout exposure. It was however an increase in proliferation after exposure during the maintenance, implying adipogenesis occurred during the maintenance as well. The effect of the plastic extracts on the proliferation and lipid accumulation in 3T3-L1 cells has been demonstrated for TBT and DEHP as well (Biemann et al., 2012). These two MDCs induced the proliferation and the lipid accumulation to a higher extent after exposure during the differentiation window in the adipogenesis assay compared to exposure during the maintenance. Meanwhile, another study reported that several plasticizers promoted lipid accumulation to a greater extent in 3T3-L1 cells by exposure during the maintenance compared to the differentiation window (Pomatto et al., 2018). These results demonstrate that MDCs can affect several mechanisms crucial for the adipogenesis and adipocyte maintenance. The proliferative and differentiative effect of PP4 and PVC4 exposure during the differentiation phase imply that this window is more sensitive for exposure, even though the extracts induced adipogenesis to a certain degree during the maintenance as well.

Regarding the lipid accumulation, exposure of PP4 and PVC4 during the differentiation window and throughout the assay resulted in the largest lipid pool compared to the maintenance exposure window (Figure 11 and 13). Thus, the exposure of 3T3-L1 cells to PP4 and PVC4 during the differentiation window has a greater impact on the lipid accumulation compared to the maintenance window, indicating the plastic chemicals are triggering the lipid accumulation in the differentiation. The lipid accumulation results are consistent with the proliferation and differentiation results implying the plastic chemicals might be affecting a mechanism occurring early in the differentiation of the cells. All things considered, both the proliferative and the lipid accumulative effects of the extracts are in line with the hypothesis that the differentiation window is a sensitive window of exposure.

The sensitivity of adipogenesis to chemical disruption during the differentiation window can be compared with the human development. The total number of adipocytes is increasing until adulthood and remains quite constant thereafter (Spalding et al., 2008). This means that most of the adipogenesis occurs early in life. The results in this thesis therefore imply that the plastic chemicals might exert a larger adipogenic effect when exposures occur during early life. After a child is born, it is exposed to plastic chemicals through toys, bottles, and similar products. However, a study from 2022 found microplastic in breast milk, suggesting the presence of plastic chemicals as well. The most abundant microplastics found in breast milk were

polyethylene, PVC, and PP, some of the same plastic polymers analyzed in this thesis (Ragusa et al., 2022). Regarding the potency of the plastic extracts during the differentiation phase and the fact that we are exposed to a variety of plastic chemicals from early life support the idea that plastic chemicals can contribute to the obesity pandemic.

4.3 Effect of plastic chemicals on cytokine release

We conducted an immunological analysis to test the hypothesis that plastic chemicals induce an inflammatory response and a shift towards the development of unhealthy adipocytes. Unhealthy adipocytes are defined by their large size, increased inflammatory response, decreased respiration, and impaired glucose uptake and insulin signaling (Ghaben and Scherer, 2019). In Völker et al. (2022a), the adipocytes exposed to the plastic extracts (except PUR3) accumulated higher levels of lipids per adipocyte compared to rosiglitazone. Based on these results it was hypothesized that the plastics could contribute to the development of unhealthy adipocytes. We investigated the TNF-α and IL-6 release by the adipocytes after the differentiation phase and at the end of the maintenance period. TNF-α and IL-6 were chosen for the analysis because they are well-known proinflammatory cytokines released by adipocytes (Ali et al., 2013, Popko et al., 2010).

The PS2 and PUR3 extracts triggered a release of IL-6 significantly higher than the SC during the differentiation window (Figure 14). We know from the experiments conducted by Zimmermann et al. (2019) that both extracts cause oxidative stress and baseline toxicity. Additionally, they were the most cytotoxic extracts to the cells used in the study of oxidative stress. The highest non-cytotoxic concentration analyzed by the PUR3 extract in this thesis was the second lowest analyzed concentrations. In short, they are both potent extracts. Several signaling pathways have been proposed to explain the inflammatory process in the adipose tissue of obese subjects, including oxidative stress, ER stress, and hypoxia (González-Muniesa et al., 2016). Obesity is associated with unregulated lipid and carbohydrate metabolism and an increase in either of these will also increase the demand on the mitochondria. In addition, there is usually relative hypoxia in adipose tissue undergoing increased demand, either because of poor oxygen supply or the adipocyte size is approaching the limits of diffusion (Ghaben and Scherer, 2019, González-Muniesa et al., 2016). Together with the increased demand of nutrient oxidation, an unusual amount of ROS is generated. Oxidative stress activates kinases that may directly induce the transcription factor NFκB, regulating the expression of inflammatory

cytokines (Monteiro and Azevedo, 2010). Previous studies have showed that oxidative stress and inflammation affect each other, and oxidative stress leads to the release of IL-6 and TNF-α by adipocytes (Li and Shen, 2019). The metabolic stress in the adipocytes results in organelle dysfunction, especially mitochondria and ER. The latter is a cytosolic organelle participating in the regulation of lipid, glucose, cholesterol, and protein metabolism. ER is also the site of lipid droplet formation. Given that it is required to secrete large amounts of substances and synthesize lipids in adipose tissue in obese, ER function might be impaired, leading to misfolded or unfolded proteins in its lumen (Monteiro and Azevedo, 2010). This condition has been showed to induce inflammatory cascades through several pathways (Zha and Zhou, 2012). PS2 and PUR3 might cause the described metabolic stresses leading to the observed cytokine release by the adipocytes. However, compared to the other plastic extracts, PS2 and PUR3 caused the lowest proliferation and lipid accumulation. Unhealthy adipocytes are associated with their large size, impaired glucose uptake and insulin signaling which are contributing to an inflammation. The induction of IL-6 might therefore be due to the toxic effect of the extracts, rather than because of the development of unhealthy adipocytes. The extracts exerting the highest cell count and lipid accumulation in the cells did not cause an elevated cytokine release, suggesting that the plastic extracts are not contributing to the development of unhealthy adipocytes. The plastic extracts might therefore not cause a shift in the development of unhealthy adipocytes, and the described potency and toxicity of PS2 and PUR3 might explain the release of the inflammatory marker, IL-6.

TNF-α was not detected in two ELISA experiments. Previously, the release of TNF-α has been demonstrated with ELISA in 3T3-L1 cells in response to plastic chemicals like BPA (Ben-Jonathan et al., 2009). However, according to a study from 2014, TNF-α is a degradable cytokine and instant freezing by liquid nitrogen does not preserve the stability of the cytokines (Ozbey et al., 2014). For this reason, potential TNF-α released by the adipocytes might have been degraded as the media samples were stored at -80°C after collection. In contrast to TNF-α, IL-6 was detected in most media samples and the detected cytokine concentration was higher in the media obtained after the differentiation window than in the media obtained from the last day of the assay. This indicates that adipocytes are sensitive to inflammatory stimuli during differentiation. It appears to be a crosstalk between insulin signaling, ROS, and adipogenesis, by which the insulin signaling generates ROS which in turn inhibit protein tyrosine phosphatase 1B, an inhibitor of the insulin signaling pathway. ROS is therefore associated with promoting

the insulin signaling pathway and adipogenesis. However, sustained high levels of ROS inhibit insulin signaling, and thus inhibit the adipogenesis (Ghaben and Scherer, 2019). If there is a certain basal level of ROS required for adipogenesis, the threshold of a damaging ROS level might be more easily obtained in response to inflammatory stimuli than in preadipocytes and mature adipocytes. Here, the elevated level of IL-6 during the differentiation might be promoted by the start of plastic extract exposure. Meanwhile, an increase in IL-6 release has been observed in differentiating adipocytes (Vicennati et al., 2002), confirming the effect observed in this thesis. Thus, a general elevated ROS in the cells during the adipogenesis might explain the sensitivity to inflammatory stimuli during the differentiation window.

The cells exclusively exposed to the SC was releasing a higher IL-6 level than the cells exposed to several of the plastic extracts. Compared to the SC, rosiglitazone along with PP4, PUR3, PUR4, and PVC4 promoted a lower IL-6 level. Rosiglitazone is known to be anti-inflammatory and has been showed to decrease IL-6 release (Li and Shen, 2019), explaining the low IL-6 concentration compared to the SC. These results may imply that several of the plastic extracts also have an anti-inflammatory effect on the cells. The second experiment did however demonstrate that the SC caused the same IL-6 concentration as rosiglitazone, PUR4 and PVC4, which might imply a potential contamination or inaccuracy in the experiment execution in one of the experiments. The increased level of IL-6 during the differentiation was, hence, potentially due to the differentiation of the cells and the elevated SC compared to the other samples might be a result of inaccuracy.

A low-grade inflammatory response triggered by excess nutrients in metabolic cells is one of the markers found in obese (González-Muniesa et al., 2016). The constant elevated cytokine production in the adipose tissue is associated with reduced insulin resistance, reduced capacity of adipogenesis, and decreased expression of PPARγ and C/EBPα (Jiang et al., 2019). In the experiments conducted in this thesis, we seemingly did not see the development of unhealthy adipocytes. It might be that the adipocytes need more time of maintenance before an inflammatory response is initiated, to develop obesity takes years of a person's life. At the same time, it might be that the plastic extracts simply are not leading to the development of unhealthy adipocytes. The association of inflammation with obesity is clear, however, whether the plastic extracts are contributing to this state needs further research.

4.4 Mechanisms by which plastic chemicals induce adipogenesis

In our previous study, only PS2 and PVC2 activated PPARγ, and none of the extracts activated the glucocorticoid receptor (Völker et al., 2022a). Both receptors are key regulators in the adipogenesis, and a common idea is that PPARγ activation is a main mechanism where chemicals can trigger adipogenesis. Our previous results therefore demonstrated that plastic chemicals may act through various mechanisms independent of the glucocorticoid receptor and PPARγ. In the further investigation of the underlying mechanisms of the induction of adipogenesis by the plastic extract, qPCR was conducted for the four target genes. These were selected based on earlier RNA sequencing data, which we aimed to verify and to include further plastic exposures to. Alteration in gene expression was compared to the SC, and the target genes were in general downregulated in the cells exposed to rosiglitazone, except for *Manf* (Figure 18). The four target genes were however upregulated in the adipocytes exposed to PP4, PS2, PUR4, and PVC2. Further, *LPP3* and *Manf* were downregulated and *Enpp2* and *Serpinb6a* were upregulated in the adipocytes exposed to PVC4.

The reference genes are markers of the adipogenesis and were upregulated in the adipocytes as expected in (Figure 16). The reference genes were PPARγ, the master regulator of the adipogenesis (Huang et al., 2009), the fatty acid binding protein FABP4, which is specific for late phase of adipogenesis (Pomatto et al., 2018) and adipsin, one of the adipokines secreted by adipocytes (Tafere et al., 2020). Upregulation of these genes compared to the cells treated with the SC therefore confirms the development of adipocytes.

The target gene *Enpp2* was upregulated in the adipocytes exposed to all the plastic samples compared to the rosiglitazone treatment, similar as for *Lpp3*, except for the down regulation in adipocytes exposed to PVC4 (Figure 17). Differences in gene expression in adipocytes treated with plastic extracts compared to rosiglitazone exposure implicate different mechanisms are altered. *Enpp2* encodes the secreted glycoprotein autotaxin (ATX) which is abundantly expressed in adipose tissue and has been found to be substantially upregulated in obese mice (Zhang et al., 2021, Ferry et al., 2003). ATX is mainly hydrolyzing lysophosphatidylcholine (LPC) forming the bioactive lipid compound, lysophosphatidic acid (LPA). By binding to a diverse of extracellular G protein-coupled receptors (LPAR), it can influence many cellular responses, including proliferation, growth, survival, development, and vasoregulation (Jose and Kienesberger, 2021). LPA induce preadipocyte proliferation, however treatment with LPA

in preadipocytes and mature adipocytes decrease PPARγ expression, impair the response of rosiglitazone-activated PPARγ genes, reduce lipid accumulation, and reduce the expression of adipocyte mRNA markers. Thus, a high local production of LPA may exert an inhibitory effect on adipogenesis by the binding of $LPAR_1$ (Simon et al., 2005). LPA is mainly regulated by ATX, thus the LPA concentration is dependent on the expression of ATX (Harper et al., 2019). In our adipocytes exposed to the different plastic extracts, *Enpp2* is upregulated indicating an elevated level of the adipogenic inhibitor LPA. However extracellular LPA is in general degraded through the dephosphorylation by lipid phosphate phosphatases (LPPs), like LPP3 into monoacylglycerol (Jose and Kienesberger, 2021). All plastic samples, except PVC4 caused an upregulation of *Lpp3* preventing high LPA concentrations. In other words, ATX was upregulated in the adipocytes exposed to the plastic extracts, and an increased LPA concentration might have been avoided in the adipocytes exposed to PP4, PS2, PUR4, and PVC2 by the upregulation of *Lpp3* degrading LPA. PVC4 caused a downregulation of *Lpp3* and an upregulation of *Enpp2* in the adipocytes. The combination of downregulated *Lpp3* and upregulated of *Enpp2* might lead to the accumulation of LPA. PVC4 was however one of the extracts causing the highest lipid accumulation in the cells, and since an increased LPA concentration may exert an inhibitory effect on adipogenesis, an LPA accumulation is therefore contradictive to our results. On the other hand, an increased LPA accumulation has been observed in response to hypoxia (Harper et al., 2019), which might be the case in adipocytes when their size becomes too large for the oxygen to diffuse through them (Halberg et al., 2009). An LPA accumulation might therefore be a result of the high lipid accumulation in these cells, suggesting hypoxia in the cells exposed to PVC4.

The *Enpp2* and *Lpp3* may be upregulated as a result of inflammatory stimuli. Previous nonadipocyte studies have shown LPA to stimulate expression of IL-6, which in turn stimulates the expression of ATX (Castelino et al., 2016). Further on, the ATX-LPA signaling pathway has been observed to increase the expression of antioxidative genes protecting the cell against ROS (Venkatraman et al., 2015). *Lpp3* is also suggested to be upregulated by LPA itself, in addition to inflammatory stimuli in various cell types (Mao et al., 2019). We know that most of the plastic extracts causes oxidative stress in the cells which could explain the upregulation of *Enpp2* and the downstream upregulation of *Lpp3.* At the same time, Zimmerman et al. (2019) did not demonstrate oxidative stress caused by the PP4 extract. These results were however obtained from experiments with short-time exposure, which does not

exclude a possible toxic effect of the PP4 extract over time. On the other hand, rosiglitazone caused a downregulation of both genes, which can be explained by its anti-inflammatory properties (Li and Shen, 2019). The downregulation of both genes was also observed when 3T3F442A cells were treated with rosiglitazone (Boucher et al., 2005). Thus, *Enpp2* and *Lpp3* might be upregulated in response to inflammation and oxidative stress, while rosiglitazone causes a downregulation of *Enpp2* in adipocytes.

Manf is one of the genes found to be upregulated in the adipocytes exposed to rosiglitazone and the plastic extracts compared to the SC, PVC4 was on the other hand downregulated compared to the SC. Circulating mesencephalic astrocyte-derived neurotrophic factor (MANF) is a protein showed to be positively correlated with BMI in humans (Wu et al., 2021). MANF is primarily located in the ER and is upregulated and secreted during ER stress (Tang et al., 2022). The membranous network is important for the integration of metabolic signals crucial in cellular homeostasis. The metabolic stress the adipocytes are facing in obese subjects might lead to ER stress (Monteiro and Azevedo, 2010). The upregulation of *Manf* in the adipocytes exposed to rosiglitazone, the PP4, PS2, PUR4, and PVC2 extracts may therefore indicate an ER stress as a result of the metabolic stress the cells are exposed to.

The last target gene, *Serpinb6a*, was upregulated in the adipocytes exposed to the plastic extracts, however, not in the cells exposed to rosiglitazone. As far as the author knows, there is not yet described a connection between the expression of *Serpinb6a* and the adipocyte homeostasis or metabolic alteration. The gene was included because previous RNA sequencing indicated an upregulation in the adipocytes exposed to plastics. It is therefore hypothesized if *Serpinb6a* might be involved in the development of unhealthy adipocytes.

The expression of the housekeeping genes was not consistent in the RNA samples (Figure 15). In the normalization of qPCR data, using housekeeping genes is the most common approach. They have the potential to remove most technical variation in cDNA concentrations between the samples, however they must be stably expressed to meet this potential (Hellemans and Vandesompele, 2014). The two housekeeping genes *Gapdh* and *Nono* were not stably expressed and was thus not used for the normalization. The large variation might be due to the fact that the RNA is obtained from a diverse population of cells. Even though the RNA is collected at the end of the adipogenesis assay preadipocytes and not fully mature adipocytes

are present. In other words, the housekeeping genes were not stably expressed to use for normalization.

There was a difference in the expression of the target genes in the sequencing and the qPCR executed in this thesis. Historically, qPCR is often performed to verify the data obtained in large-scale transcriptomic studies. However, it appears to be a very small fraction of the genes that are severely contradictory (Coenye, 2021). Unfortunately, the expression of *Lpp3* was downregulated in the sequencing data, the opposite of the results obtained in this thesis. An upregulation of *Enpp2* and downregulation of *Lpp3* might lead to an increased level of LPA, as described for PVC4. Technical inaccuracy might explain the differences between the sequencing and qPCR results.

5. Conclusion and further directions

In this thesis we found that six plastic extracts promote the adipogenesis in 3T3-L1 cells, confirming the reproducibility of the adipogenesis assays performed by Völker et al. (2022a). The results demonstrated that the six plastic products contain MDCs. In further experiments, 3T3-L1 cells were exposed to the extracts in three different windows of the adipogenesis assay: during the differentiation, the maintenance and throughout the assay. This, to investigate whether the cells were sensitive to plastic extract exposure in a specific window of the adipogenesis assay. The exposure of the cells to the positive control, rosiglitazone, and the six plastic extracts PP4, PS2, PUR3, PUR4, PVC2, and PVC4 suggested that adipocytes are very sensitive to chemical disruption during the differentiation window. In a further investigation of sensitive exposure windows of the development of adipocytes, the commitment to the adipocyte lineage would be interesting to look more into. By exposing mesenchymal stem cells, like C3H/10T1/2 to the plastic extracts before the induction of the terminal differentiation, an increase in adipocyte number could indicate whether the plastic chemicals could induce cell determination.

The cytokine release by the adipocytes exposed to the plastic chemicals was investigated. TNF-α was not detected in the media obtained from the cells during the adipogenesis assay, probably due to instability of the cytokine. However, we found an elevated IL-6 concentration in the differentiation window compared to the last day of the assay, indicating that the cells are sensitive to inflammatory stimuli during differentiation. The adipocytes exposed to PS2 and PUR3 released significantly higher levels of IL-6 compared to the adipocytes exposed to the SC. The release of IL-6 might have been caused by the development of unhealthy adipocytes, or by the toxic effect of the extracts. The link between the plastic chemical exposure and the cytokine release was not clear and need further research. To identify whether TNF-α is expressed in response to the chemical exposure, the RNA encoding the TNF-α could be quantified by qPCR because of the instability of the cytokine. A quantification of IL-6 released by the adipocytes exposed exclusively during the differentiation would be interesting to investigate since a toxic exposure can lead to impaired cell function and adipogenesis over time.

In the investigation on the underlying mechanisms affected by the plastic extracts, we conducted qPCR on RNA samples extracted from the cells after exposure throughout the

adipogenesis assay. *Enpp2* and *Lpp3* might be upregulated in response to inflammation and oxidative stress in the adipocytes exposed to the plastic extracts. These genes were not upregulated in the adipocytes exposed to rosiglitazone, which can be explained by its anti-inflammatory properties. Similar with rosiglitazone, *Lpp3* was not upregulated in the adipocytes exposed to PVC4. The combination of upregulation of *Enpp2* and downregulation of *Lpp3* might indicate the presence of hypoxia in the cells exposed to PVC4. Further on, upregulation of *Manf* observed in the cells exposed to rosiglitazone, the PP4, PS2, PUR4, and PVC2 extracts, might indicate ER stress as a result of metabolic stress. *Serpinb6a* was upregulated in the adipocytes exposed to the plastic extracts and not the rosiglitazone, and it was therefore hypothesized whether it could be involved in the development of unhealthy adipocytes. To further elucidate the mechanisms affected by the plastic chemicals, a quantification of enzymes involved in detoxification could indicate the toxicity of the extracts, especially regarding the mechanisms affected in adipocytes exposed to PS2 and PUR3. Based on the biological variations and the differences in the results obtained in this thesis and in the RNA sequencing, a verification of the gene expression could further clarify the mechanisms affected by the plastic extracts. In this thesis we demonstrated that plastic chemicals could affect the human health and contribute to obesity, by exposure early in life.

Literature

ALI, A. T., HOCHFELD, W. E., MYBURGH, R. & PEPPER, M. S. 2013. Adipocyte and Adipogenesis. *European Journal of Cell Biology,* 92**,** 229-236.

AMATO, A. A., WHEELER, H. B. & BLUMBERG, B. 2021. Obesity and Endocrine-Disrupting Dhemicals. *Endocrine Connections,* 10**,** R87-r105.

BAHMAD, H. F., DAOUK, R., AZAR, J., SAPUDOM, J., TEO, J. C. M., ABOU-KHEIR, W. & AL-SAYEGH, M. 2020. Modeling Adipogenesis: Current and Future Perspective. *Cells,* 9.

BEN-JONATHAN, N., HUGO, E. R. & BRANDEBOURG, T. D. 2009. Effects of Bisphenol A on Adipokine Release from Human Adipose Tissue: Implications for the Metabolic Syndrome. *Molecular and Cellular Endocrinology,* 304**,** 49-54.

BIEMANN, R., NAVARRETE SANTOS, A., NAVARRETE SANTOS, A., RIEMANN, D., KNELANGEN, J., BLÜHER, M., KOCH, H. & FISCHER, B. 2012. Endocrine Disrupting Chemicals Affect the Adipogenic Differentiation of Mesenchymal Stem Cells in Distinct Ontogenetic Windows. *Biochemical and Biophysical Research Communications,* 417**,** 747-752.

BOUCHER, J., QUILLIOT, D., PRADÈRES, J. P., SIMON, M. F., GRÈS, S., GUIGNÉ, C., PRÉVOT, D., FERRY, G., BOUTIN, J. A., CARPÉNÉ, C., VALET, P. & SAULNIER-BLACHE, J. S. 2005. Potential Involvement of Adipocyte Insulin Resistance in Obesity-Associated Up-Regulation of Adipocyte Lysophospholipase D/Autotaxin Expression. *Diabetologia,* 48**,** 569-77.

CASTELINO, F. V., BAIN, G., PACE, V. A., BLACK, K. E., GEORGE, L., PROBST, C. K., GOULET, L., LAFYATIS, R. & TAGER, A. M. 2016. An Autotaxin/Lysophosphatidic Acid/Interleukin-6 Amplification Loop Drives Scleroderma Fibrosis. *Arthritis & Rheumatology,* 68**,** 2964-2974.

CAWTHORN, W. P. & SETHI, J. K. 2008. TNF-alpha and Adipocyte Biology. *FEBS Letters,* 582**,** 117-31.

COENYE, T. 2021. Do Results Obtained with RNA-Sequencing Require Independent Verification? *Biofilm,* 3**,** 100043.

CRISTANCHO, A. G. & LAZAR, M. A. 2011. Forming Functional Fat: a Growing Understanding of Adipocyte Differentiation. *Nature Reviews Molecular Cell Biologyl,* 12**,** 722-34.

DUFAU, J., SHEN, J. X., COUCHET, M., DE CASTRO BARBOSA, T., MEJHERT, N., MASSIER, L., GRISETI, E., MOUISEL, E., AMRI, E. Z., LAUSCHKE, V. M., RYDÉN, M. & LANGIN, D. 2021. *In Vitro* and *Ex Vivo* Models of Adipocytes. *American Journal of Physiology-Cell Physiology,* 320**,** C822-c841.

DUNCAN, R. E., AHMADIAN, M., JAWORSKI, K., SARKADI-NAGY, E. & SUL, H. S. 2007. Regulation of Lipolysis in Adipocytes. *Annual review of nutrition,* 27**,** 79-101.

EGUSQUIZA, R. J. & BLUMBERG, B. 2020. Environmental Obesogens and Their Impact on Susceptibility to Obesity: New Mechanisms and Chemicals. *Endocrinology,* 161.

FAJAS, L. 2003. Adipogenesis: a Cross-Talk between Cell Proliferation and Cell Differentiation. *Annals of Medicine,* 35**,** 79-85.

FARMER, S. R. 2006. Transcriptional Control of Adipocyte Formation. *Cell Metabolism,* 4**,** 263-273.

FERRY, G., TELLIER, E., TRY, A., GRÉS, S., NAIME, I., SIMON, M. F., RODRIGUEZ, M., BOUCHER, J., TACK, I., GESTA, S., CHOMARAT, P., DIEU, M., RAES, M., GALIZZI, J. P., VALET, P., BOUTIN, J. A. & SAULNIER-BLACHE, J. S. 2003. Autotaxin is Released from Adipocytes, Catalyzes Lysophosphatidic Acid Synthesis, and Activates Preadipocyte Proliferation: Up-Regulated Expression with Adipocyte Differentiation and Obesity. *Journal of Biological Chemistry,* 278**,** 18162-18169.

FROMME, H., MATTULAT, A., LAHRZ, T. & RÜDEN, H. 2005. Occurrence of Organotin Compounds in House Dust in Berlin (Germany). *Chemosphere,* 58**,** 1377-83.

FRYKLUND, C., MORÉN, B., NEUHAUS, M., PERIWAL, V. & STENKULA, K. G. 2022. Rosiglitazone Treatment Enhances Intracellular Actin Dynamics and Glucose Transport in Hypertrophic Adipocytes. *Life Sciences,* 299**,** 120537.

FURUKAWA, S., FUJITA, T., SHIMABUKURO, M., IWAKI, M., YAMADA, Y., NAKAJIMA, Y., NAKAYAMA, O., MAKISHIMA, M., MATSUDA, M. & SHIMOMURA, I. 2004. Increased Oxidative Stress in Obesity and Its Impact on Metabolic Syndrome. *The Journal of Clinical Investigation,* 114**,** 1752-61.

GEUEKE, B. Dossier. Non-Intentionally Added Substances (NIAS). Food Packag. Forum, 2018.

GHABEN, A. L. & SCHERER, P. E. 2019. Adipogenesis and Metabolic Health. *Nature Reviews Moleculare Cell Biology,* 20**,** 242-258.

GIMBLE, J. M., ROBINSON, C. E., WU, X., KELLY, K. A., RODRIGUEZ, B. R., KLIEWER, S. A., LEHMANN, J. M. & MORRIS, D. C. 1996. Peroxisome Proliferator-Activated Receptor-gamma Activation by Thiazolidinediones Induces Adipogenesis in Bone Marrow Stromal Cells. *Molecular pharmacology,* 50**,** 1087-1094.

GONZÁLEZ-MUNIESA, P., GARCIA-GERIQUE, L., QUINTERO, P., ARRIAZA, S., LOPEZ-PASCUAL, A. & MARTINEZ, J. A. 2016. Effects of Hyperoxia on Oxygen-Related Inflammation with a Focus on Obesity. *Oxidative Medicine and Cellular Longevity,* 2016**,** 8957827.

GREEN, H. & MEUTH, M. 1974. An Established Pre-Adipose Cell Line and Its Differentiation in Culture. *Cell,* 3**,** 127-133.

GREGOIRE, F. M., SMAS, C. M. & SUL, H. S. 1998. Understanding Adipocyte Differentiation. *Physiological Reviews,* 78**,** 783-809.

GREGOR, M. F. & HOTAMISLIGIL, G. S. 2011. Inflammatory Mechanisms in Obesity. *Annual Review of Immunology,* 29**,** 415-445.

GROH, K. J., BACKHAUS, T., CARNEY-ALMROTH, B., GEUEKE, B., INOSTROZA, P. A., LENNQUIST, A., LESLIE, H. A., MAFFINI, M., SLUNGE, D., TRASANDE, L., WARHURST, A. M. & MUNCKE, J. 2019. Overview of Known Plastic Packaging-Associated Chemicals and Their Hazards. *Science of The Total Environment,* 651**,** 3253-3268.

GUERRE-MILLO, M. 2004. Adipose Tissue and Adipokines: for Better or Worse. *Diabetes & Metabolism,* 30**,** 13-19.

GUSTAFSON, B. & SMITH, U. 2006. Cytokines Promote Wnt Signaling and Inflammation and Impair the Normal Differentiation and Lipid Accumulation in 3T3-L1 Preadipocytes. *Journal of Biological Chemistry,* 281**,** 9507-9516.

HALBERG, N., KHAN, T., TRUJILLO, M. E., WERNSTEDT-ASTERHOLM, I., ATTIE, A. D., SHERWANI, S., WANG, Z. V., LANDSKRONER-EIGER, S., DINEEN, S., MAGALANG, U. J., BREKKEN, R. A. & SCHERER, P. E. 2009. Hypoxia-Inducible Factor 1alpha Induces Fibrosis and Insulin Resistance in White Adipose Tissue. *Molecular and Cellular Biology,* 29**,** 4467-83.

HALES, C. M., CARROLL, M. D., FRYAR, C. D. & OGDEN, C. L. 2020. *Prevalence of Obesity and Severe Obesity Among Adults: United States, 2017-2018* [Online]. Hyattsville: National Center for Health Statistics. Available: https://www.cdc.gov/nchs/products/databriefs/db360.htm#Suggested_citation [Accessed: 03.11 2022].

HAN, C. Y. 2016. Roles of Reactive Oxygen Species on Insulin Resistance in Adipose Tissue. *Diabetes and Metabolism Journal,* 40**,** 272-279.

HARPER, K., BROCHU-GAUDREAU, K., SAUCIER, C. & DUBOIS, C. M. 2019. Hypoxia Downregulates LPP3 and Promotes the Spatial Segregation of ATX and LPP1 During Cancer Cell Invasion. *Cancers,* 11**,** 1403.

HAUCK, A. K., HUANG, Y., HERTZEL, A. V. & BERNLOHR, D. A. 2019. Adipose Oxidative Stress and Protein Carbonylation. *Journal of Biological Chemistry,* 294**,** 1083-1088.

HEINDEL, J. J. & BLUMBERG, B. 2019. Environmental Obesogens: Mechanisms and Controversies. *Annual Review of Pharmacology and Toxicology,* 59**,** 89-106.

HEINDEL, J. J., BLUMBERG, B., CAVE, M., MACHTINGER, R., MANTOVANI, A., MENDEZ, M. A., NADAL, A., PALANZA, P., PANZICA, G., SARGIS, R., VANDENBERG, L. N. & VOM SAAL, F. 2017. Metabolism Disrupting Chemicals and Metabolic Disorders. *Reproductive Toxicology,* 68**,** 3-33.

HEINRICH BÖLL STIFTUNG 2019. *Plastic Atlas,* Berlin, Germany, Heinrich Böll Fundation and Break Free From Plastic.

HELLEMANS, J. & VANDESOMPELE, J. 2014. Selection of Reliable Reference Genes for RT-qPCR Analysis. *In:* BIASSONI, R. & RASO, A. (eds.) *Quantitative Real-Time PCR: Methods and Protocols.* New York, NY: Springer New York.

HIRSCH, C. & SCHILDKNECHT, S. 2019. *In Vitro* Research Reproducibility: Keeping Up High Standards. *Frontiers in pharmacology,* 10**,** 1484.

HUANG, H., SONG, T. J., LI, X., HU, L., HE, Q., LIU, M., LANE, M. D. & TANG, Q. Q. 2009. BMP Signaling Pathway is Required for Commitment of C3H10T1/2 Pluripotent Stem Cells to the Adipocyte Lineage. *Proceedings of the National Academy of Science of the United States of America,* 106**,** 12670-5.

JIANG, N., LI, Y., SHU, T. & WANG, J. 2019. Cytokines and Inflammation in Adipogenesis: an Updated Review. *Frontiers of Medicine,* 13**,** 314-329.

JOSE, A. & KIENESBERGER, P. C. 2021. Autotaxin-LPA-LPP3 Axis in Energy Metabolism and Metabolic Disease. *International Journal of Molecular Sciences,* 22**,** 9575.

KATZ, T. A. & WALKER, C. L. 2019. Chapter 1-4 - Implications for Chromatin Biology in Toxicology. *In:* MCCULLOUGH, S. D. & DOLINOY, D. C. (eds.) *Toxicoepigenetics.* Academic Press.

KLINGELHUTZ, A. J., GOURRONC, F. A., CHALY, A., WADKINS, D. A., BURAND, A. J., MARKAN, K. R., IDIGA, S. O., WU, M., POTTHOFF, M. J. & ANKRUM, J. A. 2018. Scaffold-Free Generation of Uniform Adipose Spheroids for Metabolism Research and Drug Discovery. *Scientific Reports,* 8**,** 523.

KOCH, H. M. & CALAFAT, A. M. 2009. Human Body Burdens of Chemicals Used in Plastic Manufacture. *Philosophical Transactions of the Royal Society of London. Series B, Biological Science,* 364**,** 2063-78.

KRAUS, N. A., EHEBAUER, F., ZAPP, B., RUDOLPHI, B., KRAUS, B. J. & KRAUS, D. 2016. Quantitative Assessment of Adipocyte Differentiation in Cell Culture. *Adipocyte,* 5**,** 351-358.

KROTKIEWSKI, M., BJÖRNTORP, P. & SMITH, U. 1983. Impact of Obesity on Metabolism in Men and Women. Importance of Regional Adipose Tissue Distribution. *Journal of Clinical Investigation,* 72**,** 1150-1162.

LI, J. & SHEN, X. 2019. Effect of Rosiglitazone on Inflammatory Cytokines and Oxidative Stress After Intensive Insulin Therapy in Patients with Newly Diagnosed Type 2 Diabetes. *Diabetology Metabolic Syndrome,* 11**,** 35.

LITHNER, D., LARSSON, A. & DAVE, G. 2011. Environmental and Health Hazard Ranking and Assessment of Plastic Polymers Based on Chemical Composition. *Science of The Total Environment,* 409**,** 3309-24.

MACDOUGALD, O. A. & LANE, M. D. 1995. Transcriptional Regulation of Gene Expression During Adipocyte Differentiation. *Annual Review of Biochemistry,* 64**,** 345-73.

MAO, G., SMYTH, S. S. & MORRIS, A. J. 2019. Regulation of PLPP3 Gene Expression by NF-κB Family Transcription Factors. *Journal of Biological Chemistry,* 294**,** 14009-14019.

MARTÍNEZ, J. A., CORDERO, P., CAMPIÓN, J. & MILAGRO, F. I. 2012. Interplay of Early-Life Nutritional Programming on Obesity, Inflammation and Epigenetic Outcomes. *Proceedings of the Nutrition Society,* 71**,** 276-283.

MEHRZAD, R. 2022. *The Link Between Obesity and Cancer,* Amsterdam, Elsevier Science Technology.

MONTEIRO, R. & AZEVEDO, I. 2010. Chronic Inflammation in Obesity and The Metabolic Syndrome. *Mediators of Inflammation,* 2010.

NAPPI, F., BARREA, L., DI SOMMA, C., SAVANELLI, M. C., MUSCOGIURI, G., ORIO, F. & SAVASTANO, S. 2016. Endocrine Aspects of Environmental "Obesogen" Pollutants. *Internal Journal of Environmental Research and Public Health,* 13.

NIEMELÄ, S., MIETTINEN, S., SARKANEN, J. & ASHAMMAKHI, N. 2008. Adipose Tissue and Adipocyte Differentiation: Molecular and Cellular Aspects and Tissue Engineering Applications. *Topics in tissue engineering,* 4**,** 26.

OGDEN, C. L., YANOVSKI, S. Z., CARROLL, M. D. & FLEGAL, K. M. 2007. The Epidemiology of Obesity. *Gastroenterology,* 132**,** 2087-2102.

OZBEY, G., GORCZYNSKI, R. & ERIN, N. 2014. Stability of Cytokines In Supernatants of Stimulated Mouse Immune Cells. *European Cytokine Network,* 25**,** 30-34.

PHANIENDRA, A., JESTADI, D. B. & PERIYASAMY, L. 2015. Free Radicals: Properties, Sources, Targets, and Their Implication in Various Diseases. *Indian Journal of Clinical Biochemistry,* 30**,** 11-26.

POMATTO, V., COTTONE, E., COCCI, P., MOZZICAFREDDO, M., MOSCONI, G., NELSON, E. R., PALERMO, F. A. & BOVOLIN, P. 2018. Plasticizers Used In Food-Contact Materials Affect Adipogenesis In 3T3-L1 cells. *The Journal of Steroid Biochemistry and Molecular Biology,* 178**,** 322-332.

POPKO, K., GORSKA, E., STELMASZCZYK-EMMEL, A., PLYWACZEWSKI, R., STOKLOSA, A., GORECKA, D., PYRZAK, B. & DEMKOW, U. 2010. Proinflammatory Cytokines IL-6 and TNF-α and The Development of Inflammation in Obese Subjects. *European Journal of Medical Research,* 15**,** 120.

RAGUSA, A., NOTARSTEFANO, V., SVELATO, A., BELLONI, A., GIOACCHINI, G., BLONDEEL, C., ZUCCHELLI, E., DE LUCA, C., D'AVINO, S., GULOTTA, A., CARNEVALI, O. & GIORGINI, E. 2022. Raman Microspectroscopy Detection and Characterisation of Microplastics in Human Breastmilk. *Polymers,* 14**,** 2700.

REGULATION10/2011/EU 2011. COMMISSION REGULATION (EU) No 10/2011 on plastic materials and articles intended to come into contact with food.

RIO, D. C., ARES, M., JR., HANNON, G. J. & NILSEN, T. W. 2010. Purification of RNA Using TRIzol (TRI reagent). *Cold Spring Harbor Protocols,* 2010**,** pdb.prot5439.

ROSEN, E. D. 2005. The Transcriptional Basis of Adipocyte Development. *Prostaglandins, Leukotrienes and Essential Fatty Acids,* 73**,** 31-34.

ROSEN, E. D. & SPIEGELMAN, B. M. 2000. Molecular Regulation of Adipogenesis. *Annual Review of Cell and Developmental Biology,* 16**,** 145-171.

RUBIN, C. S., HIRSCH, A., FUNG, C. & ROSEN, O. M. 1978. Development of Hormone Receptors and Hormonal Responsiveness *in Vitro*. Insulin Receptors and Insulin Sensitivity In The Preadipocyte and Adipocyte Forms of 3T3-L1 cells. *Journal of Biological Chemistry,* 253**,** 7570-7578.

RUIJTER, J. M., RAMAKERS, C., HOOGAARS, W. M. H., KARLEN, Y., BAKKER, O., VAN DEN HOFF, M. J. B. & MOORMAN, A. F. M. 2009. Amplification Efficiency: Linking Baseline and Bias In The Analysis of Quantitative PCR Data. *Nucleic Acids Research,* 37**,** e45-e45.

SALANS, L. B., KNITTLE, J. L. & HIRSCH, J. 1968. The Role of Adipose Cell Size and Adipose Tissue Insulin Sensitivity In The Carbohydrate Intolerance of Human Obesity. *Journal of Clinical Investigation,* 47**,** 153-165.

SIMON, M. F., DAVIAUD, D., PRADÈRE, J. P., GRÈS, S., GUIGNÉ, C., WABITSCH, M., CHUN, J., VALET, P. & SAULNIER-BLACHE, J. S. 2005. Lysophosphatidic Acid Inhibits Adipocyte Differentiation via Lysophosphatidic Acid 1 Receptor-dependent Down-regulation of Peroxisome Proliferator-activated Receptor γ2. *Journal of Biological Chemistry,* 280**,** 14656-14662.

SKURK, T., ALBERTI-HUBER, C., HERDER, C. & HAUNER, H. 2007. Relationship between Adipocyte Size and Adipokine Expression and Secretion. *The Journal of Clinical Endocrinology & Metabolism,* 92**,** 1023-1033.

SPALDING, K. L., ARNER, E., WESTERMARK, P. O., BERNARD, S., BUCHHOLZ, B. A., BERGMANN, O., BLOMQVIST, L., HOFFSTEDT, J., NÄSLUND, E., BRITTON, T., CONCHA, H., HASSAN, M., RYDÉN, M., FRISÉN, J. & ARNER, P. 2008. Dynamics of Fat Cell Turnover In Humans. *Nature,* 453**,** 783-787.

STUDENT, A. K., HSU, R. Y. & LANE, M. D. 1980. Induction of Fatty Acid Synthetase Synthesis In Differentiating 3T3-L1 Preadipocytes. *Journal of Biological Chemistry,* 255**,** 4745-4750.

TAFERE, G. G., WONDAFRASH, D. Z., ZEWDIE, K. A., ASSEFA, B. T. & AYZA, M. A. 2020. Plasma Adipsin as a Biomarker and Its Implication in Type 2 Diabetes Mellitus. *Diabetes, Metabolic Syndrome and Obesity,* 13**,** 1855-1861.

TANG, Q., LI, Y. & HE, J. 2022. MANF: an Emerging Therapeutic Target for Metabolic Diseases. *Trends in Endocrinology & Metabolism,* 33**,** 236-246.

TEUTEN, E. L., SAQUING, J. M., KNAPPE, D. R., BARLAZ, M. A., JONSSON, S., BJÖRN, A., ROWLAND, S. J., THOMPSON, R. C., GALLOWAY, T. S., YAMASHITA, R., OCHI, D., WATANUKI, Y., MOORE, C., VIET, P. H., TANA, T. S., PRUDENTE, M., BOONYATUMANOND, R., ZAKARIA, M. P., AKKHAVONG, K., OGATA, Y., HIRAI, H., IWASA, S., MIZUKAWA, K., HAGINO, Y., IMAMURA, A., SAHA, M. & TAKADA, H. 2009. Transport and Release of Chemicals from Plastics to The Environment and to Wildlife. *Philosophical Transactions of the Royal Society of London. Series B, Biological Science,* 364**,** 2027-45.

VANDENBERG, L. N., HAUSER, R., MARCUS, M., OLEA, N. & WELSHONS, W. V. 2007. Human Exposure to Bisphenol A (BPA). *Reproductive Toxicology,* 24**,** 139-177.

VENKATRAMAN, G., BENESCH, M. G. K., TANG, X., DEWALD, J., MCMULLEN, T. P. W. & BRINDLEY, D. N. 2015. Lysophosphatidate Signaling Stabilizes Nrf2 and Increases The Expression of Genes Involved In Drug Resistance and Oxidative Stress Responses: Implications for Cancer Treatment. *The FASEB Journal,* 29**,** 772-785.

VICENNATI, V., VOTTERO, A., FRIEDMAN, C. & PAPANICOLAOU, D. A. 2002. Hormonal Regulation of Interleukin-6 Production in Human Adipocytes. *International Journal of Obesity,* 26**,** 905-911.

VOM SAAL, F. S., AKINGBEMI, B. T., BELCHER, S. M., BIRNBAUM, L. S., CRAIN, D. A., ERIKSEN, M., FARABOLLINI, F., GUILLETTE, L. J., HAUSER, R., HEINDEL, J. J., HO, S.-M., HUNT, P. A., IGUCHI, T., JOBLING, S., KANNO, J., KERI, R. A., KNUDSEN, K. E., LAUFER, H., LEBLANC, G. A., MARCUS, M., MCLACHLAN, J. A., MYERS, J. P., NADAL, A., NEWBOLD, R. R., OLEA, N., PRINS, G. S., RICHTER, C. A., RUBIN, B. S., SONNENSCHEIN, C., SOTO, A. M.,

TALSNESS, C. E., VANDENBERGH, J. G., VANDENBERG, L. N., WALSER-KUNTZ, D. R., WATSON, C. S., WELSHONS, W. V., WETHERILL, Y. & ZOELLER, R. T. 2007. Chapel Hill Bisphenol A Expert Panel Consensus Statement: Integration of Mechanisms, Effects in Animals and Potential to Impact Human Health at Current Levels of Exposure. *Reproductive Toxicology,* 24**,** 131-138.

VÖLKER, J., ASHCROFT, F., VEDØY, Å., ZIMMERMANN, L. & WAGNER, M. 2022a. Adipogenic Activity of Chemicals Used in Plastic Consumer Products. *Environmental Science & Technology,* 56**,** 2487-2496.

VÖLKER, J., VEDØY, Å., ASHCROFT, F., ZIMMERMANN, L. & WAGNER, M. 2022b. *CellProfiler pipelines for the adipogenesis assay and nuclear count (reporter gene assays)* [Online]. Available: https://zenodo.org/record/5513372#.Y2TfZS1Q1QJ [Accessed 04.11 2022].

WELLEN, K. E. & HOTAMISLIGIL, G. S. 2003. Obesity-Induced Inflammatory Changes In Adipose Tissue. *Journal of Clinical of Investigation,* 112**,** 1785-8.

WIESINGER, H., WANG, Z. & HELLWEG, S. 2021. Deep Dive into Plastic Monomers, Additives, and Processing Aids. *Environmental Science & Technology,* 55**,** 9339-9351.

WU, T., LIU, Q., LI, Y., LI, H., CHEN, L., YANG, X., TANG, Q., PU, S., KUANG, J., LI, R., HUANG, Y., ZHANG, J., ZHANG, Z., ZHOU, J., HUANG, C., ZHANG, G., ZHAO, Y., ZOU, M., JIANG, W., MO, L. & HE, J. 2021. Feeding-Induced Hepatokine, Manf, Ameliorates Diet-Induced Obesity by Promoting Adipose Browning via p38 MAPK Pathway. *Journal of Experimental Medicine,* 218.

ZEBISCH, K., VOIGT, V., WABITSCH, M. & BRANDSCH, M. 2012. Protocol for Effective Differentiation of 3T3-L1 Cells to Adipocytes. *Analytical Biochemistry,* 425**,** 88-90.

ZHA, B. S. & ZHOU, H. 2012. ER Stress and Lipid Metabolism in Adipocytes. *Biochemistry Research International,* 2012**,** 312943.

ZHANG, X., LI, M., YIN, N. & ZHANG, J. 2021. The Expression Regulation and Biological Function of Autotaxin. *Cells,* 10**,** 939.

ZIMMERMANN, L., DIERKES, G., TERNES, T. A., VÖLKER, C. & WAGNER, M. 2019. Benchmarking the *in Vitro* Toxicity and Chemical Composition of Plastic Consumer Products. *Environmental Science & Technology,* 53**,** 11467-11477.

Appendix

Table A.1: Materials are listed with belonging producer and catalog number.

Materials	Supplier	Catalog no.
3T3-L1	ZenBio Inc.	SP-L1, lot 3T3L1062104
AdipoRed kit assay	Lonza	PT-7009
Bovine calf serum (BCS)	HyClone	SH300/2,03
Dexamethasone	Sigma-Aldrich	D4902
Dimethyl sulfoxide (DMSO)	Sigma-Aldrich	D8418
DMEM, high glucose, glutamax supplement, pyruvate	Gibco	10569010
DMEM - high glucose	Sigma-Aldrich	D6429-500
DMEM high glucose	Biowest	L0103-500
DuoSet ELISA ancillary reagent kit 2	R&D systems	DY008
Fetal bovine serum (FBS)	Gibco	A4766801
HEPES	Sigma-Aldrich	H0887
IBMX	Sigma-Aldrich	I5879
Insulin human	Sigma-Aldrich	I3536-100MG
LightCycler 480 SYBR Green I Master	Roche	04887352001
Methanol	Sigma	≥98 %, CAS: 10034998
Mouse Il-6 DuoSet ELISA	R&D systems	DY406-05
Mouse TNF-α DuoSet ELISA	R&D systems	DY410-05
NucBlue live cell ready probes reagent	Thermo Fisher	R37605
Paraformaldehyde	Thermo Scientific	11400580
Penicillin/streptomycin	VWR	L0022-100
Quantitect rev. Transcription kit (200)	Qiagen	205313
RNeasy mini kit	Qiagen	74004
Rosiglitazone	Sigma-Aldrich	R2408
Trypsin/EDTA	Sigma-Aldrich	59418C
TRIzol^{tm}	Invitrogen	15596026

Table A.2: The content in phosphate-buffered saline (PBS).

1 L Phosphate-buffered saline (PBS)	
1.42 g	Na_2HPO_4
0.24 g	KH_2PO_4
8 g	NaCl
0.2 g	KCl
Adjust to 1 L	Ultrapure H_2O (PURELAB flex, ELGA)

GENERAL ELISA PROTOCOL (DuoSet, R&D systems)

Plate Preparation

1. Dilute the Capture Antibody to the working concentration in PBS without carrier protein. Immediately coat a 96-well microplate with 100 µL per well of the diluted Capture Antibody. Seal the plate and incubate overnight at room temperature.

2. Aspirate each well and wash with Wash Buffer, repeating the process two times for a total of three washes. Wash by filling each well with Wash Buffer (400 µL) using a squirt bottle, manifold dispenser, or autowasher. Complete removal of liquid at each step is essential for good performance. After the last wash, remove any remaining Wash Buffer by aspirating or by inverting the plate and blotting it against clean paper towels.

3. Block plates by adding 300 µL of Reagent Diluent to each well. Incubate at room temperature for a minimum of 1 hour.

4. Repeat the aspiration/wash as in step 2. The plates are now ready for sample addition.

Assay Procedure

1. Add 100 µL of sample or standards in Reagent Diluent, or an appropriate diluent, per well. Cover with an adhesive strip and incubate 2 hours at room temperature.

2. Repeat the aspiration/wash as in step 2 of Plate Preparation.

3. Add 100 µL of the Detection Antibody, diluted in Reagent Diluent, to each well. Cover with a new adhesive strip and incubate 2 hours at room temperature.

4. Repeat the aspiration/wash as in step 2 of Plate Preparation.

5. Add 100 µL of the working dilution of Streptavidin-HRP to each well. Cover the plate and incubate for 20 minutes at room temperature. Avoid placing the plate in direct light.

6. Repeat the aspiration/wash as in step 2.

7. Add 100 µL of Substrate Solution to each well. Incubate for 20 minutes at room temperature. Avoid placing the plate in direct light.

8. Add 50 µL of Stop Solution to each well. Gently tap the plate to ensure thorough mixing.

9. Determine the optical density of each well immediately, using a microplate reader set to 450 nm. If wavelength correction is available, set to 540 nm or 570 nm. If wavelength correction is not available, subtract readings at 540 nm or 570 nm from the readings at 450 nm. This subtraction will correct for optical imperfections in the plate. Readings made directly at 450 nm without correction may be higher and less accurate.

3T3-L1 RNA extraction (Invitrogen and Qiagen)

1. Lyse and homogenize samples in TRIzol reagent
    a. Remove growth media
    b. Add 0.4-0.4 mL TRIzol reagent per 10^5-10^7 cells directly to the culture dish to lyse the cells.
    c. Pipet the lysate up and down several times to homogenize.
2. Store at -20 up to a year
3. Thaw samples on ice and keep them on ice until step 9.
4. Add 200 uL chloroform per 1 mL TRIzol reagent used for lysis, then securely cap the tube.
5. Vortex samples 5 sec
6. Incubate for 10 minutes
7. Centrifuge the sample for 20 min at 12,000 g at 4°C. The mixture separates into a lower red phenol-chloroform, and interphase and a colorless upper aqueous phase.
8. Transfer the aqueous phase containing the RNA to a new tube
9. Transfer the aqueous phase containing the RNA to a new tube by angling the tube at 45° and pipetting the solution out.
10. Add 1 volume of 70% ethanol to the lysate and mix well by pipetting. Do not centrifuge. Proceed immediately to step 3.
11. Transfer up to 700 uL of the sample, including any precipitate, to a RNeasy Mini spin column placed in a 2 mL collection tube. Close lid, close the lid and centrifuge for 15 sec at ≥8000 g. Discard the flow through.
12. Add 700 uL Buffer RW1 to the RNeasy spin column. Close the lid, and centrifuge for 15 sec at ≥8000 g. Discard the flow through.
13. Add 500 uL Buffer RPE to the RNeasy spin column. Close the lid, and centrifuge for 15 sec at ≥8000 g. Discard the flow through.
14. Add 500 uL Buffer RPE to the RNeasy spin column. Close the lid, and centrifuge for 2 min at ≥8000 g.
    Optional: Place the RNeasy spin column in a new 2 mL collection tube. Centrifuge at full speed for 1 min to dry the membrane.
15. Place the RNeasy spin column in a new 1.5 mL collection tube. Add 30-50 µL RNAse-free water directly to the spin column membrane. Close the lid, and centrifuge for 1 min at ≥8000 g to elute the RNA.
16. Repeat step 14, using the eluate from step 14. Reuse the collection tube from step 14.
17. Nanodrop the samples
18. Store at -80°C

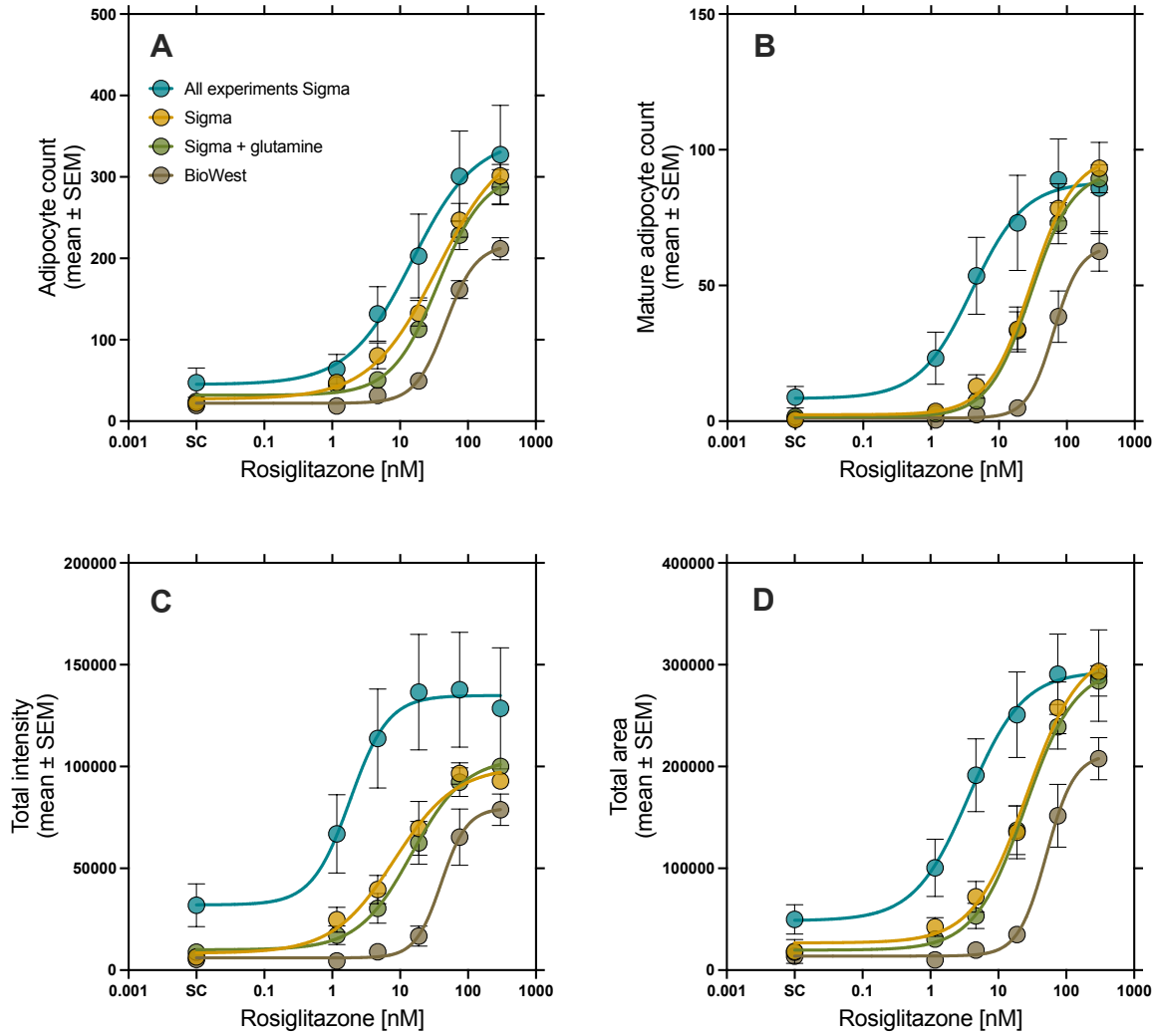

Figure A.1: Effect of rosiglitazone exposure to 3T3-L1 throughout the adipogenesis assay for comparison of different media. Media comparison was conducted with Sigma cell culture media, Sigma media added glutamine and BioWest cell media, the results were compared to the average of all experiments conducted with Sigma cell media. The four endpoints A) Adipocyte count, B) mature adipocyte, C) total intensity of the NileRed staining and D) Total area of lipid droplets, were estimated per field and fitted with a four-parameter logistic regression with the average ± SEM. In the graphs presenting the average of all experiments conducted with Sigma media in the adipocyte count (N = 5), mature adipocyte count (N = 5), total intensity of lipid staining (N = 6) and total area occupied by lipid droplets (N = 5) represents the mean of the biological replicates (N), which are a mean of four technical replicates from each experiment. The results from the media comparison are mean of the four technical replicates from the single experiment.

Table A.3: Highest non-cytotoxic concentration (HNC) of the plastic extracts after exposure of 3T3-L1 cells throughout the adipogenesis assay.

Plastic extract	HNC (mg plastic well^{-1})
PP4	3.0
PS2	3.0
PUR3	0.375
PUR4	3.0
PVC2	3.0
PVC4	3.0

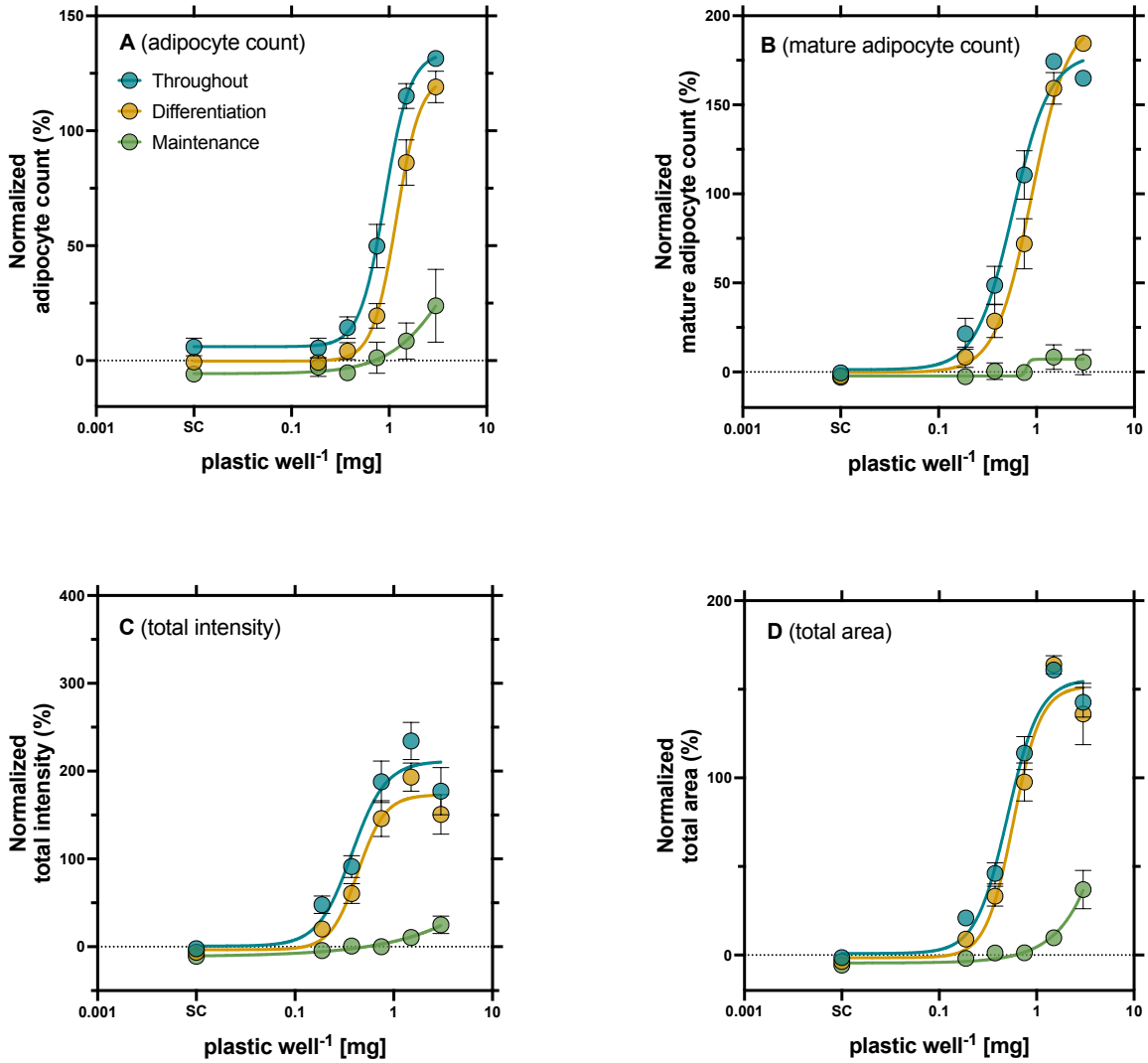

Figure A.2: Effect of PP4 exposure on A) adipocyte count (N = 2), B) mature adipocyte count (N = 2), C) total intensity of the staining (N = 3) and D) total area of lipid droplets (N = 3) in 3T3-L1 during the three windows of adipogenesis assay. The data is fitted with a four-parameter logistic regression ± SEM and normalized to the effect of the throughout exposure of rosiglitazone. The biological replicates (N) are the average of four technical replicates.

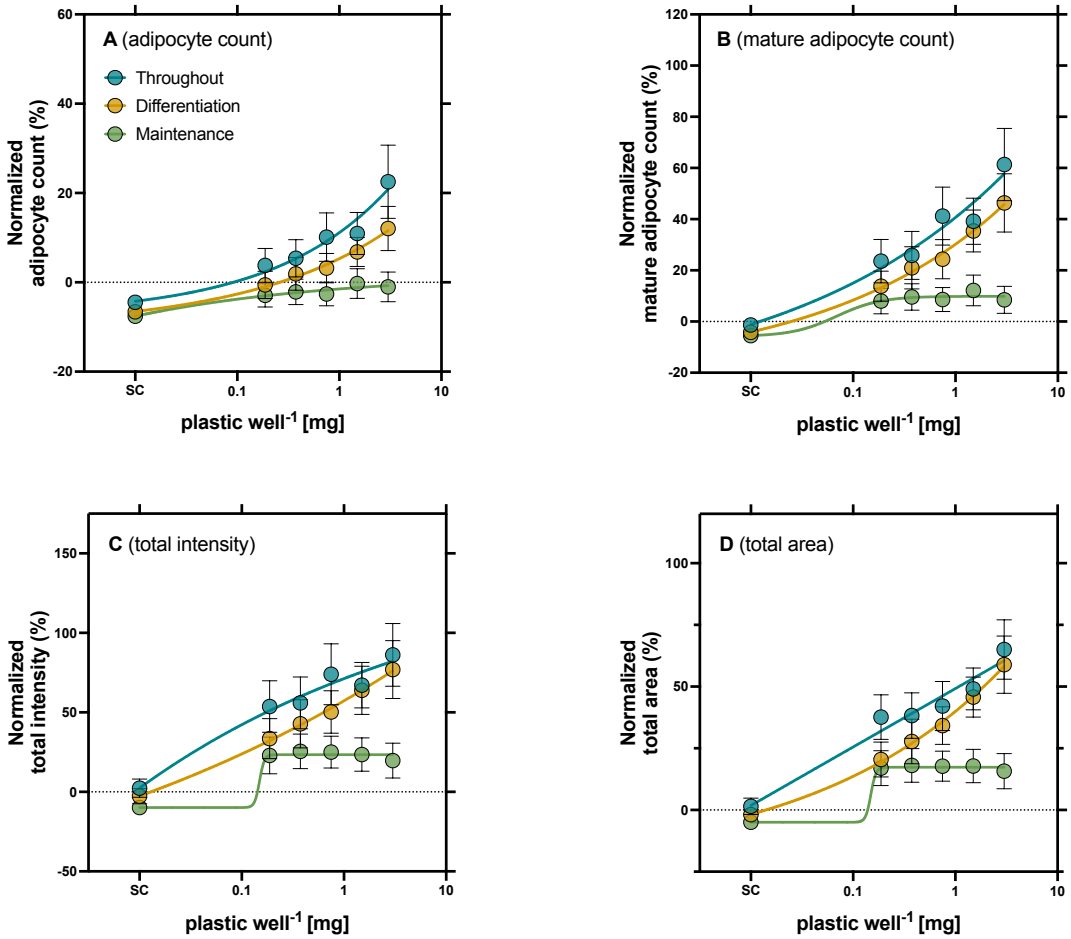

Figure A.3: Effect of the PS2 exposure on A) adipocyte count (N = 3), B) mature adipocyte count (N = 3), C) total intensity of staining (N = 3) and D) total area of lipid droplets (N = 3) in 3T3-L1 cells throughout, during the differentiation and maintenance window of the adipogenesis assay. The biological replicates (N) are a mean of four technical replicates. The data is fitted with a four-parameter logistic regression ± SEM and normalized to the throughout exposure of rosiglitazone.

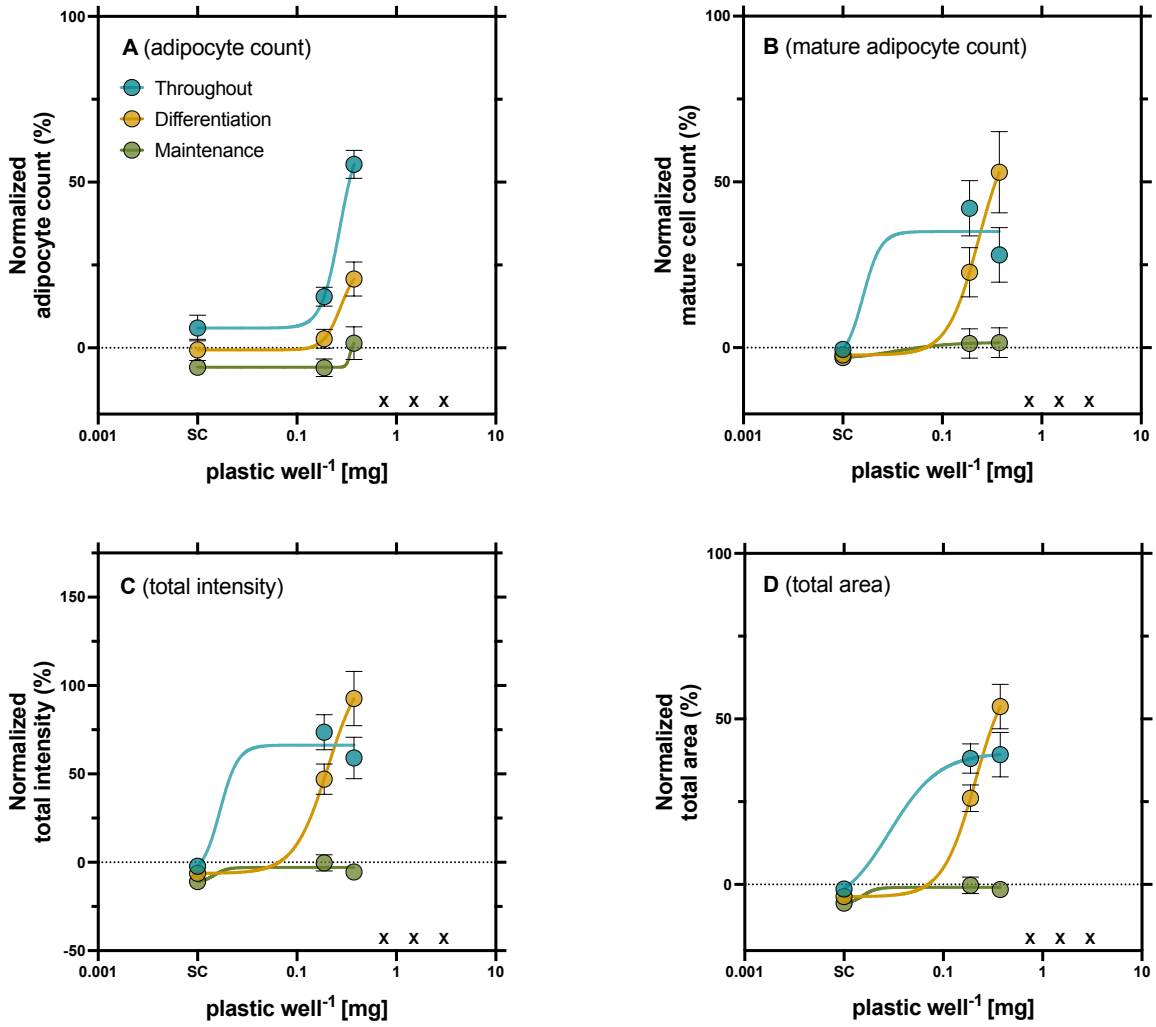

Figure A.4: The effect of PUR3 exposure of 3T3-L1 on A) adipocyte count (N=2), B) mature adipocyte count (N=2), C) total intensity of the staining (N=3) and D) total area of lipid droplets (N=3) during different windows of the adipogenesis assay. The data is fitted with a four-parameter logistic regression ± SEM, normalized to the throughout exposure of rosiglitazone and the concentrations are logarithmically transformed. The "x" represents the analyzed cytotoxic concentrations of PUR3.

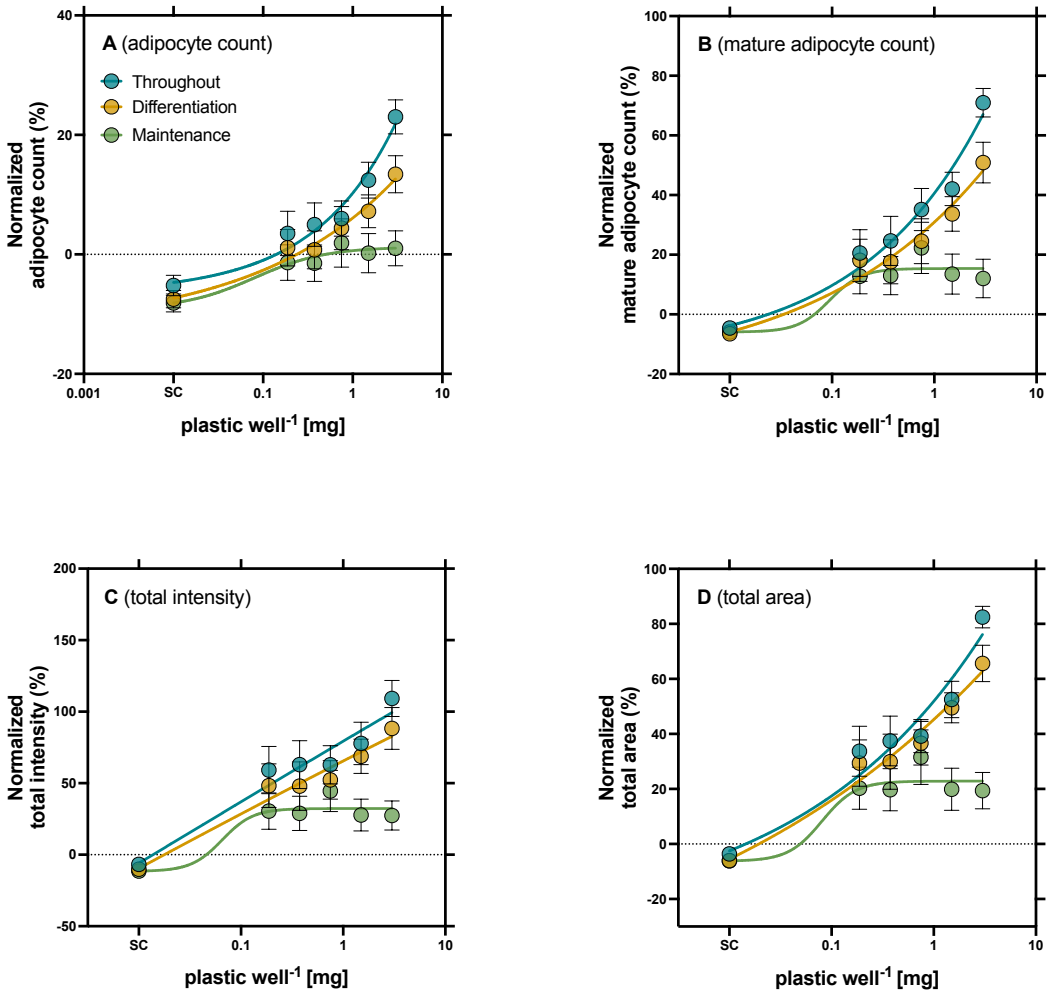

Figure A.5: The effect of PUR4 exposure on A) adipocyte count, B) mature adipocyte count, C) total intensity of the lipid staining, D) total area of the lipid droplet count in 3T3-L1 cells throughout, during the differentiation and maintenance window of the adipogenesis assay. There are three biological replicates per concentration which are a mean of the four technical replicates obtained in each experiment. The data is fitted with a four-parameter logistic regression ± SEM and normalized to the throughout exposure of rosiglitazone.

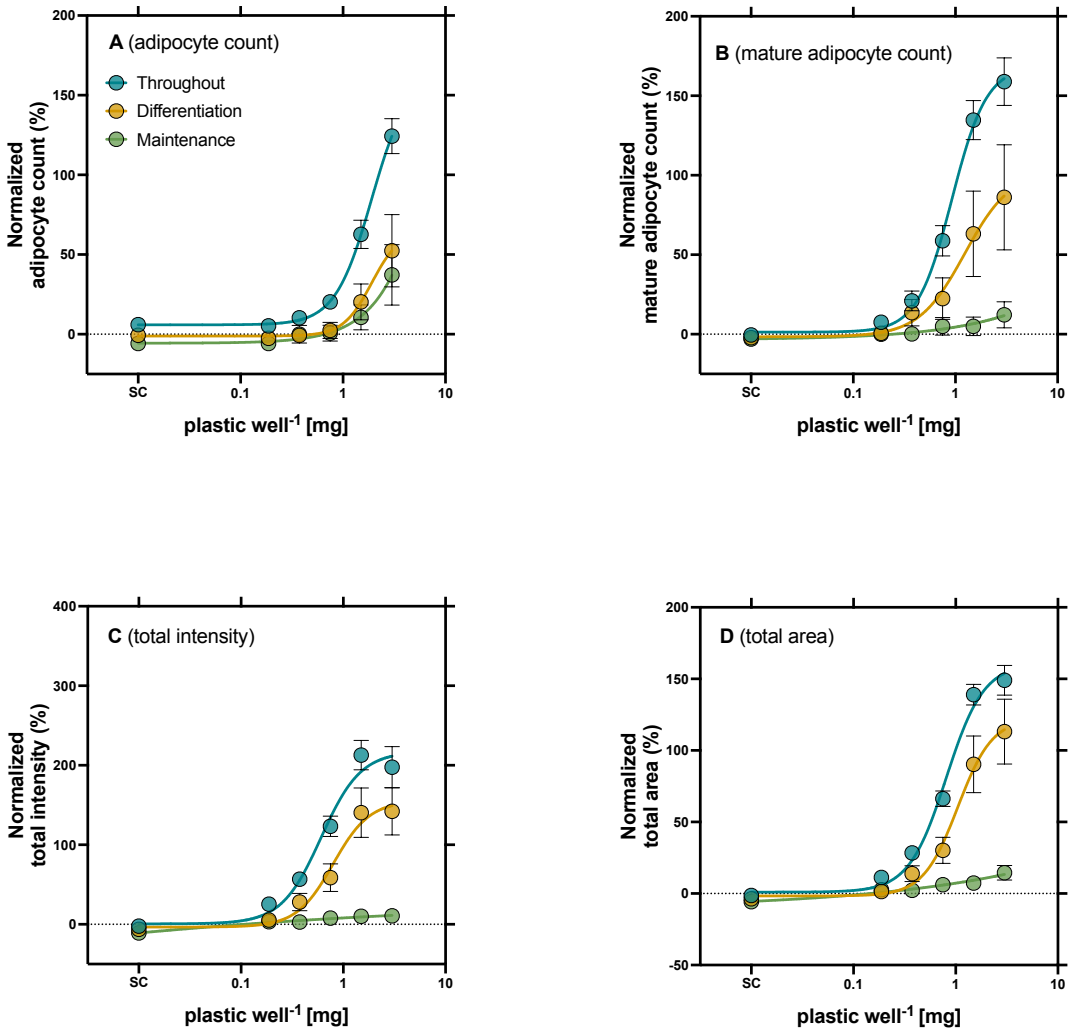

Figure A.6: The effect of PVC2 exposure of 3T3-L1 on the A) adipocyte count (N = 2), B) mature adipocyte count (N = 2), C) total intensity of lipid staining (N = 3) and D) total area of lipid droplets (N = 3). The data is fitted with a four-parameter logistic regression ± SEM and normalized to the throughout exposure of rosiglitazone. The biological replicates (N) are an average of the four technical replicates from each experiment.

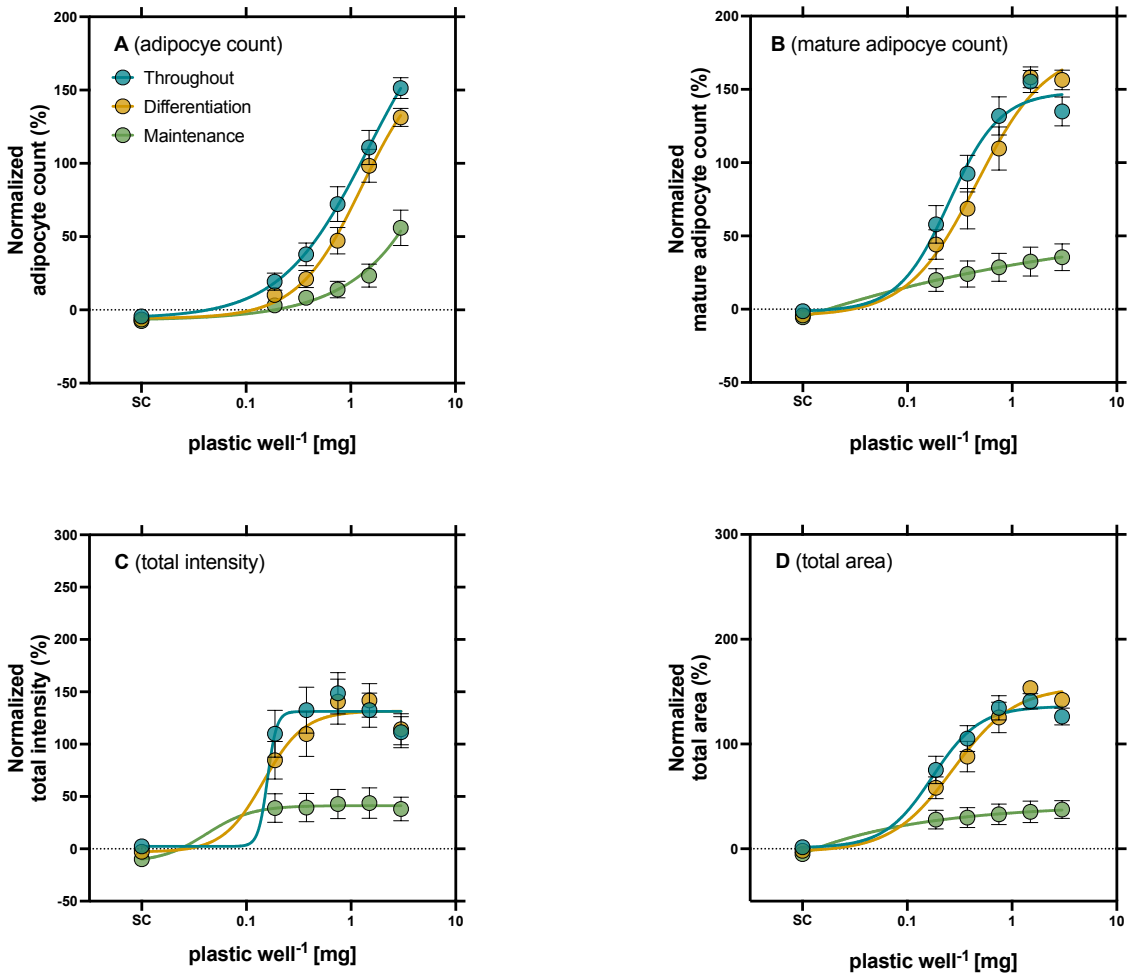

Figure A.7: Effect of PVC4 exposure in three windows to 3T3-L1 cells on A) adipocyte count, B) mature adipocyte count, C) total intensity of the NileRed staining and D) total area of the lipid droplet. There are three biological replicates per concentration which are a mean of the four technical replicates obtained in each experiment. The data is fitted with a non-linear regression (four-parameter logistic function) ± SEM and normalized to the throughout exposure data.

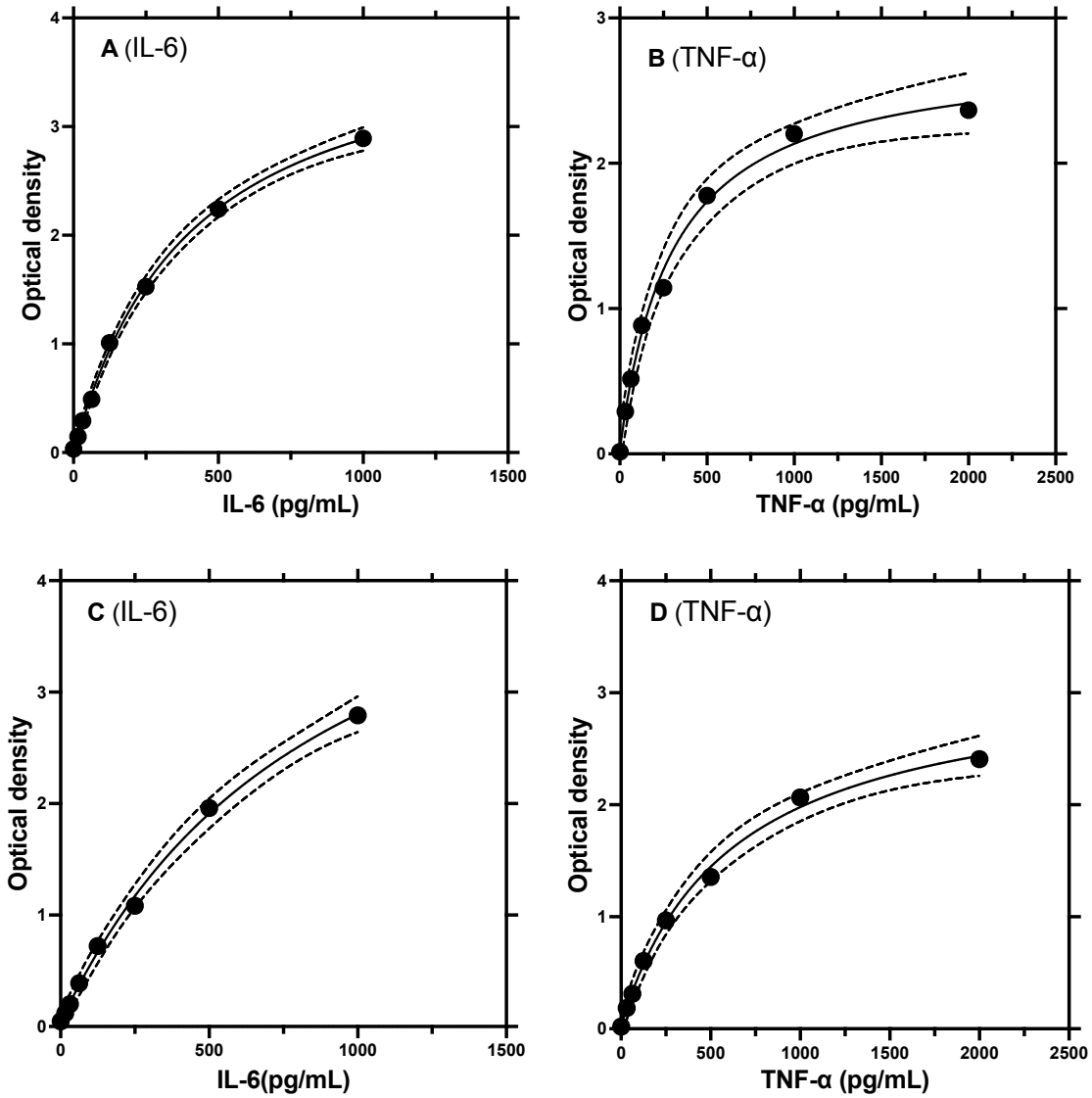

Figure A.8: Standard curve of IL-6 and TNF-α from both experiments. The A) IL-6 and B) TNF-α standard curves are from the first experiment and C) IL-6 and D) TNF-α are from the repeated experiment. The graphs include one technical replicate, fitted with a four-parameter sigmoidal curve.

Table A.4: Results from one-way ANOVA in the comparison of the effect of the plastic extracts on the IL-6 release from 3T3-L1. The IL-6 release was compared to the SC at day 5 and day 11 in both experiments.

ANOVA	DF	F-VALUE	P-VALUE	ALPHA
DAY 5 EXP.1	(11, 24)	66.89	<0.0001	0.05
DAY 11 EXP.1	(13, 28)	98.96	<0.0001	0.05
DAY 5 EXP.2	(7, 16)	207.7	<0.0001	0.05
DAY 11 EXP.2	(2, 5)	122.9	<0.0001	0.05

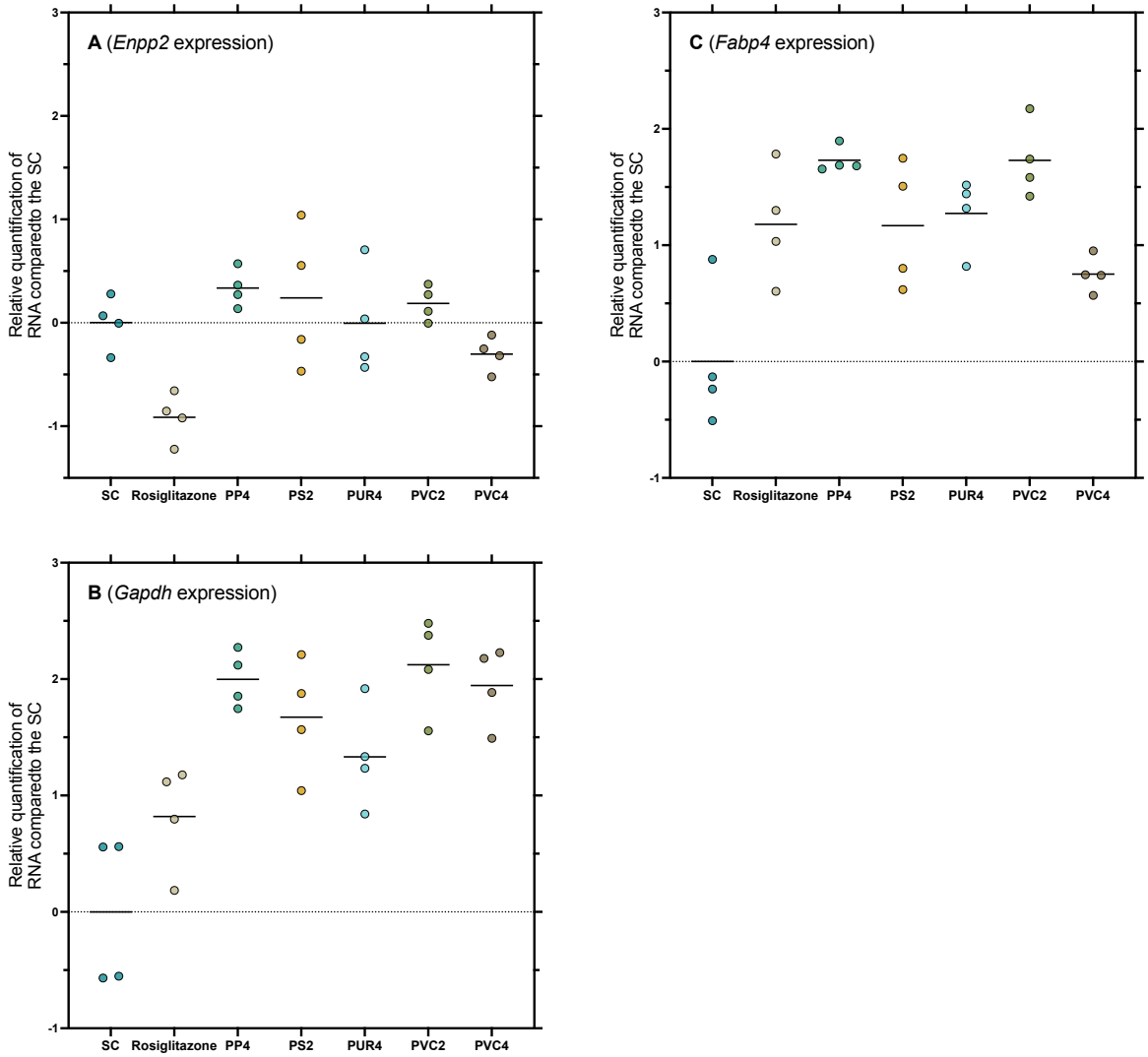

Figure A.9: Gene expression of *Enpp2, Fabp4* and *Gapdh* in 3T3-L1 in response to exposure of plastic extracts throughout the adipogenesis assay obtained from the first qPCR results. The relative gene expression is scaled to the SC, normalized to the gene expression of *Ywhaz* and transformed logarithmically. The graphs represent the mean of the four biological replicates in a relative quantification of A) *Enpp2*, B) *Fabp4* and C) *Gapdh* expression compared to the SC.

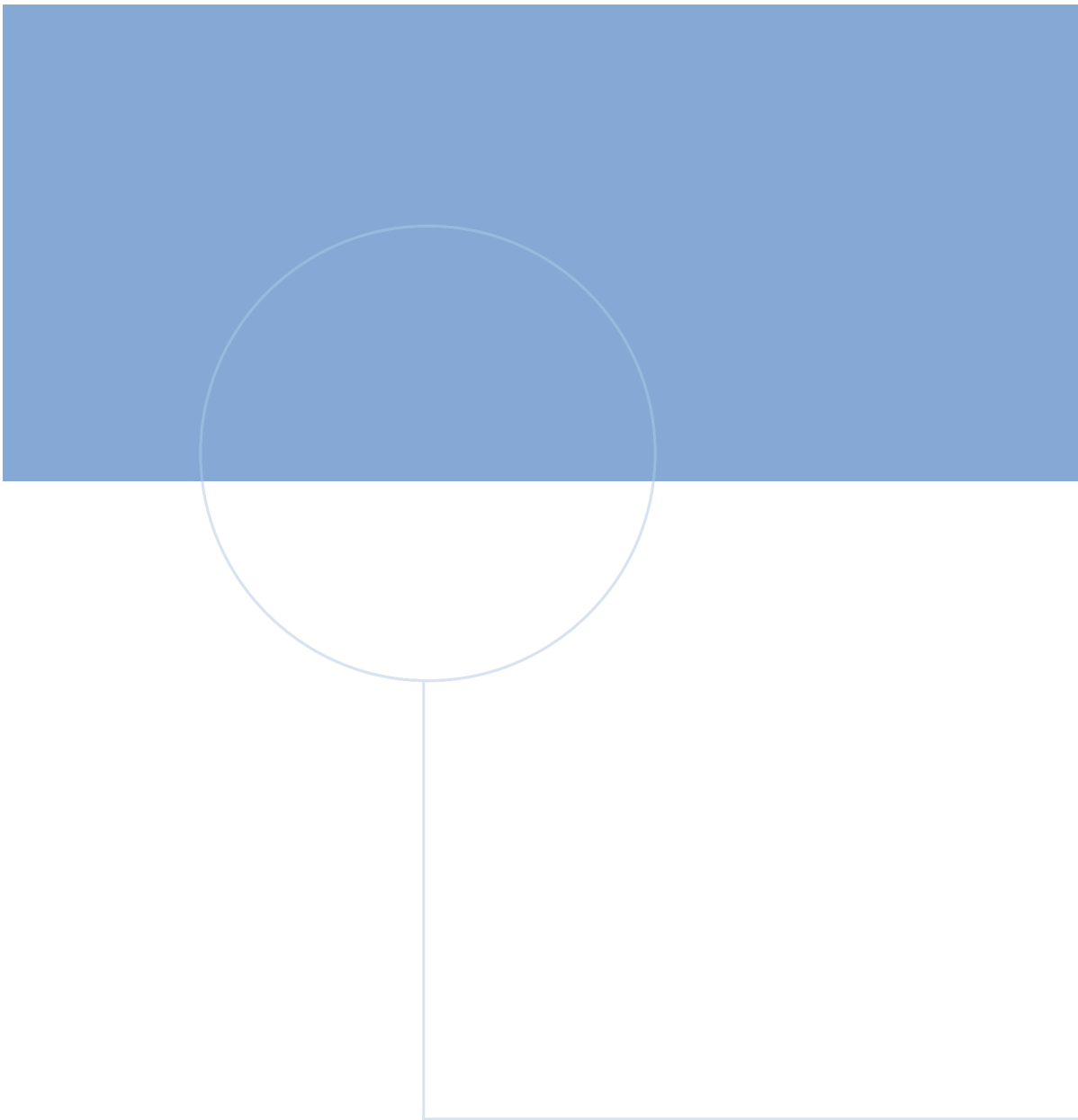

NTNU

Norwegian University of
Science and Technology